

UNIVERSITY OF BELGRADE
FACULTY OF CHEMISTRY

Afya A. Baroud

**SYNTHESIS, CHARACTERIZATION AND CYTOTOXICITY OF
BIS(BIPYRIDINE) RUTHENIUM(II) COMPLEXES WITH
PICOLINIC ACID DERIVATIVES**

Doctoral dissertation

Belgrade, 2017.

UNIVERZITET U BEOGRADU
HEMIJSKI FAKULTET

Afya A. Baroud

**SINTEZA, KARAKTERIZACIJA I CITOTOKSIČNOST
BIS(BIPIRIDIN) RUTENIJUM(II) KOMPLEKSA SA
DERIVATIMA PIKOLINSKE KISELINE**

doktorska disertacija

Beograd, 2017

Mentor

Full Professor dr Sanja Grgurić-Šipka
Faculty of Chemistry, University of Belgrade

Commission members

Associate Research Professor dr Sandra Arandelović,
Institute for Oncology and Radiology of Serbia

Assistant Professor dr Aleksandar Savić
Faculty of Chemistry, University of Belgrade

Assistant Research Professor dr Ljiljana Mihajlović-Lalić
Innovation Center of the Faculty of Chemistry

Date:

Acknowledgements

- It is a genuine pleasure to express my deep sense of thanks and gratitude to Prof. Sanja Grgurić-Šipka, dr Ljiljana Mihajlović-Lalić and dr Aleksandar Savić who helped me to get to this stage.
- I thank profusely dr Sandra Arandelović for her kind help and co-operation throughout experimental part of biological study.
- I thank deeply to Prof. Kristof Van Hecke for kind help and solving crystal structures.
- I express my deep sense of gratitude to my parents, who exerted their best to complete my educational career.
- It is my privilege to thank my husband Mr. Sliman Barood for his constant encouragement throughout my study period.

**SYNTHESIS, CHARACTERIZATION AND CYTOTOXICITY OF BIS(BIPYRIDINE)
RUTHENIUM(II) COMPLEXES WITH PICOLINIC ACID DERIVATIVES
SUMMARY**

SUMMARY

Bis(bipyridine)ruthenium(II) complexes (**1-5**) of general formula $[\text{Ru}(\text{L})(\text{bpy})_2]\text{PF}_6$, where $\text{bpy} = 2,2'$ -bipyridine; **HL** = 3-methylpyridine-2-carboxylic acid (**HL1**), 6-methylpyridine-2-carboxylic acid (**HL2**), 5-bromopyridine-2-carboxylic acid (**HL3**), 6-bromopyridine-2-carboxylic acid (**HL4**) and pyridine-2,4-dicarboxylic acid (**HL5**) were synthesized and fully characterized. For compounds **3**, **4** and **5** single-crystal X-ray diffraction analyses were also performed. The electrochemical character of the complexes was investigated by cyclic voltammetry revealing Ru(II)/Ru(III) electron transfer in the positive range of potentials. On the opposite potential side, multiple partially reversible peaks are dominant representing subsequent reductions of the bulky bipyridyl moiety. Cytotoxicity studies by MTT assay for 72 h of drug action, revealed that complexes **2-4** exhibited moderate activity in cervical human tumor cells (HeLa), with IC_{50} values (μM): 132.3 ± 5.0 (**2**), 184.0 ± 16.2 (**3**), 147.7 ± 8.0 (**4**). Complex **2** exhibited activity in colon cancer LS-174 cells (180.9 ± 10.1), while complexes were devoid of activity in lung cancer A549 and non-tumor MRC-5 cells, in the range of concentrations up to $200 \mu\text{M}$ for complexes **1-4** and up to $300 \mu\text{M}$ for complex **5**. Moderate cytotoxicity of complexes **1-5** may be due to faster ligand dissociation kinetics, and greater off-target reactivity, when once in solution. Still, minor variations in the structure of the co-ligand resulted in variations of IC_{50} values obtained in HeLa cells. Combinational studies of the most

active complex **2**, with pharmacological modulators of cell redox status, L-buthionine-sulfoximine (L-BSO) or N-acetyl-L-cysteine (NAC), showed that when L-BSO potentiated, complex **2** induced a sub-G1 peak of the cell cycle, in the HeLa cell line. Also, the obtained results for the same complex indicated that there is no influence on cell survival, at the same time. In addition to the cytotoxicity studies, UV-vis and cyclic voltammetry were performed in order to investigate the binding mode of the complex **2** to DNA. The results obtained using mutually complement methods suggested an intercalation mode of the complex-DNA interaction.

Keywords: bis(Bipyridine)ruthenium(II) complexes, Crystal structure, Redox properties, Cytotoxicity, Picolinic ligands.

Area of science: Chemistry

Sub-area of science: General and inorganic chemistry

UDC number: 546

SINTEZA, KARAKTERIZACIJA I CITOTOKSIČNOST BIS(BIPIRIDIN) RUTENIJUM(II) KOMPLEKSA SA DERIVATIMA PIKOLINSKE KISELINE

REZIME

Bis(bipiridin)rutenijum(II) kompleksi (**1-5**) opšte formule $[\text{Ru}(\text{L})(\text{bpy})_2]\text{PF}_6$, gde je bpy = 2,2'-bipiridin; **HL** = 3-metilpiridin-2-karboksilna kiselina (**HL1**), 6-metilpiridin-2-karboksilna kiselina (**HL2**), 5-bromopiridin-2-karboksilna kiselina (**HL3**) 6-brompiridin-2-karboksilna kiselina (**HL4**) i piridin-2,4-dikarboksilna kiselina (**HL5**) su sintetisani i potpuno okarakterisani. Za jedinjenja **3**, **4** and **5** urađena je difrakcionom analizom X-zraka na monokristalu. Elektrohemijski karakter kompleksa je ispitivan cikličnom voltametrijom, ukazujući na Ru(II)/Ru(III) transfer elektrona, u opsegu pozitivnih potencijala. Sa druge strane, u opsegu negativnih potencijala, zapaženi su višestruki reverzibilni pikovi koji predstavljaju sukcesivne redukcije bipiridinskog dela. Citotoksično delovanje ovih jedinjenja ispitano je primenom MTT testa nakon 72 h delovanja kompleksa. Dobijeni rezultati ukazuju da kompleksi **2-4** ispoljavaju umerenu aktivnost prema humanoj ćelijskoj liniji grlića materice (HeLa), sa IC_{50} vrednostima (μM): 132.3 ± 5.0 (**2**), 184.0 ± 16.2 (**3**), 147.7 ± 8.0 (**4**). Kompleks **2** ispoljio je aktivnost prema ćelijama kancera debelog creva LS-174 cells (180.9 ± 10.1), dok je aktivnost izostala prema tumorskim ćelijama pluća A549 i netumorskim ćelijskim linijama MRC-5, u opsegu koncentracija do $200 \mu\text{M}$ za komplekse **1-4** i do $300 \mu\text{M}$ za kompleks **5**. Umerena citotoksična aktivnost kompleksa **1-5** je najverovatnije uslovljena brзом disocijacijom liganada pri samom rastvaranju kompleksa pri fiziološkim uslovima. Male varijacije u strukturi koliganda rezultovale

su u promeni IC_{50} vrednosti na HeLa ćelijskoj liniji. Kombinovane studije najaktivnijeg kompleksa **2** sa farmakološkim modulatorima ćelijskog redoks statusa, L-butioninsulfoksaminom (L-BSO) ili N-acetil-L-cisteionom (NAC), pokazale su da u slučaju L-BSO, kompleks **2** izaziva sub-G1 pik u ćelijskom ciklusu, na HeLa linijama. Istovremeno, dobijeni rezultati sa istim kompleksom su pokazali da nema uticaja na ćelijsko preživljavanje. Pored ispitivanja citotoksičnosti, UV-vis spektroskopijom i cikličnom voltametrijom ispitivano je vezivanje kompleksa **2** za DNK. Dobijeni su rezultati koji ukazuju na interkalaciju kompleksa sa DNK.

Ključne reči: bis(bipiridin)rutenijum(II) kompleksi, kristalna struktura, redoks svojstva, citotoksičnost, pikolinato ligandi.

Naučna oblast: Hemija

Uža naučna oblast: Opšta i neorganska hemija

UDK broj: 546

Abbreviations

SAR	structure activity relationship
DNA	Deoxyribonucleic acid
FT-IR	Fourier transform infrared spectroscopy
HPLC	High-performance liquid chromatography
CCDC	Cambridge Crystallographic Data Center
DMSO	dimethyl sulfoxide
PEEK	polyether ether ketone
NAC	N-acetyl-L-cysteine
L-BSO	L-Buthionine-sulfoximine
MTT	3-(4,5-dymethylthiazol-yl)-2,5-diphenyltetrazolium bromide
EtOH	ethanol
PBS	phosphate buffer solution
FACS	fluorescence activated cell sorting
CSD	Cambridge Structural Database
Byp	bipyridine
GSH	glutathione

Contents

1. INTRODUCTION	1
2. GENERAL PART.....	4
2.1. Platinum complexes in treatment of cancer	4
2.2. Other platinum complexes	6
2.3. An alternative to platinum therapy: Ruthenium complexes.....	8
2.4. Ligands and corresponding complexes: Structures and biological features	14
3. EXPERIMENTAL PART.....	21
3.1. Materials and methods for the synthesis and characterization.....	21
3.2. Syntheses.....	21
3.2.1. Synthesis of the starting ruthenium complex, $[\text{RuCl}_2(\text{bpy})_2]$	21
3.2.2. Synthesis of complex 1, $[\text{Ru}(\text{L1})(\text{bpy})_2]\text{PF}_6$	22
3.2.3. Synthesis of complex 2, $[\text{Ru}(\text{L2})(\text{bpy})_2]\text{PF}_6$	23
3.2.4. Synthesis of complex 3, $[\text{Ru}(\text{L3})(\text{bpy})_2]\text{PF}_6$	24
3.2.5. Synthesis of complex 4, $[\text{Ru}(\text{L4})(\text{bpy})_2]\text{PF}_6$	25
3.2.6. Synthesis of complex 5, $[\text{Ru}(\text{L5})(\text{bpy})_2]\text{PF}_6$	26
3.3. X-ray structure determinations.....	28
3.3.1. X-ray analysis of the complexes	28
3.4. Electrochemical measurements.....	32
3.5. Biology tests.....	33
3.5.1. Reagents and cell cultures.....	33
3.5.2. MTT cytotoxicity assay	33
3.5.3. Combinational drug study.....	34
3.5.4. Effects of N-acetyl-L-cysteine (NAC) or L-Buthionine-sulfoximine (L-BSO) on complex 2 - treated HeLa cells in relation to cell survival	34

3.5.5.	Effects of N-acetyl-L-cysteine (NAC) or L-Buthionine-sulfoximine (L-BSO) on complex 2-treated HeLa cells in relation to cell cycle perturbations.....	34
3.6.	DNA-binding studies	35
3.6.1.	UV-vis study	35
3.6.2.	Cyclic voltammetry interaction study	35
4.	RESULTS AND DISCUSSION	38
4.1.	Synthesis and characterization	38
4.2.	Description of the crystal structures.....	39
4.3.	Electrochemical measurements.....	49
4.4.	Results of MTT assay	51
4.5.	Effects of NAC or L-BSO on the cell survival of HeLa cells treated with complex 2	53
4.6.	Interaction of complex 2 with DNA	56
4.6.1.	UV-vis spectroscopy	56
4.6.2.	Cyclic voltammetry.....	57
5.	CONCLUSION.....	61
6.	SUPPLEMENTARY MATERIAL.....	62
7.	Curriculum Vitae	84

1. INTRODUCTION

Precious metals have been used for medicinal purposes for at least 3500 years, when records show that gold was included in a variety of medicines in Arabia and China [1]. In general, metal based drugs have utilized their pathway and future development in the field of inorganic medicine chemistry [2-4]. Since the Rosenberg's discovery of *cisplatin*'s cytotoxicity [5,6], a large number of scientists have been inspired to design unique compounds that would eventually resolve well known limitations of commercial drugs (resistance and side effects) [7]. Among the different transition metal centers that have been exhaustively studied for therapeutic applications, Ru is particularly suitable for the design of metal-based drugs [8]. In the chemical context, Ru forms coordination bonds that are substitutionally inert and consequently Ru complexes are less susceptible to ligand substitution in biological conditions. So far, two Ru complexes (NAMI-A and KP1019) have undergone clinical trials [9,10].

The selection of the ligand system certainly represents the promising base in the design of active metal complex. The ligands moiety can be responsible for redox activity as well as for anticancer activity. It can be also improve the solubility of the complex, reduce toxicity and enhance specificity. Some studies showed how low antitumor activity of the ligand can be improved by coordinating to the metal center [11]. From a strictly chemical point of view, metal-ligand synergism intruded most probably as the main spot in designing the perfect drug structure. Moreover, the ligand carrier may originate from a structure that has a rather specific role in some biological system. In that sense, some authors emphasize the significance of picolinic acid (2-pyridinecarboxylic acid) [12-14]. This six-membered ring molecule is found in mother's milk and has a direct impact on mineral uptake in humans [15]. Beside its wide variety of physiological properties, picolinic acid is also an industrially significant compound. It is used as an active substance in a great number of dietary supplements [16,17]. Picolinic acid and its derivatives are present in the literature as multidentate ligands whose coordination modes rely on two different ligator atoms [18,19].

As modern cancer therapy imposes even more rigid criteria for the final clinical use, the whole metal drug concept is subject to significant change. Thus every extensive study includes the synthetic route followed by structural and electrochemical characterization, *in vitro* and DNA targeting tests as well as examination of protein inhibition.

References of Introduction Part

1. C. Orvig, M. J. Abrams, *Chem. Rev.* **99** (1999) 2201.
2. M. Gielen, E. R. T. Tiekinkin: *Metallotherapeutic Drugs & Metal-based Diagnostic Agents*. Chichester: JohnWiley&Sons, Ltd.; 2005.
3. M. A. Jakupec, M. Galanski, V. B. Arion, C. G. Hartinger, B. K. Keppler, *DaltonTrans.* (2008) 183.
4. G. Gasser, I. Ott, N. Metzler-Nolte, *J. Med. Chem.* **54** (2011) 3.
5. B. Rosenberg, L. VanCamp, T. Krigas, *Nature* **200** (1965) 698.
6. B. Rosenberg, L. VanCamp, J. E. Trosko, V. H. Mansour, *Nature* **222** (1969) 385.
7. Z. H. Siddik, *Oncogene* **22** (2003) 265.
8. A. Habtemariam, M. Melchart, R. Fernandez, S. Parsons, I. D. H. Oswald, A. Parkin, F. P. A. Fabbiani, J. E. Davidson, A. Dawson, R. E. Aird, D. I. Jodrell, P. J. Sadler, *J. Med.Chem.* **49** (2006) 6858.
9. A. Bergamo, G. Sava, *Chem. Soc. Rev.* **44** (2015) 8818.
10. F. Bacher, V. B. Arion, *Elsevier Reference Module in Chemistry, Molecular Sciences and Chemical Engineering*, Elsevier, Waltham, MA, 2014.
11. C. G. Hartinger, N. Metzler-Nolte, P. J. Dyson, *Organometallics* **31** (2012) 5677.
12. J. A. Fernandez-Pol, D. J. Klos, P. D. Hamilton, *Anticancer Res.* **21** (2001) 3773.
13. S. Cai, K. Sato, T. Shimizu, S. Yamabe, M. Hiraki, C. Sano, H. Tomioka, *J. Antimicrob. Chemoth.* **57** (2006) 85.
14. R. S. Grant, S. E. Coggan, G. A. Smythe, *Int. J. Tryptophan Res.* **2** (2009) 71.
15. T. Rebello, B. Lonnerdal, L. S. Hurley, *Am. J. Clin. Nutr.* **35** (1982) 1.
16. T. O. Bemer, M. M. Murphy, R. Slesinski, *Food Chem.Toxicol.* **42** (2004) 1029.
17. M. Peng, X. Yang, *J. Inorg.Biochem.* **146** (2015) 97.
18. A. Perez, L. Hernandez, E. Del Carpio, V. Lubes, *J. Mol. Liq.* **194** (2014) 193.
19. D. M. Steams, W. H. Armstrong, *Inorg. Chem.* **31** (1992) 5178.

2. GENERAL PART

2.1. Platinum complexes in treatment of cancer

cis-Diamminedichloridoplatinum(II) (*cisplatin*) was first described by Peyrone in 1845 [1]. Its activity against cancer was revealed in 1964, when Rosenberg realized that the platinum electrodes in the NH_4Cl solution used in one of his experiments affected bacterial growth [2,3]. The main species responsible for that was found to be *cis*- $[\text{Pt}(\text{NH}_3)_2\text{Cl}_2]$, which was formed slowly by reaction of the electrodes with solution of NH_4Cl . The drug entered clinical trials in 1971 and by the end of 1987 it was already the most widely used as anticancer drug in medicine [4] with anticancer activity against certain types of tumors. Unfortunately, some tumors avoid the action of *cisplatin*, demonstrating intrinsic or acquired resistance. Also, administration of *cisplatin* causes severe side-effects, namely neurotoxicity, ototoxicity, nausea, vomiting, bone marrow dysfunction and nephrotoxicity. In the blood, the high physiological chloride concentration (ca. 100 mM) ensures that the complex remains neutral until it enters the cell. This passage through membrane was thought to occur mainly by passive diffusion, but also active transport by the copper transporter Ctr1p could not be excluded [5]. Once in the cytosol, hydrolysis occurs due to the lower chloride concentration (ca. 4 mM). The mechanism of action includes interaction with DNA which is considered as an ultimate target of *cisplatin* [6]. The DNA coordination sites of *cisplatin* after hydrolysis are, in order of preference, the N7 atom of guanine, the N7 atom of adenine, the N1 adenine, and N3 of cytosine. Bifunctional binding results in chelation and subsequent formation of various adducts in DNA. Intrastrand 1,2-d(GpG) cross-links are the most abundant Pt-DNA adducts (60-65% of the platinum bound to DNA is in that form) [7], followed by intrastrand d(ApG) cross-links (around 20% of the bound platinum). Only about 1.5% of the *cisplatin* was found to be involved in interstrand adducts; some minor DNA-protein cross-links were also can be formed (Figure 1) [8-10].

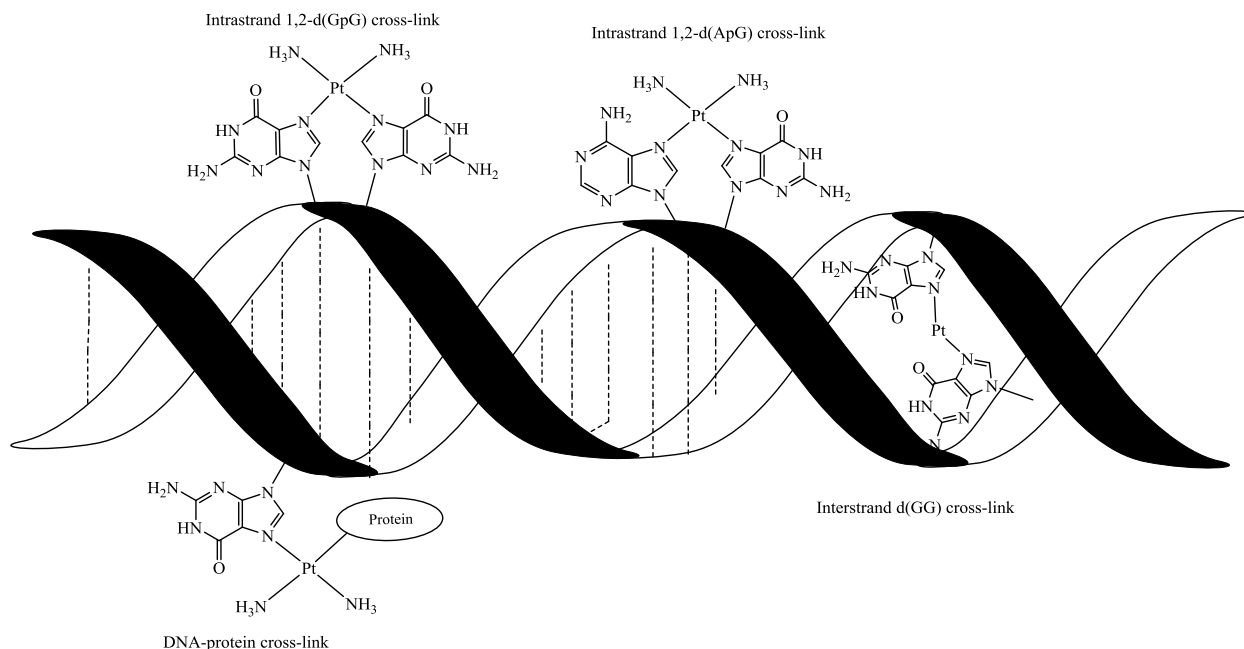


Figure 1. Schematic view of a double-stranded DNA, depicting some of the most commonly occurring Pt-DNA adducts.

This drug has guided the search for new chemical entities to overcome limitations and many other complexes of platinum and other transition metals, besides platinum, were tested to this aim leading to some thousands molecules with varying degrees of success [11-15].

Research has been focused on several fronts. For the design of improved pharmaceuticals it is crucial to understand the transport of the drug in the body, cellular uptake, and its fate inside the cell. The development of synthetic methods rapidly increased the number of compounds that were screened for anticancer activity. Also, since *cisplatin* is definitely effective against certain tumours, studies were also included the avoidance of undesired side effects, with the retention of the therapeutic value of the drug.

Thousands of platinum compounds have been synthesized in an attempt to overcome the problems of *cisplatin*. The observation of the first platinum complex and its efficacies as antitumor agent led to what was called the “structure-activity relationships” (SAR’s). This was a list of structural characteristics that a platinum complex requires in order to show an antitumor activity and the most of the new compounds were designed according to these rules. The most successful of the second-generation platinum compounds is *cis*-diammine-1,1-cyclobutanedicarboxylatoplatinum(II), known as *carboplatin* (Figure 2). It was introduced in clinics in 1986

and its activity is equivalent to *cisplatin* in the treatment of ovarian cancers, however in the treatment of testicular, head and neck cancers *cisplatin* is superior [16,17]. Also, *carboplatin* has less severe side effects than *cisplatin*, but it is cross-resistant with it. Two other second- and third-generation compounds have been approved for clinical use. *cis*-Diammine(glycolato)platinum(II) (*nedaplatin*) [18] was approved in 1995 by the Health and Welfare Ministry in Japan [19] and various studies of combined therapies of the platinum complex with other drugs are undergoing clinical trials for the treatment of urothelial, uterine, lung, esophageal or testicular cancer, amongst others [20-26]. (1*R*,2*R*-Diaminocyclohexane)oxalatoplatinum(II) (*oxaliplatin*) [27] was approved in France and in a few other European countries mainly for the treatment of metastatic colorectal cancer.

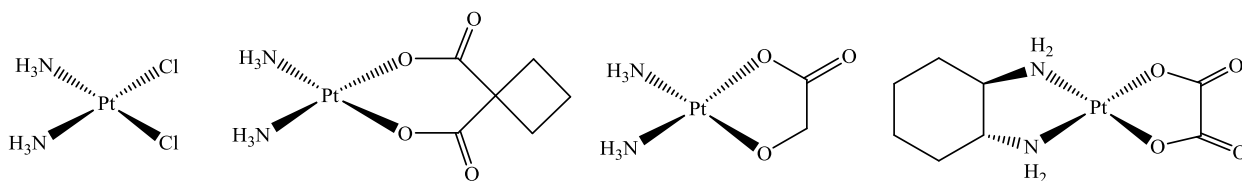


Figure 2. Molecular structure of a few selected platinum drugs: *cisplatin*, *carboplatin*, *nedaplatin* and *oxaliplatin*.

Since it has become evident that mere analogues of *cisplatin* or *carboplatin* would probably not offer any substantial clinical advantages over the existing drugs, as complexes of this kind can be expected to have similar biological consequences to *cisplatin*, some platinum complexes were synthesized despite contradicted the SAR's.

2.2. Other platinum complexes

The design of platinum(IV) complexes yielded a new concept in platinum anticancer therapy. Additional axial preferably lipophilic ligands would facilitate intestinal absorption of the drug, making oral administration possible [28]. Also, they would act as pro-drugs, which get reduced to platinum(II) by intracellular glutathione, ascorbic acid or other reducing agents. The

platinum(II) would bind subsequently to DNA and exert the desired action [29]. The most successful Pt(IV) complex is bis(acetato)amminedichlorido(cyclohexylamine)platinum(IV) (Figure 3), also known as *satraplatin* or JM216. *Satraplatin* also shows *in vivo* oral antitumor activity against a variety of murine and human subcutaneous tumor models, comparable to the activity of *cisplatin*. In addition, it has a relatively mild toxicity profile, being myelosuppression instead of nephrotoxicity the dose-limiting factor [30].

One approach covers so called sterically hindered *cis*-platinum(II) complexes that contain sterically crowded non-leaving groups. For instance, *cis*-amminedichlorido(2-methylpyridine)platinum(II) (ZD0473 or AMD473) was selected for clinical trials [31]. Phase-II clinical trials carried out with lung and metastatic breast cancer patients showed a good tolerability of the drug, but no greater efficacy over existing agents in platinum-resistant patients [32]. Studies are ongoing of combined therapy with liposomal doxorubicin or paclitaxel [33].

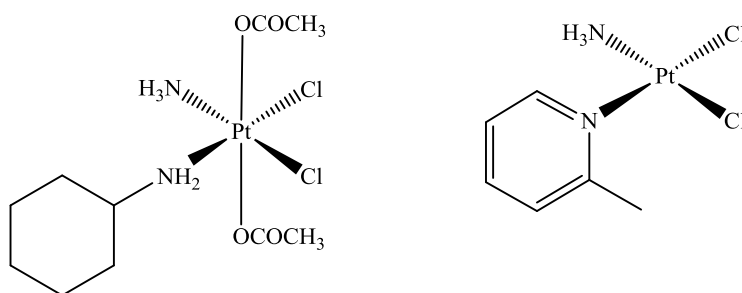


Figure 3. Molecular structure of the anticancer platinum complexes *satraplatin* or JM216 (a Pt (IV) complex, on the left) and ZD0473 (a Pt (II) complex, on the right).

In the search for complexes that followed a different mechanism to *cisplatin* the first SAR-rule, that complex must be of *cis* geometry, was revised. The *trans*-Pt(II) complexes that have been synthesized so far can be divided into several groups that respond to the general formula *trans*-[PtCl₂(L)(L')]. The pioneers were Farrell and his group, with complexes where L = a pyridine as ligand and L' = an ammine, a sulfoxide or a pyridine group [34-38]. Following his example, other groups synthesized more *trans*-Pt(II) complexes, finding in some cases very good anticancer activities. Navarro-Ranninger and her group focused on complexes with L = L' = branched aliphatic amines [39,40]. Gibson and others reported that the replacement of one of *transplatin*'s

ammine ligands by a heterocyclic ligand, such as piperidine, piperazine or 4-picoline, resulted in a radical enhancement of the cytotoxicity [41,42]. Finally the group of Natile and Coluccia synthesized complexes where L = an iminoether ligand and L' = an amine or one more iminoether ligands [43,44] (Figure 4). All these groups have reported that the cytotoxic ability of the above described *trans*-platinum complexes with bulky non-leaving groups is in some cases superior to that shown by *cisplatin*, and often better than the cytotoxicity of their respective *cis*-analogues. These *trans*-complexes are characterized by a spectrum of activity different from *cisplatin* and they often overcome resistance.

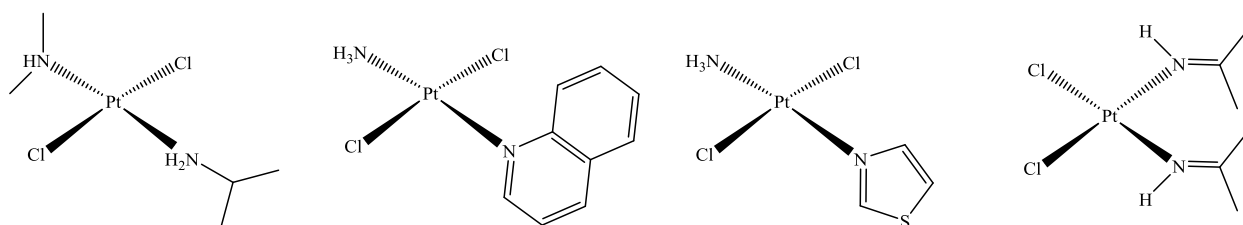


Figure 4. Examples of *trans*-platinum complexes

2.3. An alternative to platinum therapy: Ruthenium complexes

To overcome the limitations of platinum complexes many compounds based on ruthenium have been developed and tested against cancer cell lines [45]. These compounds tend to cause fewer and less severe side effects compared to platinum drugs. Chemistry of ruthenium is well suited towards potential pharmacological applications. Synthetic chemistry of ruthenium is developed; ruthenium tends to form octahedral complexes, which allows two additional ligands comparing with square planar platinum(II) complexes; coordination to different ligand atoms, varying in hardness and electronegativity; and finally availability of different oxidation states, with +2 and +3 being the most interesting. The latest is thought to be reason for less toxicity of ruthenium compounds with hypothesis of activation by reduction. This theory is based on the observation that ruthenium(III) complexes are more inert than ruthenium(II) and the cancer cells are hypoxic in the more chemical reducing environment, than healthy cells. These two factors mean that

compounds of ruthenium can be administered in the (relatively inert) +3 oxidation state, causing minimal damage to healthy cells, but being reduced to the (active) +2 oxidation state in cancer cells [46-50].

In general, two approaches are commonly used for the design of new anticancer compounds. The first one, trial-and-error approach is based on synthesis as many compounds as possible that are similar to a complex of known activity, with the aim to solve its drawbacks. These new compounds are then tested, first *in vitro* followed by *in vivo*. The second approach consists of thorough studies of the properties of some particular complex, that include its chemical, physical, pharmacological properties, the uptake of the drug, its biodistribution and its detoxifying processes with the aim to reach desired activity and overcome drawbacks. This demands multidisciplinary approach in which collaboration from different scientific fields is necessary.

The first generation of ruthenium compounds synthesized for anticancer purposes were structurally similar to *cisplatin*: several ammine and chlorido ligands were coordinated to Ru(II) and Ru(III) to form complexes with general formula $[\text{Ru}(\text{NH}_3)_{6-x}\text{Cl}_x]^{n+}$. Those complexes in which the oxidation state of the ruthenium ion was +2 were targeted DNA in an analogous way to *cisplatin* as the experiments with $[\text{Ru}(\text{NH}_3)_5\text{Cl}]^+$ and $[\text{Ru}(\text{NH}_3)_5(\text{H}_2\text{O})]^{2+}$ confirmed (Figure 5). However, cytotoxicity tests showed poor activity. Interestingly, both *cis*- $[\text{Ru}(\text{NH}_3)_4\text{Cl}_2]^+$ and especially *fac*- $[\text{Ru}(\text{NH}_3)_3\text{Cl}_3]$ displayed a comparable antitumor activity to that of *cisplatin* in a few selected cell lines [51,52]. It has been hypothesized that these complexes, once inside the cell, are reduced to less inert Ru(II) species, which bind to DNA after hydrolysis [53]. The trichloride complex, being the most promising of all these compounds, was discarded for further investigation due to its poor water solubility.

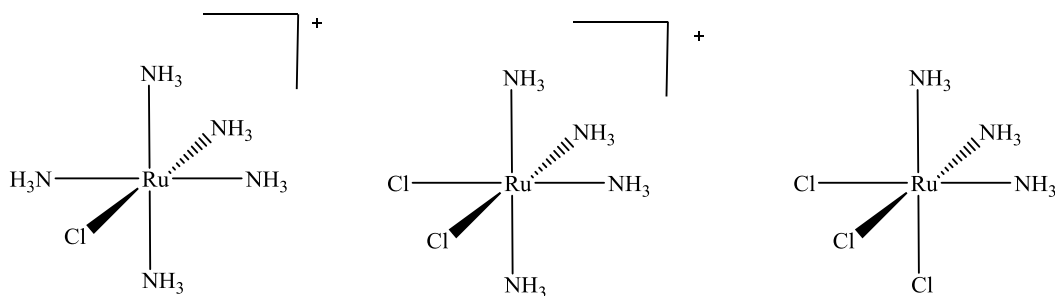


Figure 5. Examples of ammine-chlorido ruthenium complexes, $[\text{Ru}(\text{NH}_3)_5\text{Cl}]^+$, $\text{cis-}[\text{Ru}(\text{NH}_3)_4\text{Cl}_2]^+$ and $\text{fac-}[\text{Ru}(\text{NH}_3)_3\text{Cl}_3]$.

The substitution of the ammine ligands by DMSO molecules yields compounds with improved solubility. Both *cis*- and *trans*- $[\text{Ru}(\text{II})\text{Cl}_2(\text{DMSO})_4]$ (Figure 6) were shown to be able to coordinate to guanine residues of DNA *via* the N7 position with the *trans* complex being more active due to differences in kinetics. In addition, the *trans* isomer also seemed to be able to overcome *cisplatin* resistance, and along with good antimetastatic activity represented an interesting alternative to *cisplatin* [54]. Afterwards, the series of dimethyl sulfoxide-ruthenium complexes were designed, inspired on that promising compound. Noteworthy are the compounds $\text{Na}\{\text{trans-}[\text{Ru}(\text{III})\text{Cl}_4(\text{DMSO})(\text{Him})]\}$, (Him = imidazole), nicknamed NAMI, and the more stable $[\text{H}_2\text{Im}][\text{trans-Ru}(\text{III})\text{Cl}_4(\text{DMSO})(\text{Him})]$, also known as NAMI-A (Figure 6). NAMI-A is the first ruthenium complex to have ever reached clinical testing for anticancer activity. Nowadays, when surgical removal of primary cancers is efficient and successful, a complex such as NAMI-A, which presents an antimetastatic activity in a broad range of tumours including lung metastasis, is becoming of utmost interest [55-57].

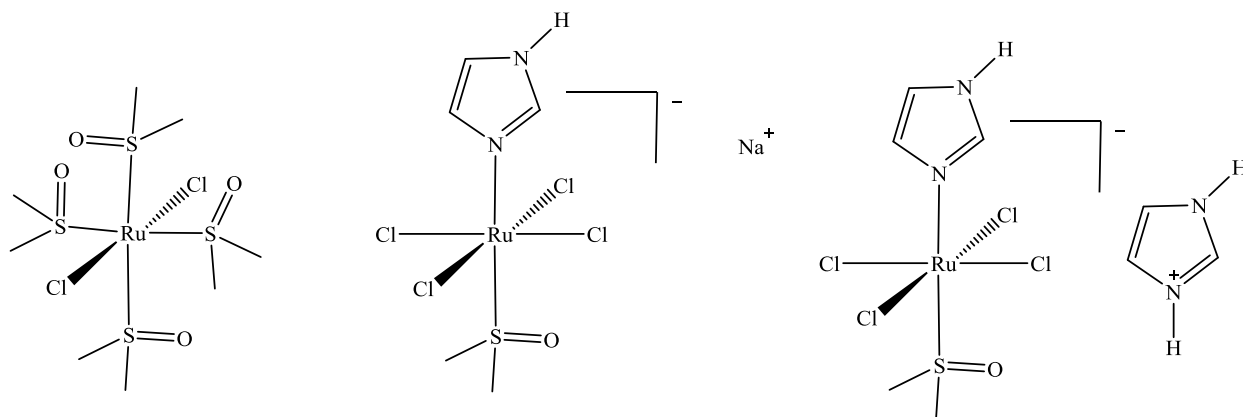


Figure 6. Examples of dimethylsulfoxide complexes. From left to right, *trans*-[Ru(II)(DMSO)₄Cl₂], Na{*trans*-[Ru(III)Cl₄(DMSO)(Him)]} (NAMI) and [H₂Im]{*trans*-[Ru(III)Cl₄(DMSO)(Him)]} (NAMI-A).

The second complex in clinical evaluation comes from Keppler's group [58]. In that research group were prepared the series of anionic ruthenium(III) complexes with monodentate heterocyclic nitrogen donor ligands, the most successful have the formula *trans*-[RuCl₄(L)₂]⁻, where L is imidazole (KP418) or indazole (KP1019 and KP1339), and the counterion (LH)⁺ or Na⁺ (Figure 7). KP1019 and KP1339 were reported effective in inhibiting platinum-resistant colorectal carcinomas in rats [59].

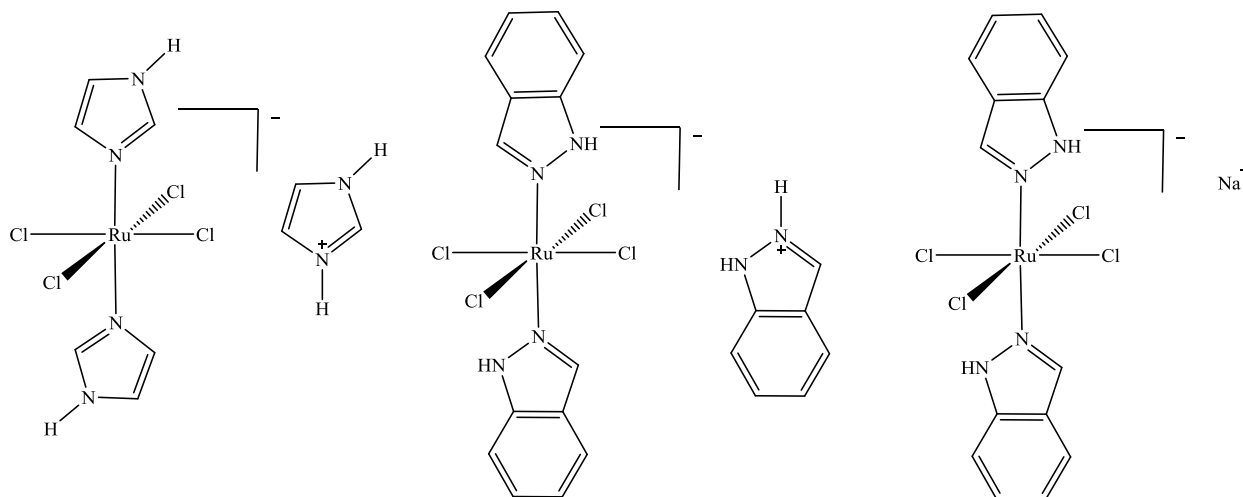


Figure 7. Molecular structure of the ruthenium(III) complexes imidazolium [tetrachloridobis(imidazole)ruthenate(III)] (KP418), indazolium *trans*-[tetrachloridobis(indazole)ruthenate(III)] (KP1019) and sodium *trans*-[tetrachloridobis(indazole)ruthenate(III)] (KP1339).

The mechanism of action of these complexes is thought to differ considerably from that of *cisplatin*. The involvement of the “activation-by-reduction” process and the transferring mediated transport into the cells seem to play a very important role in the efficiency of the “Keppler-type” complexes [60], as in the case of NAMI-A.

Organoruthenium complexes have received considerable attention in recent years, since a large number of applications in supramolecular [61] and medicinal chemistry have been developed with excellent or promising results.

Organoruthenium complexes are appealing in drug design because, like platinum complexes, they exhibit slow rates of ligands dissociation in biological systems, allowing for a more controlled release of active drug since that slow down deactivation of the drug before it reaches target and decrease potential side effects.

In particular, ruthenium arene complexes are substitutionally inert under biological systems [62] and service as an excellent platform for drug development in cancer therapies [63]. Ruthenium-arene-chloride dimeric complexes $[(\eta^6\text{-arene})\text{RuCl}_2]_2$ are good starting materials that could generate variety of ruthenium derivatives to be used as anticancer drugs [64-66]. The complex $[\text{Ru}(\eta^6\text{-}p\text{-cymene})\text{Cl}_2(\text{pta})]$ called RAPTA-C (Figure 8) has been shown to have moderate anticancer activity in various cell lines and an excellent activity against solid metastases and has been pointed out to be the best anticancer complex [67].

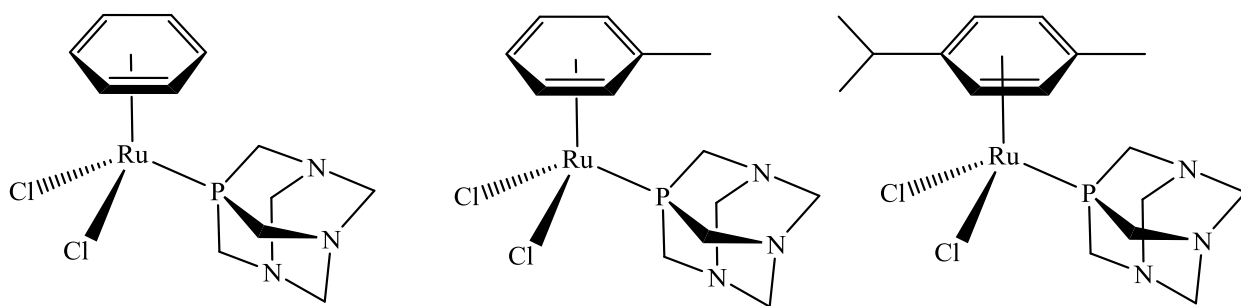


Figure 8. Molecular structure of RAPTA, RAPTA-T and RAPTA-C

Despite in depth *in vitro*, *in vivo* and theoretical studies on the behavior of the potential RAPTA anticancer drugs the mechanism of action of these complexes is not well known, but poor

correlation between the binding of RAPTA complexes to DNA and their cytotoxicity suggested that these potential anticancer drugs act through a mechanism different from the classical platinum anticancer drugs [68]. Organoruthenium systems developed by Sadler *et al.* (Figure 9) have not been shown to be much cytotoxic but they transport into cell intact better than *cisplatin* due to the presence of the lipophilic arene. This group also pointed out chloride dissociation as the limiting factor to the effectiveness of organoruthenium compounds in causing cell death [69,70].

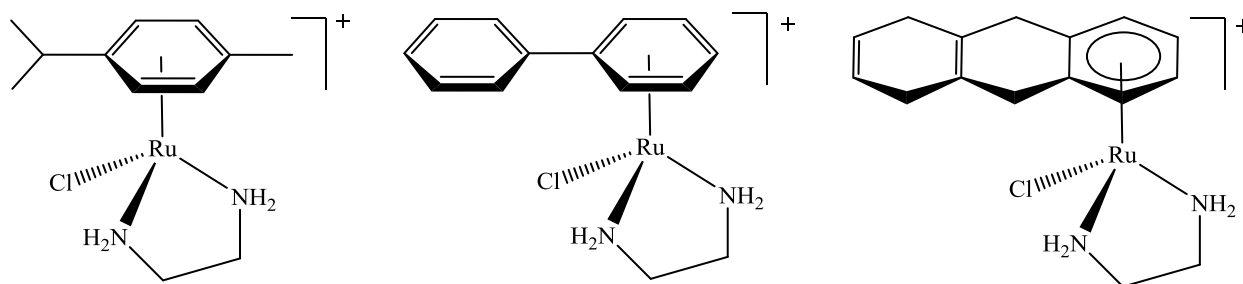


Figure 9. Molecular structure of $[\text{Ru}(\text{arene})\text{enCl}]^+$ complexes

Finally, the complexes that are notable to mention in the light of this dissertation are the ruthenium complexes with pyridine, bipyridine or terpyridine ligands [71]. Ruthenium(II) *tris* bipyridine complex has been thoroughly studied during the last 30 years as a result of their remarkable chemical stability and photophysical properties. These complexes found wide applications in different areas, from solar energy to molecular wires and switches mechanics as well as potential therapeutic agents [72].

Among those ruthenium complexes, compounds bearing a 2,2'-bipyridine moiety are also well recognized, not only as potential drugs but also as highly diverse photochemical and redox systems [73,74]. Thus, the unique combination of (electro)chemical properties makes them very attractive in terms of different potential applications (*e.g.* chemotherapy, catalysis) [75,76].

Several ruthenium polypyridyl complexes were synthesized, and their *in vitro* antitumour activity as well as DNA binding was studied [77,78].

Particularly is interesting application of such types of complexes as intercalation agents. Intercalating molecule have been subjects of many studies because intercalation distorts the helical shape of DNA. To date, many $[\text{RuL}(\text{bpy})_2]^{2+}$ and $[\text{RuL}(\text{phen})_2]^{2+}$ complexes have been described, where L is an aromatic bidentate ligand, which have been proven to interact with DNA *via* intercalation [79-84].

Among the many complexes studied, the ruthenium(II)bis(bipyridine) complex with dipyridophenazine, $[\text{Ru}(\text{bpy})_2(\text{dppz})]^{2+}$ (Figure 10), was demonstrated to have extraordinary properties, notably the ability to act as a “light switch” when bound to DNA [85]. Although such results for $[\text{Ru}(\text{bpy})_2(\text{dppz})]^{2+}$ appeared nearly two decades ago, this complex remains the subject of recent investigations which aim to clarify conditions under which it demonstrates multiple binding modes [86].

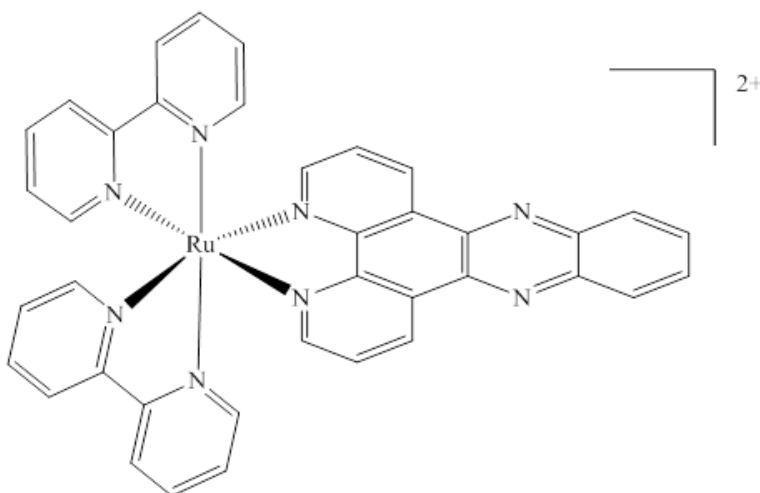


Figure 10. Molecular structure of $[\text{Ru}(\text{bpy})_2(\text{dppz})]^{2+}$

2.4. Ligands and corresponding complexes: Structures and biological features

Pyridinedicarboxylic acids are well known for their biological features. 2,4-Pyridinedicarboxylic acid demonstrated immunosuppressive and fibrosuppressive characteristic and along with 2,5- and 2,6-pyridinedicarboxylic acid acts as inhibition or activation agents for some metalloenzymes [87,88]. Usually, they coordinate to metals in a bidentate manner, *via* pyridine nitrogen and

carboxylate oxygen, leaving another carboxylate group uncoordinated. It is important to mention, ruthenium-cymene complexes with this type of ligands, have been recently reported [89-92].

References of General part

1. M. Peyrone, *Ann. Chemie Pharm.* **51** (1845) 1.
2. B. Rosenberg, L. VanCamp, J. E Trosko, V. H. Mansour, *Nature* **222** (1969) 385.
3. B. Rosenberg, L. VanCamp, T. Krigas, *Nature* **205** (1965) 698.
4. S. Dasari, P. B. Tchounwou, *Eur. J. Pharmacol.* (2014) 364.
5. S. Ishida S, J. D. J. Thiele, I. I. Herskowitz, *Proc. Natl. Acad. Sci. USA*, **99** (2002) 14298.
6. E. R. Jamieson, S. J. Lippard, *Chem. Rev.* **99** (1999) 2467.
7. A. M. Fichtinger-Schepman, J. L. van der Veer, J. H. den Hartog, P. H. Lohman, J. Reedijk, *Biochemistry* **24** (1985) 707.
8. A. Eastman, *Biochemistry* **25** (1986) 3912.
9. K. B. Lee, D. Wang, S. J. Lippard, P. A. Sharp, *Proc. Natl. Acad. Sci. USA* **99** (2002) 4239.
10. L. J. Naser, A. L. Pinto, S. J. Lippard, J. M. Essigmann, *Biochemistry* **27** (1988) 4357.
11. M. A. Fuertes, J. Castilla, C. Alonso, J. M. Pérez, *Curr. Med. Chem. Anti-Cancer Agents* **2** (2002) 2539.
12. M. Galanski, M. J. Jakupec, B. K. Keppler, *Curr. Med. Chem.* **12** (2005) 2075.
13. G. Momekov, A. Bakalova, M. Karaivanova, *Curr. Med. Chem.* **12** (2005) 2177.
14. I. Ott, R. Gust, *Archiv der Pharmazie - Chemistry in Life Sciences* **340** (2007) 117.
15. G. Gasser, I. Ott, N. Metzler-Nolte, *J. Med. Chem.* **54** (2011) 3.
16. V. Brabec, J. Kasparkova, *Drug Resist.* **8** (2005) 131.
17. N. Thatcher, M. Lind, *Semin. Oncol.* **17** (1990) 40.
18. D. S. Alberts, S. Green, E. V. Hannigan, R. Otoole, D. Stocknovack, P. Anderson, E. A. Surwit, V. K. Malvlya, W. A. Nahhas, C. L. Jolles, *J. Clin. Oncol.* **10** (1992) 706.
19. N. Uchida, Y. Takeda, H. Kasai, R. Maekawa, K. Sugita, T. Yoshioka, *Anticancer Res.* **18** (1998) 3375.
20. D. Lebowitz, R. Canetta, *Eur. J. Cancer* **34** (1998) 1522.
21. Y. Hasegawa, S. Takanashi, K. Okudera, M. Aoki, K. Basaki, H. Kondo, T. Takahata, N. Yasui-Furukori, T. Tateishi, Y. Abe, K. Okumura, *Jpn. J. Clin. Oncol.* **34** (2004) 647.
22. S. Kawase, T. Okuda, M. Ikeda, S. Ishihara, Y. Itoh, S. Yanagawa, T. Ishigaki, *Gynecol. Oncol.* **102** (2006) 493.

23. E. I. Takaoka, K. Kawai, S. Ando, T. Shimazui, H. Akaza, *Jpn. J. Clin. Oncol.* **36** (2006) 60.
24. Y. Sato, T. Takayama, T. Sagawa, T. Okamoto, K. Miyanishi, T. Sato, H. Araki, S. Iyama, S. Abe, K. Murase, R. Takimoto, H. Nagakura, M. Hareyama, J. Kato, C. Y. Niitsu, *Cancer Chemother. Pharmacol.* **58** (2006) 570.
25. T. Shirai, T. Hirose, M. Noda, K. Ando, H. Lshida, T. Hosaka, T. Ozawa, K. Okuda, T. Ohnishi, T. Ohmori, N. Horichi, M. Adachi, *Lung Cancer* **52** (2006) 181.
26. N. Shinohara, T. Harabayashi, S. Suzuki, K. Nagao, S. Nagamori, H. Matsuyama, K. Naito, K. Nonomurh, *J. Clin. Oncol.* **21** (2006) 236.
27. J. L. Misset, *Br. J. Cancer* **77** (1998) 4.
28. L. R. Kelland, G. Abel, M. J. McKeage, M. Jones, P. M. Goddard, M. Valenti, B. A. Murrer, K. R. Harrap, *Cancer Res.* **53** (1993) 2581.
29. S. Choi, C. Filotto, M. Bisanzo, S. Delaney, D. Lagasee, J. L. Whitworth, A. Jusko, C. R. Li, N.A. Wood, J. Willingham, A. Schwenker, K. Spaulding, *Inorg.Chem.* **37** (1998) 2500.
30. H. Choy, C. Park, M. Yao, *Clin. Can. Res.* **14** (2008) 1633.
31. J. Holford, S. Y. Sharp, B. A. Murrer, M. Abrams, L. R. Kelland, *Br. J. Cancer* **77** (1998) 366.
32. J. Treat, J. Schiller, E. Quoix, A. Mauer, M. Edelman, M. Modiano, P. Bonomi, R. Ramlau, E. Lemarie, *Eur. J. Cancer* **38** (2002) 13.
33. K. A. Gelmon, D. Stewart, K. N. Chi, S. Chia, C. Cripps, S. Huan, S. Janke, D. Ayers, D. Fry, J. A. Shabbits, W. Walsh, L. McIntosh, L.K. Seymour, L. K., *Ann. Oncol.* **15** (2004) 1115.
34. U. Bierbach, Y. Qu, T. W. Hambley, J. Peroutka, H. L. Nguyen, M. Doedee, N. Farrell, *Inorg. Chem.* **38** (1999) 3535.
35. N. Farrell, T. T. B. Ha, J. P. Souchard, F. L. Wimmer, S. Cros, N. P. Johnson, *J. Med. Chem.* **32** (1989) 2240.
36. M. VanBeusichem, N. Farrell, *Inorg. Chem.* **31** (1992) 634.
37. N. Farrell, L. R. Kelland, J. D. Roberts, M. VanBeusichem, *Cancer Res.* **52** (1992) 5065.
38. Y. Zou, B. van Houten, N. Farrell, *Biochemistry* **32** (1993) 9632.

39. E. I. Montero, S. Diaz, A. M. Gonzalez-Vadillo, J. M. Perez, C. Alonso, C. Navarro-Ranninger, *J. Med. Chem.* **42** (1999) 4264.
40. E. I. Montero, J. M. Perez, A. Schwartz, M.A. Fuertes, J. M. Malinge, C. Alonso, M. Leng, C. Navarro-Ranninger, *ChemBioChem* **3** (2002) 61.
41. J. Kasparikova, V. Marini, Y. Najajreh, D. Gibson, V. Brabec, *Biochemistry* **42** (2003) 6321.
42. J. Kasparikova, O. Novakova, V. Marini, Y. Najajreh, D. Gibson, J. M. Perez, V. Brabec, *J. Biol. Chem.* **278** (2003) 47516.
43. M. Coluccia, A. Nassi, F. Loseto, A. Boccarelli, M. A. Mariggio, D. Giordano, F. P. Intini, P. Caputo, G. Natile, *J. Med. Chem.* **36** (1993) 510.
44. A. Boccarelli, F. P. Intini, R. Sasanelli, M. F. Sivo, M. Coluccia, G. Natile, *J. Med. Chem.* **49** (2006) 829.
45. M. J. Clarke, *Coord. Chem. Rev.* **236** (2003) 209.
46. R. Pettinari, C. Pettinari, F. Marchetti, C. M. Clavel, R. Scopelliti, P. J. Dyson, *Organometallics* **32** (2013) 309.
47. A. L. Noffke, A. Habtemariam, A. M. Pizarro, P. J. Sadler, *Chem. Commun.* **48** (2012) 5219.
48. I. Bratsos, E. Mitri, F. Ravalico, E. Zangrando, T. Gianferrara, A. Bergamo, E. Alessio, *Dalton Trans.* **41** (2012) 7358.
49. T. Gianferrara, I. Bratsos, E. Alessio, *Dalton Trans.* 2009 7588.
50. S. M. Meier, M. Hanif, Z. Adhireksan, V. Pichler, M. Novak, E. Jirkovsky, M. A. Jakupec, V. B. Arion, C. A. Davey, B. K. Keppler, C. G. Hartinger, *Chem. Sci.* **4** (2013) 1837.
51. M. J. Clarke, M. Buchbinder, A. D. Kelman, *Inorg. Chim. Acta* **27** (1978) 87.
52. M. J. Clarke, S. Bitler, D. Rennert, M. Buchbinder, A. D. Kelman, *J. Inorg. Biochem.* **12** (1980) 79.
53. M. J. Kendrick, M. T. May, M. J. Plishka, K. D. Robinson, *Metals in biological systems*. Chichester, 1992.
54. K. H. Antman, *Oncologist* **6** (2001) 1.
55. E. Alessio, G. Mestroni, G. Nardin, W. M. Attia, M. Calligaris, G. Sava, S. Zotzet, *Inorg. Chem.* **27** (1988) 4099.

56. M. Coluccia, G. Sava, F. Loseto, A. Nassi, A. Boccarelli, D. Giordano, E. Alessio, G. Mestroni, *Eur. J. Cancer* **129** (1993) 1873.
57. A. Bergamo, B. Gava, E. Alessio, G. Mestroni, B. Serli, M. Cocchietto, S. Zorzet, G. Sava, *Int. J. Oncol.* **21** (2002) 1331.
58. C. A. Smith, A. J. Sutherland-Smith, B. K. Keppler, F. Kratz, E. N. Baker, *J. Biol. Inorg. Chem.* **1** (1996) 424.
59. S. Kapitza, M. Pongratz, M. A. Jakupec, P. Heffeter, W. Berger, L. Lackinger, B. K. Keppler, B. Marian, *J. Cancer Res. Clin. Oncol.* **131** (2005) 101.
60. L. Messori, P. Orioli, D. Vullo, E. Alessio, E. Iengo, *Eur. J. Biochem.* **267** (2000) 1206.
61. M. J. Chow, W. H. Ang, *Inorganic and Organometallic Transition Metal Complexes with Biological Molecules and Living Cells*, 2017, 119.
62. A. M. Pizarro, A. Habtemariam, P. J. Sadler, *Top. Organomet. Chem.* **32** (2010) 21.
63. M. Patra, T. Joshi, V. Pierroz, K. Ingram, M. Kaiser, S. Ferrari, B. Spingler, J. Keiser, G. Gasser, *Chem. Eur. J.* **19** (2013) 14768.
64. H. L. Bozec, D. Touchard, P. H. Dixneuf, *Organometallic Chemistry of Arene Ruthenium and Osmium Complexes* **29** (1989) 163.
65. R. A. Zelonka, M. C. Baird, *Can. J. Chem.* **50** (1972) 3063.
66. M. A. Bennett, A. K. Smith, *J. Chem. Soc. Dalton Trans.* (1974) 223.
67. C. Scolaro, A. Bergamo, L. Brescacin, R. Delfino, M. Cocchietto, G. Laurenczy, T. J. Geldbach, G. Sava, P. J. Dyson, *J. Med. Chem.* **48** (2005) 4161.
68. P. Nowak-Sliwinska, J. R. van Beijnum, A. Casini, A. A. Nazarov, G. Wagnieres, H. van den Bergh, P. J. Dyson, A. W. Griffioen, *J. Med. Chem.* **54** (2011) 3895.
69. F. Y. Wang, A. Habtemariam, E. P. L. van der Geer, R. Fernandez, M. Melchart, R. J. Deeth, R. Aird, S. Guichard, F. P. A. Fabbiani, P. Lozano-Casal, I. D. H. Oswald, D. I. Jodrell, S. Parsons, P. J. Sadler, *Proc. Natl. Acad. Sci. U. S. A.* **102** (2005) 18269.
70. Y. Fu, A. Habtemariam, A. M. Pizarro, S. H. van Rijt, D. J. Healey, P. A. Cooper, S. D. Shnyder, G. J. Clarkson, P. J. Sadler, *J. Med. Chem.* **53** (2010) 8192.
71. I. Kostova, *Curr. Med. Chem.* **13** (2006) 1085.
72. X. Gong, P. King Ng, W. Kin Chan, *Advanc. Mat.* **10** (1998) 1337.

73. S. Bellinger-Buckley, T. Chang, S. Bag, D. Schweinfurth, W. Zhou, B. Torok, B. Sarkar, M. Tsai, J. Rochford, *Inorg. Chem.* **53** (2014) 5556.
74. Y. Zhang, L. Lai, P. Cai, G. Cheng, X. Xu, Y. Liu, *New J. Chem.* **39** (2015) 5805.
75. J. Q. Wang, P. Y. Zhang, L. N. Ji, H. Chao, *J. Inorg. Biochem.* **146** (2015) 89.
76. H. Ohtsu, K. Tanaka, *Angew. Chem.* **51** (2012) 9792-9795.
77. A. Rilak, I. Bratsos, E. Zangrando, J. Kljun, I. Turel, T. D. Bugarčić, E. Alessio, *Inorg. Chem.* **53** (2014) 6113.
78. D. Lazić, A. Arsenijević, R. Puchta, T. D. Bugarčić, A. Rilak, *Dalton Trans.* **45** (2016) 4633.
79. A. E. Friedman, J. C. Chambron, J. P. Sauvage, N. J. Turro, J. K. Barton, *J. Am. Chem. Soc.* **112** (1990) 4960.
80. R. J. Morgan, S. Chatterjee, A. D Baker, T. C. Strekas, *Inorg. Chem.* **30** (1991) 2687.
81. A. E. Friedman, C. V. Kumar, N. J. Turro, J. K. Barton, *Nucleic Acids Res.* **19** (1991) 2595.
82. R. M. Hartshorn, J. K. Barton, *J. Am. Chem. Soc.* **114** (1992) 5919.
83. F. Gao, H. Chao, F. Zhou, Y. X. Yuan, B. Peng, L. N. Ji, *J. Inorg. Biochem.* **100** (2006) 1487.
84. F. Gao, H. Chao, F. Zhou, L. C. Xu, K. C. Zheng, L. N. Ji, *Helv. Chim. Acta* **90** (2007) 36.
85. A. J. Bryan, A. P. de Silva, S. A. de Silva, R. A. D. D. Rupasinghe, K. R. A. S. Sandanayake, *Biosensors*, **4** (1989) 169.
86. A. J. McConnell, H. Song, J. K. Barton, *Inorg. Chem.* **52** (2013) 10131.
87. C. Dette, H. Waertzig, H. Uhl, *Pharmazie* **48** (1993) 276.
88. B. L. Martin, *Arch. Biochem. Biophys.* **345** (1997) 332.
89. S. Grgurić-Šipka, I. Ivanović, G. Rakić, N. Todorović, N. Gligorijević, S. Radulović, V. B. Arion, B. K. Keppler, Ž. Lj. Tešić, *Eur. J. Med. Chem.* **45** (2010) 1051.
90. I. Ivanović, S. Grgurić-Šipka, G. Rakić, N. Gligorijević, S. Radulović, A. Roller, Ž. Lj. Tešić, B. K. Keppler, *J. Serb. Chem. Soc.* **76** (2011) 53.
91. I. Ivanović, K. K. Jovanović, N. Gligorijević, S. Radulović, V. B. Arion, K. S. A. M. Sheweshein, Ž. Lj. Tešić, S. Grgurić-Šipka, *J. Organomet. Chem.* **749** (2014) 343.
92. N. Gligorijević, S. Arandelović, L. Filipović, K. Jakovljević, R. Janković, S. Grgurić-Šipka, I. Ivanović, S. Radulović, Ž. Lj. Tešić, *J. Inorg. Biochem.* **108** (2012) 53.

3. EXPERIMENTAL PART

3.1. Materials and methods for the synthesis and characterization

All experiments were performed under atmospheric conditions with commercially available chemicals and solvents used as received. In particular, ligands **HL1-5** were purchased from Sigma Aldrich. The starting complex, $[\text{RuCl}_2(\text{bpy})_2]$ was synthesized according to a previously described but slightly modified synthetic route [1,2].

Elemental analysis was performed on an Elemental Vario EL III microanalyzer and the results are presented within Tables 1-6. A Nicolet 6700 FT-IR spectrometer was used for recording infrared spectra. Signal intensities were reported with wavenumbers and denoted by the following abbreviations: vs = very strong, s = strong, m = medium, w = weak. LTQ Orbitrap XL Mass Spectrometer (Heated ESI) was used for recording all mass spectra in acetonitrile (HPLC grade) in a positive mode. The obtained peaks were assigned and interpreted according to dimensionless mass/charge ratio. ^1H NMR spectra were recorded on a Bruker Avance III 500 spectrometer in DMSO with TMS as the reference. For proton assignments, following abbreviations were used: (br) s = (broad) singlet, d = doublet, dd = doublet of doublets, t = triplet, q = quartet, p = pentet, m = multiplet (m) and Ar = aromatic protons. A rough estimation of the compounds' melting points was done using an electrothermal melting point apparatus.

3.2. Syntheses

3.2.1. Synthesis of the starting ruthenium complex, $[\text{RuCl}_2(\text{bpy})_2]$

The synthesis was performed according to a slightly modified method of Sullivan-a [1]. $\text{RuCl}_3 \cdot x\text{H}_2\text{O}$ (1.30 g, 5 mmol), 2,2'-bipyridine (1.56 g, 10 mmol) and LiCl (2.1 g, 50 mmol) were added in 12.5 mL DMF and refluxed for 8 h with stirring. Afterwards, the solution was cooled to room temperature and 100 mL of a mixture of acetone/water (1:1) was added. A green-black solid was separated by filtration. The solid was added into 100 mL water and stirred for 10

h at r.t. followed by filtration. The product was then washed three times with 12.5 mL of water and ether.

The yield was 80% based on the ruthenium salt; IR (cm^{-1}): 3491.4(w), 3098.9(w), 3068.5(w), 3037.6(w), 1604.4(m), 1450.4(m), 1417.3(m), 1261.4(m), 1014.3(m), 762.0(s).

Table 1. Elemental analysis of the starting ruthenium complex.

Element	Anal. calcd for $\text{C}_{20}\text{H}_{16}\text{N}_4\text{Cl}_2\text{Ru}\cdot 1.5 \text{H}_2\text{O}$ (%)	Found (%)
C	47.72	47.89
H	3.80	3.59
N	11.13	11.13

3.2.2. Synthesis of complex **1**, $[\text{Ru}(\text{L1})(\text{bpy})_2]\text{PF}_6$

$[\text{RuCl}_2(\text{bipy})_2]$ (100 mg, 0.21 mmol) was dissolved in ethanol (15 mL) and stirred for 20 min at 40 °C. The ligand, 3-methylpyridine-2-carboxylic acid, **HL1** (28.3 mg, 0.21 mmol) was dissolved in a small volume of ethanol (5 mL) and added to the solution of the starting complex. In the following 3 hours the reaction mixture was stirred under reflux and afterwards left to cool to room temperature. After adding an equimolar amount of a counterion, NH_4PF_6 (33.7 mg, 0.21 mmol), dark red precipitate was isolated by filtration. The crude product was washed with a small amount of water and diethyl ether.

(1): Yield: 71 %. ^1H NMR (500 MHz, DMSO-d_6): δ 8.81 (dd, 2H, Ar), 8.75-8.69 (m, 3H, Ar), 8.16 (q, 2H, Ar), 7.98 (p, 2H, Ar), 7.83-7.78 (m, 4H, Ar), 7.64 (t, 1H, Ar), 7.54 (br s, 1H, Ar), 7.39-7.33 (m, 4H, Ar), 2.67 (s, 3H, $-\text{CH}_3$). ^{13}C NMR (125.80 MHz, DMSO-d_6): 171.86 (C=O),

157.41, 156.98, 151.37, 150.74, 140.79, 139.18, 136.81, 136.66, 136.40, 135.53, 127.46, 127.30, 126.97, 126.89, 126.53, 124.12, 123.76, 123.67, 123.46, 56.01, 19.45 and 18.54 ($-\text{CH}_3$). IR (cm^{-1}): 3423.2 (w), 1645.0 (s), 1446.8 (m), 1333.6 (m), 1268.0 (w), 1239.1 (w), 839.8 (vs), 766.2 (s), 730.7 (w), 558.2 (s). ESI-MS (m/z , (relative abundance, %)): 550.08 [$\text{M}^+ - \text{PF}_6^-$, 100]. M.p.: above 300 °C.

Table 2. Elemental analysis of the complex **1**.

Element	Anal. calcd for $\text{C}_{27}\text{H}_{22}\text{N}_5\text{O}_2\text{RuPF}_6 \cdot 0.5 \text{H}_2\text{O}$ (%)	Found (%)
C	46.09	45.55
H	3.30	3.44
N	9.95	9.53

3.2.3. Synthesis of complex **2**, $[\text{Ru}(\text{L}2)(\text{bpy})_2]\text{PF}_6$

$[\text{RuCl}_2(\text{bipy})_2]$ (100 mg, 0.21 mmol) was dissolved in ethanol (15 mL) and stirred for 20 min at 40 °C. The ligand, 6-methylpyridine-2-carboxylic acid, **HL2** (28.3 mg, 0.21 mmol) was dissolved in a small volume of ethanol (5 mL) and added to solution of the starting complex. In the following 3 hours the reaction mixture was stirred under reflux and afterwards left to cool to room temperature. After adding an equimolar amount of a counterion, NH_4PF_6 (33.7 mg, 0.21 mmol), dark red precipitate was isolated by filtration. The crude product was washed with a small amount of water and diethyl ether.

(2): Yield: 65 %. ^1H NMR (500 MHz, DMSO-d_6): δ 8.82 (br t, 2H, Ar), 8.19 (br t, 2H, Ar), 8.08 (br s, 1H, Ar), 7.99 (sept, 2H, Ar), 7.94–7.85 (m, 4H, Ar), 7.82–7.78 (m, 2H, Ar), 7.62 (br t, 2H,

Ar), 7.50-7.30 (m, 4H, Ar), 1.68 (s, 3H, -CH₃). ¹³C NMR (125.80 MHz, DMSO-d₆): 172.03 (C=O), 157.71, 157.43, 157.31, 153.70, 151.95, 151.07, 148.92, 137.94, 137.89, 136.72, 135.23, 129.04, 127.84, 127.42, 127.14, 126.83, 125.41, 125.37, 124.49, 123.83, 123.42, 23.62 (-CH₃). IR (cm⁻¹): 3089.3 (w), 1650.4 (m), 1604.0 (m), 1466.8 (m), 1450.0 (m), 1159.3 (w), 840.5 (vs), 766.6 (s), 557.3 (s). ESI-MS (*m/z*, (relative abundance, %)): 550.08 [M⁺-PF₆⁻, 100]. M.p.: above 300 °C.

Table 3. Elemental analysis of the complex **2**.

Element	Anal. calcd for C ₂₇ H ₂₂ N ₅ O ₂ RuPF ₆ (%):	Found (%)
C	46.69	46.33
H	3.19	3.28
N	10.08	9.84

3.2.4. Synthesis of complex **3**, [Ru(L3)(bpy)₂]PF₆

[RuCl₂(bipy)₂] (100 mg, 0.21 mmol) was dissolved in ethanol (15 mL) and stirred for 20 min at 40 °C. The ligand, 5-bromopyridine-2-carboxylic acid (41.7 mg, 0.21 mmol), **HL3** was dissolved in a small volume of ethanol (5 mL) and added to solution of the starting complex. In the following 3 hours the reaction mixture was stirred under reflux and afterwards left to cool to room temperature. After adding an equimolar amount of a counterion, NH₄PF₆ (33.7 mg, 0.21 mmol), dark red precipitate was isolated by filtration. The crude product was washed with a small amount of water and diethyl ether. Recrystallization of the amorphous product from an EtOH-ACN mixture gave deep red crystals suitable for X-ray analysis.

(3): Yield: 63 %. ^1H NMR (500 MHz, DMSO- d_6): δ 8.82 (t, 2H, Ar), 8.74 (br q, 2H, Ar), 8.68 (d, 2H, Ar), 8.21 (p, 4H, Ar), 8.11 (d, 1H, Ar), 8.06-7.95 (m, 1H, Ar), 7.87 (dd, 1H, Ar), 7.80 (t, 1H, Ar), 7.64 (t, 1H, Ar), 7.55 (d, 1H, Ar), 7.51 (s, 1H, Ar), 7.38 (br t, 2H, Ar). ^{13}C NMR (125.80 MHz, DMSO- d_6): 170.63 (C=O), 158.53, 157.47, 157.18, 156.95, 152.36, 151.49, 137.12, 137.03, 135.84, 127.68, 127.48, 127.02, 126.72, 124.29, 124.04, 123.97, 123.80, 123.58. IR (cm^{-1}): 3080.5 (w), 1647.5 (s), 1603.4 (m), 1447.1 (m), 1373.7 (w), 1327.4 (w), 1160.5 (w), 1027.2 (w), 840.8 (vs), 767.9 (s), 727.5 (m), 556.0 (s), 506.1 (w). ESI-MS (m/z , (relative abundance, %)): 615.97 [$\text{M}^+\text{-PF}_6^-$, 100]. M.p.: above 300 °C.

Table 4. Elemental analysis of the complex **3**.

Element	Anal. calcd for $\text{C}_{26}\text{H}_{19}\text{N}_5\text{O}_2\text{RuBrPF}_6$ (%):	Found (%)
C	41.12	40.75
H	2.52	2.63
N	9.22	9.38

3.2.5. Synthesis of complex 4, $[\text{Ru}(\text{L4})(\text{bpy})_2]\text{PF}_6$

$[\text{RuCl}_2(\text{bipy})_2]$ (100 mg, 0.21 mmol) was dissolved in ethanol (15 mL) and stirred for 20 min at 40 °C. The ligand, 6-bromopyridine-2-carboxylic acid **HL4** (41.7 mg, 0.21 mmol) was dissolved in a small volume of ethanol (5 mL) and added to solution of the starting complex. In the following 3 hours the reaction mixture was stirred under reflux and afterwards left to cool to room temperature. After adding an equimolar amount of a counterion, NH_4PF_6 (33.7 mg, 0.21 mmol), dark red precipitate was isolated by filtration. The crude product was washed with a

small amount of water and diethyl ether. Recrystallization of the amorphous product from an EtOH-ACN mixture gave deep red crystals suitable for X-ray analysis.

(4): Yield: 38 %. ^1H NMR (500 MHz, DMSO- d_6): δ 8.84 (t, 2H, Ar), 8.76-8.71 (m, 2H, Ar), 8.65 (dd, 2H, Ar), 8.39 (t, 1H, Ar), 8.33 (d, 1H, Ar), 8.26-8.20 (m, 1H, Ar), 8.09-7.78 (m, 4H, Ar), 7.68 (t, 1H, Ar), 7.43 (d, 1H, Ar), 7.38 (t, 1H, Ar), 7.34 (t, 1H, Ar), 7.27 (t, 1H, Ar), 7.17 (d, 1H, Ar). ^{13}C NMR (125.80 MHz, DMSO- d_6): 171.18 (C=O), 157.94, 157.35, 153.19, 152.32, 151.59, 149.35, 139.94, 138.59, 138.52, 137.14, 137.03, 136.88, 135.58, 134.22, 127.56, 127.13, 126.80, 126.54, 125.95, 123.97, 123.85, 123.61, 123.52. IR (cm^{-1}): 3091.3 (w), 1647.4 (m), 1604.9 (w), 1449.8 (m), 840.9 (vs), 766.2 (s), 556.8 (m). ESI-MS (m/z , (relative abundance, %)): 615.97 [M^+ - PF_6^- , 100]. M.p.: above 300 °C.

Table 5. Elemental analysis of the complex **4**.

Element	Anal. calcd for $\text{C}_{26}\text{H}_{19}\text{N}_5\text{O}_2\text{RuBrPF}_6$ (%):	Found (%)
C	41.12	40.83
H	2.52	2.75
N	9.22	9.22

3.2.6. Synthesis of complex **5**, $[\text{Ru}(\text{L5})(\text{bpy})_2]\text{PF}_6$

$[\text{RuCl}_2(\text{bipy})_2]$ (100 mg, 0.21 mmol) was dissolved in ethanol (15 mL) and stirred for 20 min at 40 °C. The ligand, 2,4-pyridinedicarboxylic acid **HL5** (35 mg, 0.21 mmol) was dissolved in a small volume of ethanol (5 mL) and added to solution of the starting complex. In the

following 3 hours the reaction mixture was stirred under reflux and afterwards left to cool to room temperature. After adding an equimolar amount of a counterion, NH_4PF_6 (33.7 mg, 0.21 mmol), dark red precipitate was isolated by filtration. The crude product was washed with a small amount of water and diethyl ether.

(5): Yield: 74 %. ^1H NMR (500 MHz, DMSO-d_6): 8.84-8.81 (*m*, 2H, Ar-H), 8.76 (*t*, 2H, Ar-H), 8.69 (*d*, 1H, Ar-H), 8.25 (*d*, 1H, Ar-H), 8.19 (*t*, 2H, Ar-H), 8.02 (*p*, 2H, Ar-H), 7.97 (*d*, 1H, Ar-H), 7.84-7.78 (*m*, 3H, Ar-H), 7.72 (*d*, 1H, Ar-H), 7.62-7.60 (*m*, 2H, Ar-H), 7.39 (*p*, 2H, Ar-H). IR (cm^{-1}): 3089 (w), 1605 (m), 1469 (m), 1450 (m), 1315 (w), 1161 (w), 1030 (w), 840 (s), 767 (s), 727 (w), 556 (m). ESI-MS (*m/z*, (relative abundance, %)): 580.05 [$\text{M}^+\text{-PF}_6^-$, 100]. M.p.: above 300 °C.

Table 6. Elemental analysis of the complex **5**.

Element	Anal. calcd for $\text{C}_{27}\text{H}_{20}\text{N}_5\text{O}_4\text{RuPF}_6 \cdot 0.5\text{H}_2\text{O}$ (%):	Found (%)
C	44.21	43.83
H	2.89	2.87
N	9.55	9.59

3.3. X-ray structure determinations

3.3.1. X-ray analysis of the complexes

For the reported structures, X-ray intensity data were collected, at 100 K, on an Agilent Supernova Dual Source (Cu at zero) diffractometer equipped with an Atlas CCD detector using ω scans and CuK α ($\lambda = 1.54184 \text{ \AA}$) radiation. The images were interpreted and integrated with the program CrysAlisPro (Rigaku Oxford Diffraction) [3]. Using Olex2 [4], the structures were solved by direct methods using the ShelXS structure solution program and refined by full-matrix least-squares on F^2 using the ShelXL program package [5]. Non-hydrogen atoms were anisotropically refined and the hydrogen atoms in the riding mode and isotropic temperature factors fixed at 1.2 times $U(\text{eq})$ of the parent atoms (1.5 times $U(\text{eq})$ for methyl and hydroxyl groups). The hydrogen atoms of the solvent water molecule and the pyridine-2-carboxylate-4-carboxylic acid carboxyl group were located from a difference Fourier electron density map and restrained refined with isotropic temperature factors fixed at 1.5 times $U(\text{eq})$ of the parent atoms. CCDC 1482372-1482373 and 1524673 contain the supplementary crystallographic data for this paper and can be obtained free of charge via www.ccdc.cam.ac.uk/conts/retrieving.html (or from the Cambridge Crystallographic Data Centre, 12, Union Road, Cambridge CB2 1EZ, UK; fax: +44-1223-336033; or deposit@ccdc.cam.ac.uk). Crystal data and structure refinement for the complexes **3**, **4** and **5**, are shown in the Tables 7, 8, 9.

Table 7. Crystal data and structure refinement for the complex **3**.

Empirical formula	C ₂₆ H ₁₉ N ₅ O ₂ RuBrPF ₆
Formula weight	851.54
Temperature (K)	100
Crystal system	Monoclinic
Space group	<i>P</i> 2 ₁ / <i>n</i>
<i>a</i> (Å)	11.0258(2)
<i>b</i> (Å)	14.1182(3)
<i>c</i> (Å)	20.8563(5)
α (°)	90
β (°)	92.332(2)
γ (°)	90
<i>V</i> (Å ³)	3243.90(12)
<i>Z</i>	4
ρ_{calc} (g cm ⁻³)	1.744
μ (Cu-K α , mm ⁻¹)	6.531
<i>F</i> (000)	1704
<i>h,k,l</i>	15,17,19
<i>N</i> _{ref}	6531
<i>R</i> _{int}	0.0731
<i>R</i> ₁	0.0368
<i>wR</i> ₂	0.0993
Reflections collected	31031
Θ (max)	75.255

Table 8. Crystal data and structure refinement for the complex **4**.

Empirical formula	C ₂₆ H ₁₉ N ₅ O ₂ RuBrPF ₆
Formula weight	759.40
Temperature (K)	100
Crystal system	Monoclinic
Space group	<i>I</i> 2/A
<i>a</i> (Å)	18.0576(9)
<i>b</i> (Å)	18.0576(9)
<i>c</i> (Å)	21.4772(13)
α (°)	90
β (°)	109.681(6)
γ (°)	90
<i>V</i> (Å ³)	5213.9(5)
<i>Z</i>	8
ρ_{calc} (g cm ⁻³)	1.935
μ (Cu-K α , mm ⁻¹)	7.977
<i>F</i> (000)	2992
h,k,l	22,17,26
<i>N</i> _{ref}	5079
<i>R</i> _{int}	0.0440
<i>R</i> ₁	0.0462
<i>wR</i> ₂	0.1368
Reflections collected	14143
Θ (max)	75.762

Table 9. Crystal data and structure refinement for the complex **5**.

Empirical formula	C ₂₇ H ₂₂ F ₆ N ₅ O ₅ PRu
Formula weight	742.54
Temperature (K)	100
Crystal system	Monoclinic
Space group	<i>P2₁/n</i>
<i>a</i> (Å)	12.4042(3)
<i>b</i> (Å)	14.3080(5)
<i>c</i> (Å)	15.9245(5)
α (°)	90
β (°)	98.475(3)
γ (°)	90
<i>V</i> (Å ³)	2795.41(15)
<i>Z</i>	4
ρ_{calc} (g cm ⁻³)	1.764
μ (Cu-K α , mm ⁻¹)	5.895
<i>F</i> (000)	1488
<i>h,k,l</i>	15,17,19
<i>N</i> _{ref}	5603
<i>R</i> _{int}	0.0520
<i>R</i> ₁	0.0427
<i>wR</i> ₂	0.1077
Reflections collected	17213
Θ (max)	75.501

3.4. Electrochemical measurements

Electrochemical measurements were performed with a CHI-760B instrument at room temperature. A three electrode system consisted of a boron doped diamond electrode (Windsor Scientific Ltd, Slough, Berkshire, United Kingdom) embedded in a polyether ether ketone (PEEK) body with an inner diameter of 3 mm, a resistivity of 0.075 Ω cm and a boron doping level of 1000 ppm (as declared by the supplier) used as working electrode, a non-aqueous Ag/AgCl electrode used as the reference electrode and a platinum wire that was used as a counter electrode in the potential range of -2.3 V to 1.0 V. For the purpose of experiments, 1.0 mM solutions of the synthesized complexes in DMSO were prepared and TBAP was added as a supporting electrolyte. Cyclic voltammograms were obtained at 20 mV s^{-1} for **1-4**; 50 , 100 , 150 , 200 , 300 , 500 mV s^{-1} for **4**.

For the complex **5** the voltammetric measurement was performed in a three-electrode cell, which consisted of a glassy carbon electrode (Model 6.1204.300), an auxiliary platinum electrode with large surface area (Model CHI221, cell top including platinum wire counter electrode) and an Ag/AgCl reference electrode (Model CHI111). Cyclic voltammograms were obtained at 20 mV s^{-1} for 25 , 50 , 100 , 150 , 200 and 300 mV s^{-1} .

3.5. Biology tests

3.5.1. Reagents and cell cultures

Human cervical adenocarcinoma (HeLa), human alveolar basal adenocarcinoma (A549), human colon cancer (LS-174), human chronic myelogenous leukaemia (K562) and human fetal lung fibroblast (MRC-5) cell lines were maintained as a monolayer culture in the Roswell Park Memorial Institute (RPMI) 1640 nutrient medium (Sigma Aldrich). The nutrient medium was supplemented with 10% heat inactivated fetal calf serum (FCS) (Sigma Aldrich), 4-(2-hydroxyethyl)piperazine-1-ethanesulfonic acid (HEPES) (25 mM), penicillin (100 units/mL), streptomycin (200 $\mu\text{g/mL}$), and L-glutamine (3 mM). Cells were maintained as a monolayer culture in tissue culture flasks (Thermo Scientific NuncTM), in an incubator at 37 °C, in a humidified atmosphere composed of 5% CO₂.

3.5.2. MTT cytotoxicity assay

The antiproliferative activity of the tested complexes was determined using the 3-(4,5-dimethylthiazol-yl)-2,5-diphenyltetrazolium bromide (MTT, Sigma Aldrich) assay [6]. Cells were seeded into 96-well cell culture plates (Thermo Scientific NuncTM), in number of 4000 c/w (HeLa), 5000 c/w (K562), 7000 c/w (LS-174 and MRC-5) and 8000 c/w (A549), in 100 μL of culture medium. After 24 h of growth, cells were exposed to the serial dilutions of tested agents. Stock solutions were prepared immediately prior to use by dissolving in dimethyl sulfoxide (DMSO), so that the DMSO content did not exceed 1% (v/v). The antiproliferative effect of the complexes and ligand was evaluated in a range of concentrations up to 200 μM , for 72 h of continuous drug action. After the treatment, 20 μL of MTT solution, 5 mg/mL in phosphate buffer solution (PBS), pH 7.2, was added to each well. The samples were incubated for 4 h at 37 °C with 5% CO₂ in humidified atmosphere. Formazan crystals were dissolved in 100 μL of 10% sodium dodecyl sulfate (SDS). The absorbance was recorded on a microplate reader (ThermoLabsystems Multiskan EX 200e240 V) after 24 h at a wavelength of 570 nm. The IC₅₀

value (μM) was defined as the concentration of a drug which produces 50% inhibition of cell survival and was determined based on the cell survival diagrams.

3.5.3. Combinational drug study

Reagents N-acetyl-L-cysteine (NAC) and L-Buthionine-sulfoximine (L-BSO) were purchased from Sigma-Aldrich. NAC and L-BSO were dissolved in a physiological saline solution, at a final concentration of 30 mM, and sterilized by filtration (0.2 μm pore-size filters). The stock solutions were wrapped in foil and kept at $-20\text{ }^{\circ}\text{C}$.

3.5.4. Effects of N-acetyl-L-cysteine (NAC) or L-Buthionine-sulfoximine (L-BSO) on complex **2** - treated HeLa cells in relation to cell survival

In the combinational study, L-Buthionine-sulfoximine (L-BSO) or N-acetyl-L-cysteine (NAC) was used in pre-treatment with the selected complex **2**. Briefly, HeLa cells were pre-treated with subtoxic concentrations of L-BSO (1 μM) or NAC (20 μM) for 3 h, and after washing out, the treatment continued with tested complex **2** alone, applied in selected concentrations (50, 100, 200 μM). Viability of HeLa cells, after 72 h of continual treatment with the tested complex **2** alone, or in combination with NAC (20 μM)/L-BSO (1 μM), was measured by MTT (3-(4,5-dimethylthiazol-2-yl)-2,5-diphenyltetrazolium bromide) assay, as previously described.

3.5.5. Effects of N-acetyl-L-cysteine (NAC) or L-Buthionine-sulfoximine (L-BSO) on complex **2** -treated HeLa cells in relation to cell cycle perturbations

Cell cycle phase distribution analysis was performed by flow-cytometry of the DNA content in fixed HeLa cells, after staining with propidium iodide (PI) [7]. The cells were seeded at a density of 2×10^5 cells/well in 6-well plates and growth in nutrition medium. After 24 h, the cells were exposed to NAC (20 μM) or L-BSO (1 μM) for 3 h, and after washing out, the cells were continually exposed to the investigated complex **2** for 48 h with IC_{50} (132 μM) concentration. Control cells were incubated only in nutrient medium. After 48 h of continual

treatment, the cells were collected by trypsinization, washed twice with ice-cold PBS, and fixed for 30 min in 70% EtOH. After fixation, the cells were washed again with PBS, and incubated with RNaseA (1 mg/mL) for 30 min at 37 °C. The cells were then stained with PI (at concentration of 400 µg/mL) 15 min before flow-cytometric analysis. Cell cycle phase distributions were analyzed using a fluorescence activated cell sorting (FACS) Calibur Becton Dickinson flow cytometer and Cell Quest computer software.

3.6. DNA-binding studies

DNA (isolated from salmon testes) was purchased from Sigma Aldrich. The studies were performed for complex **2**.

3.6.1. UV-vis study

The absorption titration measurements were performed using a Varian spectrophotometer in the wavelength range from 300-800 nm. The complex concentration was fixed at 20 ppm in PBS at pH 7, and titration was done with different aliquots of DNA standard solution to make DNA concentrations of 0, 20, 50, 100, 150 and 250 ppm. After preparing complex-DNA solutions they were allowed to incubate for 5 min at room temperature before the adsorption spectra were recorded.

3.6.2. Cyclic voltammetry interaction study

Cyclic voltammetry measurements were done in the same concentration range 0-250 ppm of the DNA presented in the phosphate buffer solution of the 20 ppm of complex **2**. The voltammetric measurements were performed using a potentiostat/galvanostat (AUTOLAB PGSTAT 302 N, Metrohm Autolab B.V., The Netherlands) controlled by the corresponding electrochemical software (NOVA 1.9). The cell (10 mL) consisted of a three-electrode system, a boron-doped diamond electrode (Windsor Scientific Ltd, Slough, Berkshire, United Kingdom)

embedded in a polyether ether ketone (PEEK) body with an inner diameter of 3 mm, a resistivity of $0.075 \Omega \text{ cm}$ and a boron doping level of 1000 ppm (as declared by the supplier) as a working electrode, an Ag/AgCl (saturated KCl) as a reference electrode and a Pt wire as a counter electrode. All potentials reported in this paper are referred *versus* the Ag/AgCl (saturated KCl) reference electrode. Also, all experiments were done at ambient temperature after 5 min of incubation period.

References of Experimental Part

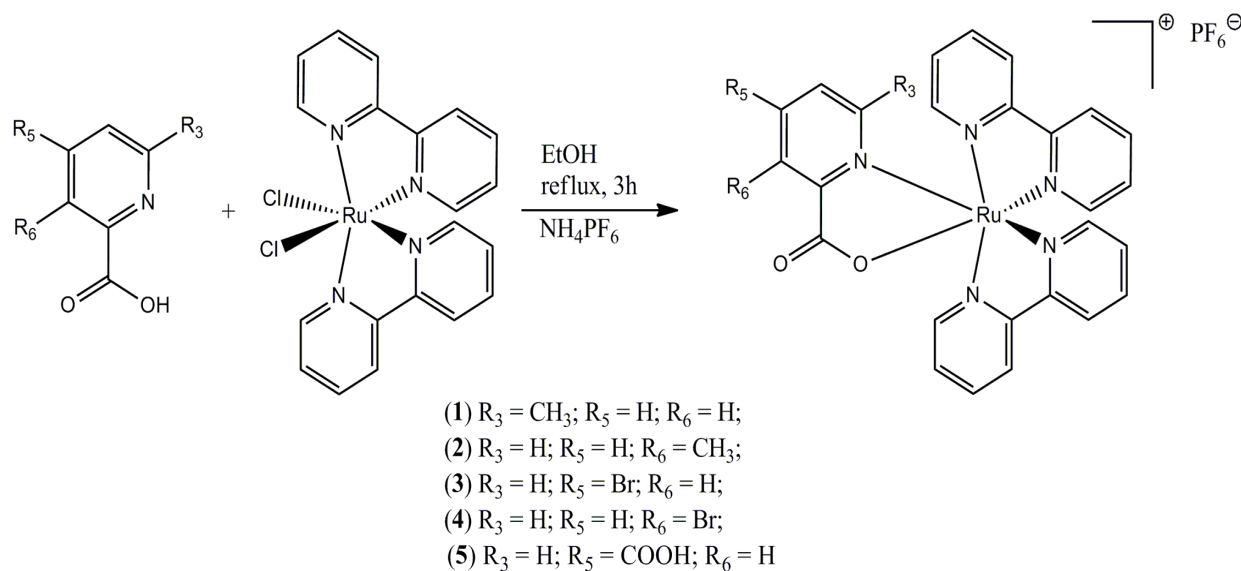
1. B. P. Sullivan, D. J. Salmon, T. J. Meyer, *Inorg. Chem.* **17** (1978) 3334.
2. A. Savić, A. A. Baroud, S. Grgurić-Šipka, *Maced. J. Chem. Chem. En.* **33** (2014) 59.
3. Rigaku Oxford Diffraction. *CrysAlis PRO*. Rigaku Oxford Diffraction, Yarnton, England. (2015).
4. O. V. Dolomanov, L. J. Bourhis, R. J. Gildea, J. A. K. Howard, H. Puschmann, *OLEX2: a complete structure solution, refinement and analysis program. J. Appl. Crystallogr.* **42** (2009) 339.
5. G. M. Sheldrick. A short history of *SHELX*, *Acta Cryst.* **A64** (2008) 112.
6. R. Supino. *In Vitro Toxicity Testing Protocols*, S. O'Hare, C.K. Atterwill (Eds), pp. 137, Humana Press, New Jersey (1995).
7. M. G. Ormerod. *Flow Cytometry, a Practical Approach*, M. G. Ormerod (Eds), 3rd Edn, pp. 119, Oxford University Press, New York (1994).

4. RESULTS AND DISCUSSION

4.1. Synthesis and characterization

The general procedure of all the synthesized complexes included dissolving of the metal precursor and equimolar amount of the ligand in ethanol (Scheme 1).

The reaction mixture was refluxed for 3 h and then left to cool to room temperature. After adding the appropriate amount of NH_4PF_6 to the solution, the intensive color change from dark purple to dark red was observed. Isolated amorphous precipitate was rinsed with a small amount of water and diethyl ether. Obtained compounds were air stable and showed no traces of decomposition. Concerning their solubility, complexes **1-5** were soluble in some polar (*e.g.*, DMSO, CHCl_3 , CH_2Cl_2 , CH_3CN) and nonsoluble in apolar solvents with a significant remark for **1** and **2**, which are very soluble in water.



Scheme 1: Synthesis of $[\text{RuL}(\text{bpy})_2]\text{PF}_6$ complexes **1-5**.

IR spectra of synthesized complexes **1-5**, generally revealed an asymmetric stretching vibration that originates from the C=O bond and is located between 1645.0 and 1650.4 cm^{-1} (1645.0 cm^{-1} for complex **1**; 1650.4 cm^{-1} for complex **2**; 1647.5 cm^{-1} for complex **3**; 1647.4 cm^{-1} for complex **4**). The coordination of the metal center *via* oxygen is suggested by comparison to the band of the free carboxylic group at $\sim 1700 \text{ cm}^{-1}$ in the spectra of the corresponding ligand(s). The very intensive vibration found at 840 cm^{-1} is assigned to C-H stretching modes.

In the ESI-MS spectra of **1-5** recorded in acetonitrile, the $[\text{M}^+-\text{PF}_6^-]$ signal was detected (at m/z : 550.08 for complexes **1** and **2**; 615.97 for complexes **3** and **4**; 580.05 for complex **5**)

As for ^1H NMR assignation, all products share a common structural feature, *i.e.* aromatic protons originating from pyridine and bipyridyl moieties. In the ^1H NMR spectra of **1** and **2**, the CH_3- group in position 3 and 6, show well-defined singlets at 2.67 and 1.68 ppm, respectively. In the ^1H NMR spectrum of the complex **5**, carboxylic protons were not detected because the co-ligand is coordinated to ruthenium through the oxygen atom of the carboxylic group in position 2 of the pyridine ring, while the carboxylic group in position 4 was deprotonated in DMSO.

In the ^{13}C NMR spectra of complexes **1-4** all aromatic carbons were detected in the range: 158.53-123.42 ppm, while the carbons from C=O group were detected at 171.86 ppm (**1**), 172.03 ppm (**2**), 170.63 (**3**), 171.18 (**4**).

4.2. Description of the crystal structures

The complex **3** crystallized in the monoclinic centro-symmetric space group $P2_1/n$ and the asymmetric unit contains one $[\text{Ru}(5\text{-bromopyridine-2- carboxylate})(\text{bpy})_2]^+$ complex cation, one PF_6^- counter anion and two ethanol solvent molecules. The Ru^{2+} ion is coordinated by five N-atoms and one O-atom and the coordination environment around the Ru^{2+} center can be described as a distorted octahedron. The Ru-N(bpy) distances in the range of 2.042(2)-2.058(3) Å, while the Ru-N(L) and Ru-O distances are 2.070(2) Å and 2.095(2) Å, respectively (Figure 11, Table 10).

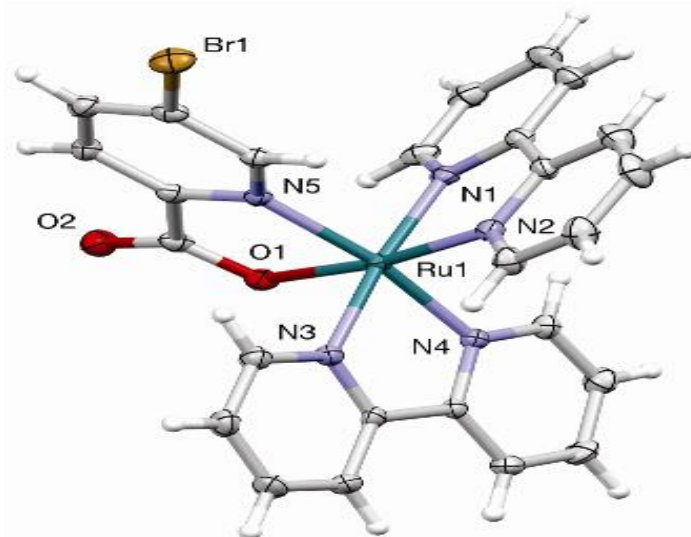


Figure 11. Molecular structure of the cation of complex **3**, showing thermal displacement ellipsoids at the 50% probability level and atom labeling scheme of the hetero-atoms. The PF_6^- counter anion and two solvent EtOH molecules are omitted for clarity.

The pairs of pyridine rings in the two bpy ligands are almost planar and show dihedral angles of $4.01(16)^\circ$ and $1.70(15)^\circ$, respectively (between least-squares planes through the respective rings).

The pyridine bromine atom forms C-Br $\cdots\pi$ interactions with the symmetry-equivalent pyridine ring N3/C11-C15 (C-Br \cdots centroid distance of $3.6545(14)$ Å).

In the packing, several π - π stacking interactions are observed between the five pyridine rings (centroid \cdots centroid distances in the range of $3.7820(18)$ - $5.9751(18)$ Å). Additionally, C-H $\cdots\pi$ interactions are observed between C29(H) and pyridine ring N1/C1-C5 (C(H) \cdots centroid distances of $3.508(4)$ Å).

The crystal packing is stabilized by several hydrogen bonds, i.e. between the 5-bromopyridine-2-carboxylate O2 atom and an ethanol solvent molecule ($\text{O3(H)}\cdots\text{O2} = 2.723(4)$ Å), between the two ethanol solvent molecules ($\text{O4(H)}\cdots\text{O3} = 2.874(4)$ Å) and a longer hydrogen bond between the 5-bromopyridine-2-carboxylate Br1 atom and the latter ethanol molecule ($\text{O4(H)}\cdots\text{Br1} = 3.466(3)$ Å) (Figure 12).

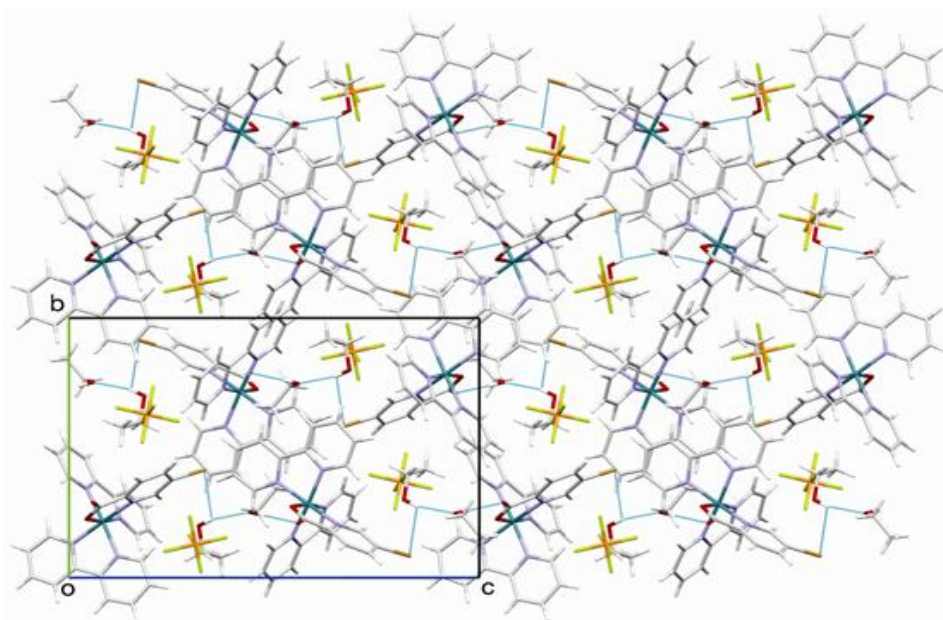


Figure 12. Packing in the crystal structure of complex **3**, along the a-axis. Hydrogen bonds, formed between bromine and carboxylate oxygen atoms of the 5-bromopyridine-2-carboxylate and ethanol solvent molecules, are indicated.

The compound **4** crystallized in the monoclinic centro-symmetric space group $I2/a$ and the asymmetric unit contains one $[\text{Ru}(6\text{-bromopyridine-2-carboxylate})(\text{bpy})_2]^+$ complex cation and one PF_6^- counter anion. Analogous to complex **3**, the Ru center is coordinated in a distorted octahedral manner, by five N-atoms and one O-atom, with the Ru-N(bpy) distances in the range of 2.046(4)-2.056(4) Å, which is comparable with symmetrical $\text{Ru}(\text{bpy})_3$ complexes in the Cambridge Structural Database (CSD, Version 5.37, 2016) [1], while the Ru-N(L) distance is longer (2.123(4) Å) and the Ru-O distance is 2.077(4) Å (Figure 13, Table 11).

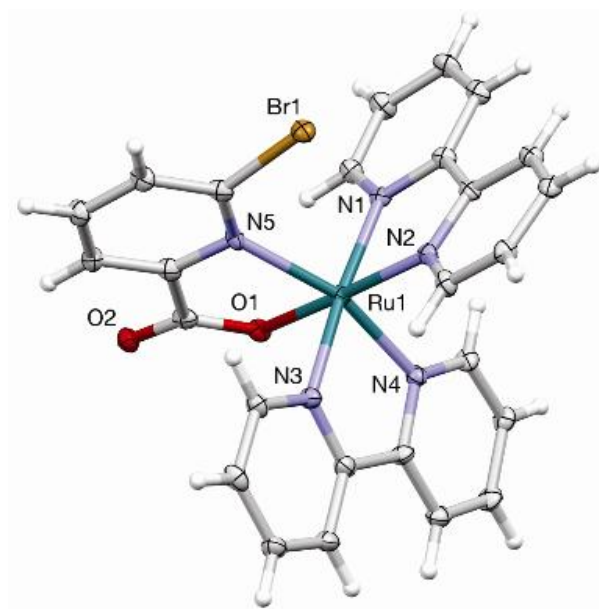


Figure 13. Molecular structure of the cation of complex **4**, showing thermal displacement ellipsoids at the 50% probability level and atom labeling scheme of the hetero-atoms. The PF_6^- counter anion is omitted for clarity.

The pairs of pyridine rings in the two bpy ligands are also almost planar and show dihedral angles of $4.6(3)^\circ$ and $5.7(3)^\circ$, respectively (between least-squares planes through the respective rings).

The pyridine bromine atom forms $\text{C-Br}\cdots\pi$ interactions with pyridine ring N2/C6-C10 and the symmetry-equivalent pyridine ring N3/C11-C15 (C-Br \cdots centroid distance of $3.477(2)$ Å and $3.887(2)$ Å, respectively).

In the packing, several π - π stacking interactions are observed between the five pyridine rings (centroid \cdots centroid distances in the range of $4.276(3)$ - $5.866(3)$ Å).

Additionally, C-H $\cdots\pi$ interactions are observed between C5(H) and C12(H) and pyridine rings (C(H) \cdots centroid distances of $3.729(6)$ Å and $3.553(6)$ Å, respectively).

Table 10. Selected bond lengths (Å) and angles (°) for compound **3**

Selected bond lengths(Å)	3
Ru1-N1	2.055(3)
Ru1-N2	2.042(3)
Ru1-N3	2.070(3)
Ru1-N4	2.058(3)
Ru1-N5	2.069(3)
Ru1-O1	2.095(2)
Selected bond angles(°)	3
N2-Ru1-N5	94.72(10)
N2-Ru1-N3	97.81(11)
N2-Ru1-N4	96.18(10)
N2-Ru1-N1	79.15(11)
N5-Ru1-O1	79.83(10)
N5-Ru1-N3	96.24(10)
N3-Ru1-O1	89.62(10)
N4-Ru1-O1	89.74(10)
N4-Ru1-N3	78.85(10)
N1-Ru1-O1	93.87(10)
N1-Ru1-N5	89.31(10)
N1-Ru1-N4	96.14(10)

Table 11. Selected bond lengths (Å) and angles (°) for compound **4**.

Selected bond lengths(Å)	4
Ru1-N1	2.046(4)
Ru1-N2	2.056(4)
Ru1-N3	2.053(4)
Ru1-N4	2.048(4)
Ru1-N5	2.123(4)
Ru1-O1	2.077(4)
Selected bond angles(°)	4
N2-Ru1-N5	103.36(16)
N2-Ru1-N3	98.65(17)
N2-Ru1-N4	92.75(16)
N2-Ru1-N1	78.96(16)
N5-Ru1-O1	79.68(14)
N5-Ru1-N3	90.34(16)
N3-Ru1-O1	87.35(16)
N4-Ru1-O1	85.15(15)
N4-Ru1-N3	79.50(17)
N1-Ru1-O1	94.80(15)
N1-Ru1-N5	94.67(16)
N1-Ru1-N4	95.97(16)

The compound **5** crystallized in the centro-symmetric space group $P2_1/n$, with one $[\text{RuL}(\text{bpy})_2]\text{PF}_6$ complex in the asymmetric unit, together with one water solvent molecule (Figure 14). The Ru(II) ion is octahedrally coordinated by four nitrogen atoms from the two bipyridine ligands, and one nitrogen and one oxygen atom from the pyridine-2-carboxylate-4-carboxylic acid. In fact, while the coordinating carboxyl group in position 2 of the 2,4-dicarboxylic acid ligand is deprotonated, the other carboxyl group in position 4 is clearly protonated. The Ru(II)-N_{bpy} distances are in the range of 2.031(4)-2.055(4) Å, while the Ru(II)-N_L and Ru(II)-O_L distances are 2.049(3) Å and 2.090(3) Å, respectively. The N-Ru-N/O angles vary between 79.07(13)° and 99.05(13)°.

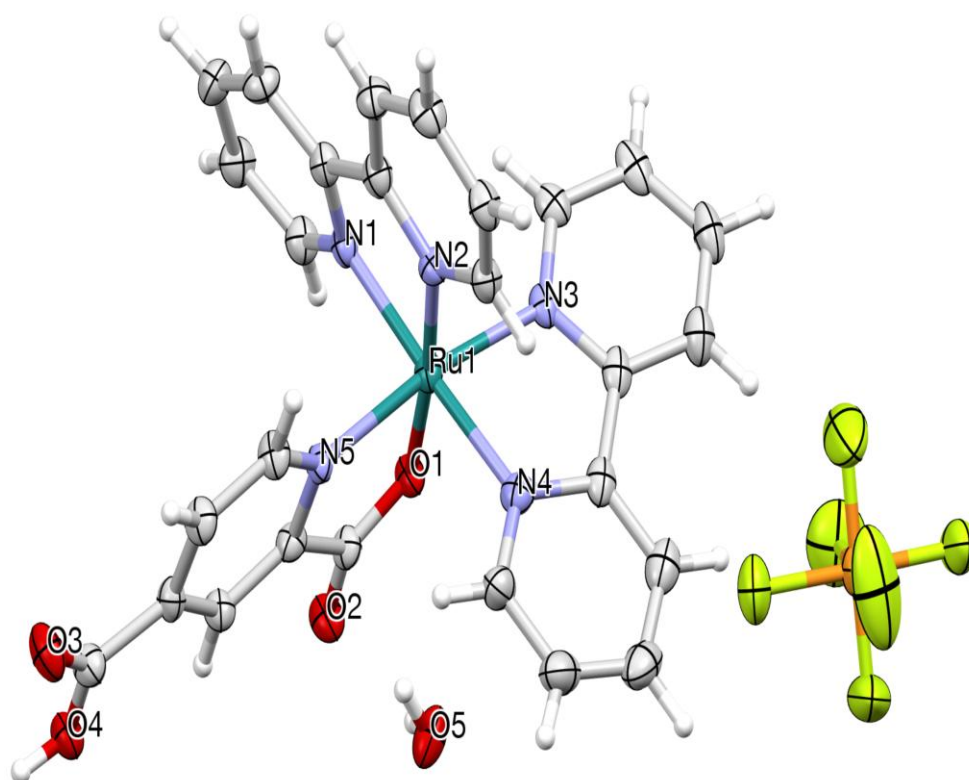


Figure 14. Asymmetric unit of the crystal structure of complex **5**, consisting of one $[\text{RuL}(\text{bpy})_2]\text{PF}_6$ complex and one water solvent molecule, with atom-labeling scheme of the hetero-atoms (except for the PF_6^- ion). Thermal displacement ellipsoids are drawn at the 50% probability level.

In the crystal packing, hydrogen bonds are formed between the pyridine-2-carboxylate-4-carboxylic acid groups and the water solvent molecule. Each water molecule forms a hydrogen bond with the deprotonated carboxylic group [O5(-H5A)⋯O2 = 2.692(4) Å] and with the protonated carboxylic groups of two symmetry-equivalent Ru(II) complexes [O5(-H5B)⋯O3ⁱ = 2.822(4) Å and O5⋯(H4-)O4ⁱⁱ = 2.552(4) Å; symmetry codes: (i) 1/2 + x, 3/2 - y, 1/2 + z; (ii) 3/2 - x, -1/2 + y, 1/2 - z], connecting four Ru(II) complexes over an inversion center (Figure 15). Furthermore, multiple π - π stacking interactions are observed between the aromatic bipyridine rings and the pyridine-2-carboxylate-4-carboxylic acid rings [ring centroid-centroid distances between 4.218(2) and 5.665(2) Å]. Selected bond lengths (Å) bond angles (°) for complex **5** are shown in the Tables 12 and 13.

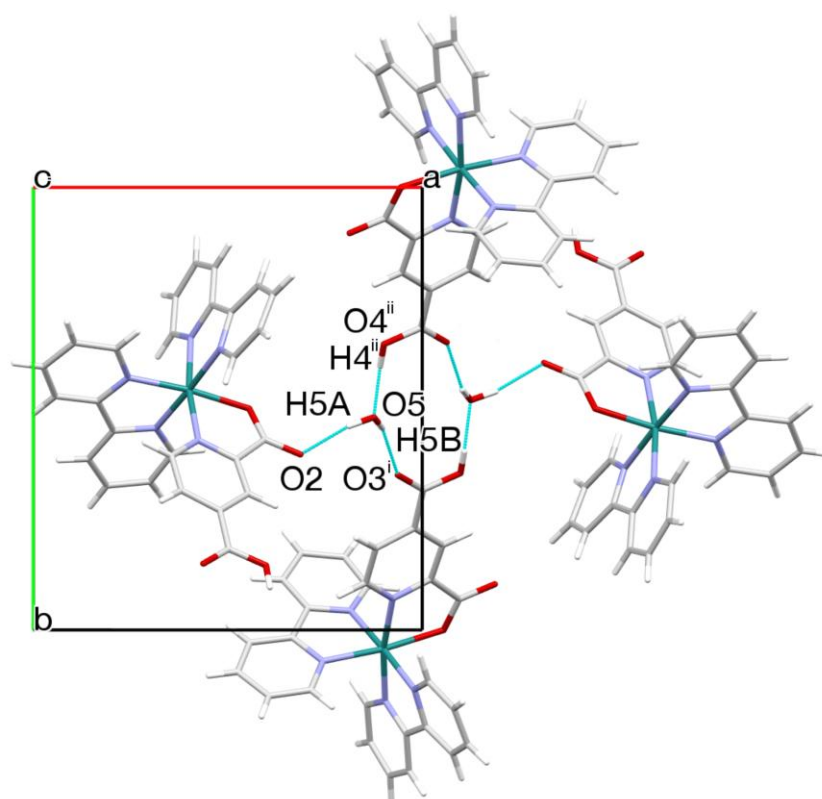


Figure 15. Part of the crystal packing of the structure of complex **5**, along the c-axis, showing hydrogen bonds between the water solvent molecules and the pyridine-2-carboxylate-4-carboxylic acid groups, with atom-labeling scheme of specific atoms involved. Symmetry codes: (i) 1/2 + x, 3/2 - y, 1/2 + z; (ii) 3/2 - x, -1/2 + y, 1/2 - z.

Table 12. Selected bond lengths (Å) for compound **5**.

Atom	Atom	Length/Å	Atom	Atom	Length/Å
Ru1	O1	2.090(3)	C6	C7	1.393(5)
Ru1	N1	2.053(3)	C7	C8	1.382(6)
Ru1	N2	2.031(3)	C8	C9	1.387(6)
Ru1	N3	2.054(3)	C9	C10	1.384(6)
Ru1	N4	2.056(4)	C11	C12	1.393(6)
Ru1	N5	2.049(3)	C12	C13	1.377(7)
O1	C21	1.279(5)	C13	C14	1.379(7)
O2	C21	1.235(5)	C14	C15	1.375(6)
O3	C27	1.213(5)	C15	C16	1.470(6)
O4	C27	1.319(5)	C16	C17	1.376(6)
N1	C1	1.344(5)	C17	C18	1.393(7)
N1	C5	1.366(5)	C18	C19	1.365(7)
N2	C6	1.365(5)	C19	C20	1.375(6)
N2	C10	1.354(5)	C21	C22	1.515(5)
N3	C11	1.351(5)	C22	C23	1.366(6)
N3	C15	1.368(5)	C23	C24	1.399(5)
N4	C16	1.366(5)	C24	C25	1.393(6)
N4	C20	1.346(5)	C24	C27	1.492(6)
N5	C22	1.368(5)	C25	C26	1.378(6)
N5	C26	1.346(5)	P1	F1	1.551(4)
C1	C2	1.369(6)	P1	F2	1.571(3)
C2	C3	1.392(6)	P1	F3	1.605(4)
C3	C4	1.386(6)	P1	F4	1.562(4)
C4	C5	1.377(6)	P1	F5	1.592(3)
C5	C6	1.470(5)	P1	F6	1.596(3)

Table 13. Selected bond angles (°) for complex **5**.

Atom	Atom	Atom	Angle/°	Atom	Atom	Atom	Angle/°
N1	Ru1	O1	95.76(12)	N3	C11	C12	121.1(4)
N1	Ru1	N3	98.62(13)	C13	C12	C11	119.9(4)
N1	Ru1	N4	177.05(13)	C12	C13	C14	118.6(4)
N2	Ru1	O1	173.99(12)	C15	C14	C13	120.2(5)
N2	Ru1	N1	79.07(13)	N3	C15	C14	121.2(4)
N2	Ru1	N3	91.27(13)	N3	C15	C16	115.0(4)
N2	Ru1	N4	99.03(13)	C14	C15	C16	123.8(4)
N2	Ru1	N5	97.22(13)	N4	C16	C15	114.3(4)
N3	Ru1	O1	92.55(11)	N4	C16	C17	121.4(4)
N3	Ru1	N4	79.10(14)	C17	C16	C15	124.3(4)
N4	Ru1	O1	86.25(12)	C16	C17	C18	119.7(5)
N5	Ru1	O1	79.38(12)	C19	C18	C17	118.4(5)
N5	Ru1	N1	87.69(13)	C18	C19	C20	120.0(5)
N5	Ru1	N3	170.27(13)	N4	C20	C19	122.4(5)
N5	Ru1	N4	94.81(14)	O1	C21	C22	116.1(3)
C21	O1	Ru1	115.6(2)	O2	C21	O1	125.4(4)
C1	N1	Ru1	125.7(3)	O2	C21	C22	118.5(4)
C1	N1	C5	118.3(4)	N5	C22	C21	114.3(3)
C5	N1	Ru1	115.7(3)	C23	C22	N5	123.1(4)
C6	N2	Ru1	115.7(3)	C23	C22	C21	122.6(4)
C10	N2	Ru1	125.7(3)	C22	C23	C24	119.2(4)
C10	N2	C6	118.6(3)	C23	C24	C27	123.4(4)
C11	N3	Ru1	125.8(3)	C25	C24	C23	117.8(4)
C11	N3	C15	118.9(4)	C25	C24	C27	118.7(4)
C15	N3	Ru1	115.3(3)	C26	C25	C24	120.0(4)

C16	N4	Ru1	115.4(3)	N5	C26	C25	122.4(4)
C20	N4	Ru1	126.3(3)	O3	C27	O4	124.5(4)
C20	N4	C16	118.0(4)	O3	C27	C24	122.2(4)
C22	N5	Ru1	114.5(3)	O4	C27	C24	113.3(3)
C26	N5	Ru1	128.0(3)	F1	P1	F2	91.3(3)
C26	N5	C22	117.5(3)	F1	P1	F3	178.8(2)
N1	C1	C2	122.4(4)	F1	P1	F4	92.3(3)
C1	C2	C3	119.5(4)	F1	P1	F5	90.72(18)
C4	C3	C2	118.5(4)	F1	P1	F6	90.30(19)
C5	C4	C3	119.4(4)	F2	P1	F3	87.7(2)
N1	C5	C4	121.7(4)	F2	P1	F5	90.1(2)
N1	C5	C6	113.6(4)	F2	P1	F6	90.1(2)
C4	C5	C6	124.7(4)	F4	P1	F2	176.4(3)
N2	C6	C5	115.2(4)	F4	P1	F3	88.7(3)
N2	C6	C7	120.9(4)	F4	P1	F5	90.0(2)
C7	C6	C5	123.9(4)	F4	P1	F6	89.68(19)
C8	C7	C6	120.0(4)	F5	P1	F3	88.45(18)
C7	C8	C9	119.0(4)	F5	P1	F6	178.94(19)
C10	C9	C8	118.9(4)	F6	P1	F3	90.53(18)
N2	C10	C9	122.5(4)				

4.3. Electrochemical measurements

For complexes **1-4** first reversible oxidation peaks were obtained in the potential range of $E_{1/2} = -0.02$ V to 0.04 V [2]. Also, these complexes showed a reversible oxidation peak at the potential range of $E_{1/2} = 0.54$ V to 0.64 V where peak potential shifts depend on the strength of the anionic ligand introduced in the Ru center. Additionally, complex **1** displayed one irreversible anodic peak at a potential of $+0.81$ V which could be attributed to the oxidation of the ligand. In the negative range of potentials all complexes showed one reversible reduction couple in the range of $E_{1/2} = -1.02$ V to -1.03 V which could be assigned to the reduction of a bipyridyl moiety [2]. A second reversible reduction for all complexes was observed at around $E_{1/2} = -1.65$ V to -1.70 V, which could be considered also as reduction of a bipyridyl group. A third redox couple was observed at around $E_{1/2} = -1.95$ V to -2.01 V, which in the case of Br-subunits (**4** and **3**) showed quasi-reversible behavior, and could be attributed to the third reduction of bipyridyl [3]. In the case of **4** the irreversible reduction peak at -2.23 V was not observed, which is obtained for all other complexes at the same potential, originating from the reduction of the R-ligands.

The results obtained from electrochemical measurements are presented in Table 14 and representative voltammograms are given in Figure 16.

Table 14. Electrochemical data for complexes **1-4** recorded in DMSO (0.1 M TBAP) at a boron doped diamond electrode with scan rate of 20 mV s^{-1} .

	$E_{1/2} / \text{V (vs. Ag/AgCl)}$						
	positive potentials range			negative potentials range			
	$A1_{(\text{ox/red})}$	$A2_{(\text{ox/red})}$	$A3_{(\text{ox/red})}$	$R1_{(\text{ox/red})}$	$R2_{(\text{ox/red})}$	$R3_{(\text{ox/red})}$	$R4_{(\text{ox/red})}$
1	0.095/0.014	0.59/0.48	0.81	-1.03/-1.13	-1.64/-1.75	-1.89/-2.01	-2.23
2	0.037/0.038	0.72/0.56	–	-1.00/-1.04	-1.59/-1.68	-1.89/-1.96	-2.23
3	0.04/0.039	0.64/0.058	–	-/-1.09	-1.64/-1.68	-/-1.92	-2.20
4	0.01/-0.04	0.66/0.48	–	–	-1.65/-1.76	-/-2.01	–

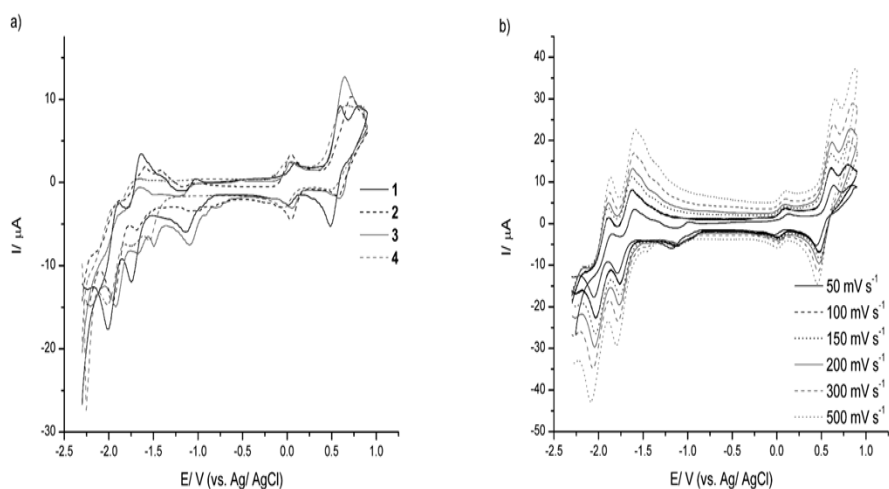


Figure 16. The cyclic voltammograms recorded in DMSO (0.1 mM TBAP) at a boron doped diamond working electrode a) for **1-4** with scan rate 20 mV s^{-1} and b) for **1** with scan rate 50, 100, 150, 200, 300, 500 mV s^{-1} .

The electrochemical character of the complex **5** was studied by cyclic voltammetry in DMSO in the $-2.50 < E < 1.00 \text{ V}$ potential range (Figure 17). The recorded voltammograms show a reversible wave at $\sim 0.30 \text{ V vs. Ag/AgCl}$, which can be readily assigned to the Ru(II)/(III) redox couple. The calculated ΔE_p values tend to slightly increase with scan rate (from 100 mV to 210 mV), indicating the partially reversible nature of the redox process. In the region of negative potentials ($-2.35 < E < -1.15 \text{ V}$), multiple partially reversible peaks can be observed. This type of reductive activity can be assigned to the subsequent reductions of the bipyridyl moiety. In comparison to the literature data [4-6], the novel Ru(II) complex shows no exception concerning its electrochemical behavior.

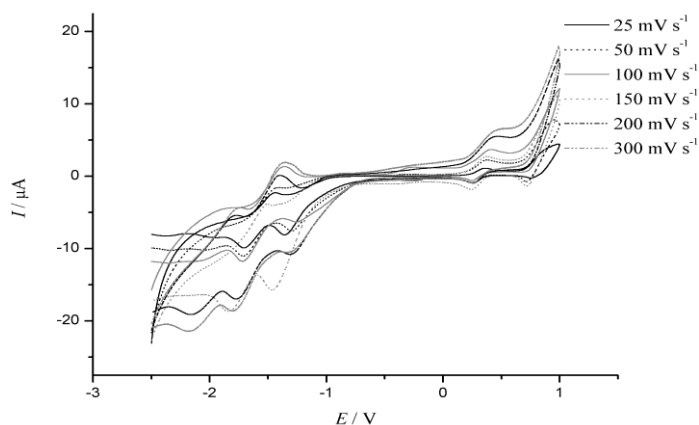


Figure 17. The cyclic voltammograms for **5** recorded in DMSO (0.1 mM TBAP) at a glassy carbon electrode for scan rates 25, 50, 100, 150, 200 and 300 mV s^{-1} .

4.4. Results of MTT assay

Cytotoxicity of the ruthenium complexes was determined by MTT assay, in few tumor cell lines: HeLa, LS-174, A549, K562, and one normal cell line, MRC-5, as presented in Table 15.

Results, obtained after 72 h of drug continual action are presented in terms of IC_{50} values (μM), (Table 15). The complexes exhibited moderate cytotoxic activity in HeLa cells, with IC_{50} (μM), ranging from 132.26 ± 4.99 (**2**), to 184.02 ± 16.16 (**3**). Complex **2** with the highest cytotoxic activity in HeLa, also was the only one to exhibit cytotoxic activity in LS-174 cells, (180.90 ± 10.12). For coordinatively saturated, as described in literature, substitutionally inert ruthenium(II) polypyridyl complexes, noncovalent association with cellular targets such as DNA, is generally assumed to be the primary mode of interaction with biological systems [7,8]. As compared to the first generations of platinum based drugs (*cisplatin*, *oxaliplatin*), ruthenium polypyridyl complexes possess structural properties that allow differential modes of binding to DNA, like specific covalent cross-linking [9], or intercalation between adjacent nucleobases. However, physicochemical parameters, such as complex stability, and ligand dissociation kinetics, also play important roles in determining their capability to reach target sites in the cell [10]. Few studies provided evidence that ruthenium polypyridyl complexes are transported to the interior of the cells, but may also remain associated with the cell membrane, particularly if they

carry extended and rigid polypyridyl ligands [11,12]. Sterically demanding ligands, such as polycyclic aromatic molecules (polypyridines), were shown to enhance cytotoxicity of the organoruthenium complexes, due to the hydrophobic interactions with DNA nucleobases or other targets in the cell. Moderate cytotoxicity of complexes **1-5** in the present study may be due to the greater off-target reactivity, when once in solution. Obtained IC₅₀ values (μM) are significantly higher, in comparison to the IC₅₀ values for *cisplatin*, reported in literature: 7.59 ± 0.04 (HeLa), 10.86 ± 0.55 (K562), 17.20 ± 0.70 (A549), 11.54 ± 0.50 (MRC-5) [13]. Still, minor variations in the structure of the co-ligand(s), resulted in variations in the IC₅₀ values, obtained in HeLa cells. Further investigations of the mechanism of action and of the structure-activity relationship of this class of ruthenium complexes, are of crucial importance for optimization of their activity.

Table 15. Cytotoxicity of the tested agents in terms of IC₅₀ values (μM), obtained for 72 h of continuous drug action, by MTT assay. IC₅₀ values present average (± SD).

Compound	IC ₅₀ ± SD (μM) [*]				
	HeLa	A549	LS-174	MRC-5	K562
1	> 200	> 200	> 200	> 200	/
2	132.26 ± 4.99	> 200	180.90 ± 10.12	> 200	/
3	184.02 ± 16.16	> 200	> 200	> 200	/
4	147.70 ± 7.99	> 200	> 200	> 200	/
5	ND	> 300	ND	> 300	177.63±2.8

^{*} > 200 denotes that IC₅₀ was not obtained in the range of concentrations tested up to 200 μM.

^{**} > 300 denotes that IC₅₀ was not obtained in the range of concentrations tested up to 300 μM.

ND Not Determined

4.5. Effects of NAC or L-BSO on the cell survival of HeLa cells treated with complex **2**

Taking into account redox-reactivity of Ru compounds bearing bipyridine moieties [3,14], we investigated whether cytotoxic potential of complex **2**, in HeLa cells, could be altered in combination with pharmacological modulators of cell redox-homeostasis, such as L-buthionine-sulfoximine (L-BSO) or N-acetyl-L-cysteine (NAC) [15-18]. Glutathione, present in millimolar intracellular concentrations, is a major determinant of the cellular redox status. L-BSO acts as a specific inhibitor of γ -glutamylcysteine synthesis (γ -GCS), the rate-limiting enzyme for biosynthesis of glutathione (GSH). N-acetyl-L-cysteine (NAC), acts as GSH precursor and is effective in protecting cells from reactive oxygen species (ROS) mediated cytotoxicity [19].

A preliminary dose-response study of L-BSO or NAC, for 72 h action in HeLa cells, was performed. Results showed more than 22% decrease of cell survival, in the concentration range above 2.5 μ M of L-BSO, or above 30 μ M of NAC (results not presented). Therefore the sub-toxic concentrations of L-BSO (1 μ M) or NAC (20 μ M), were selected for further combinational drug study [20,21]. However pretreatment of HeLa cells (3 h) with BSO or NAC, did not significantly alter cell response to the action of complex **2** (Figure 18). Results suggested that ROS and GSH might not be tightly related to the mechanism of antiproliferative action of complex **2** in HeLa cells.

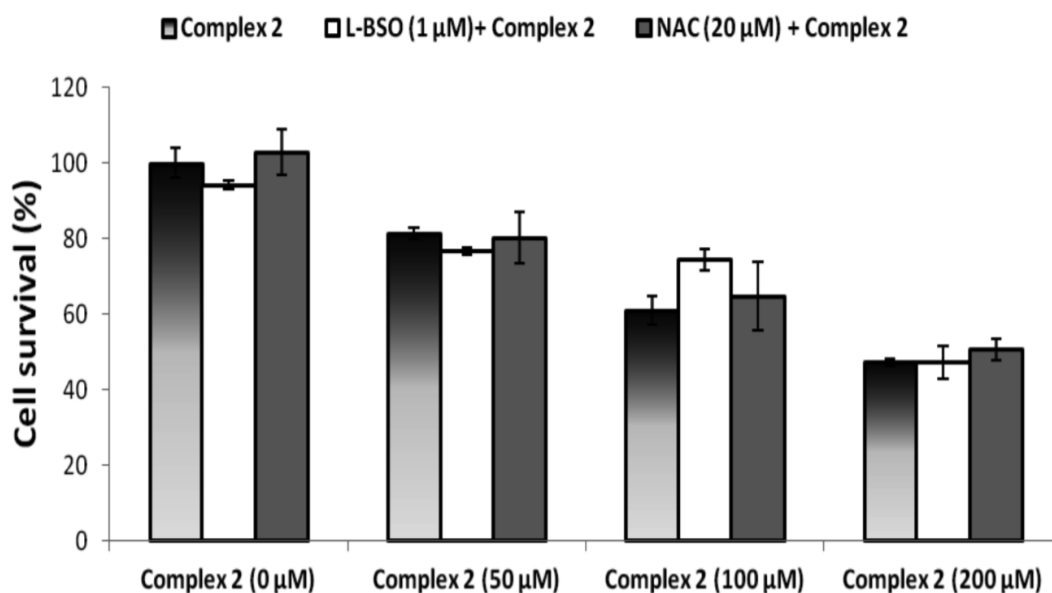


Figure 18. Effects of NAC and L-BSO on the cell survival in complex 2 treated HeLa cells. Exponentially growing cells were pre-treated with 20 μM NAC or 1 μM L-BSO and then after washing out, further treated with 50, 100 or 200 μM with the complex 2 for 72 h. Bars represent average of triplicates ± SD.

Effects of NAC or L-BSO on complex 2 induced cell cycle perturbations in HeLa cells. We performed further combinational drug study, to investigate whether pretreatment of HeLa cells by NAC (20 μM) or L-BSO (1 μM) may affect cell cycle perturbations, caused by complex 2. Sub-toxic concentrations of NAC or L-BSO, didn't affect the cell cycle profile in HeLa cells, compared to the non-treated cells (Figure 19). Complex 2 at IC₅₀ concentration (132 μM), induced slight cell cycle perturbations, characterized by the increase of sub-G1 content (7.57% compared to control 1.23%), decrease of cell number in G1 phase (52.17%, compared to control 64.66%), and arrest in the S phase (21.40% relative to control 10.99%). Slower progression of cells through S phase of the cell cycle, clearly indicated potential of complex 2 to inhibit replication in HeLa cells, through DNA-interactions or by indirect manner (ROS production). Pre-treatment of HeLa cells with NAC (3 h) caused almost no alterations of cell cycle progression, comparing to the action of complex 2, as a single agent (Figure 19). On the other hand, pretreatment with L-BSO caused more pronounced changes in Sub-G1 phase (increase to

24.21%), as well as in G1 phase (decrease of cell number to 42.23%) (Figure 19). It seems that L-BSO, at sub-toxic concentrations potentiated apoptotic stimuli caused by complex 2. This result suggested that intracellular glutathione may affect action of complex 2 or may at least influence its intracellular availability for interaction with potential cellular targets.

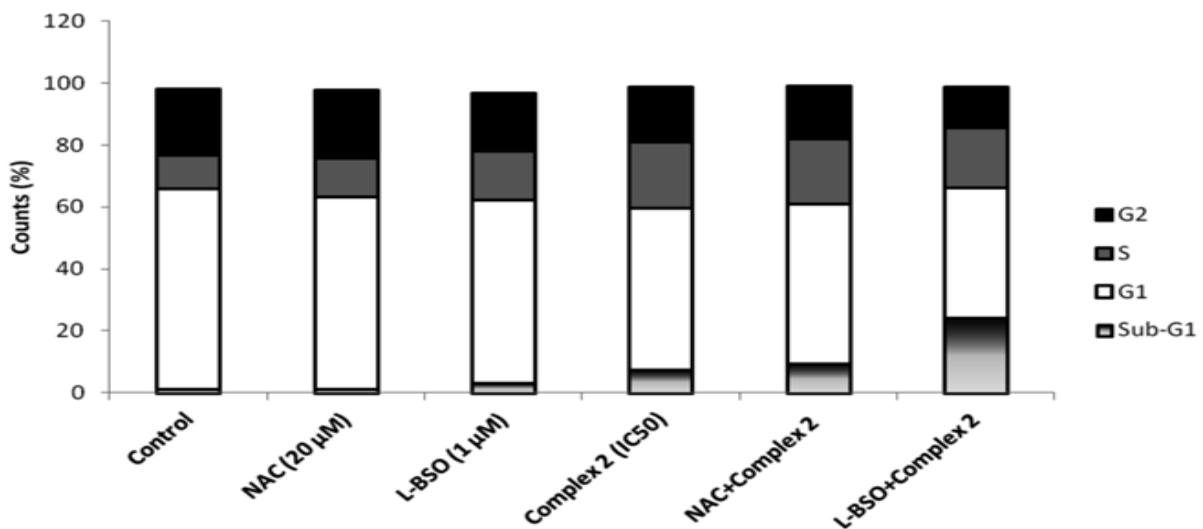


Figure 19. Effects of NAC and L-BSO on the cell cycle of complex 2-treated HeLa cells. Exponentially growing cells were pre-treated with 20 μM NAC or 1 μM L-BSO and then after washing out, further treated with complex 2 (IC₅₀ 132 μM) for 72 h. Bars represent average of duplicates.

4.6. Interaction of complex **2** with DNA

4.6.1. UV-vis spectroscopy

Potential interaction of the complex **2** with DNA was studied in PBS at room temperature and the corresponding absorption spectrum in the absence and presence of DNA is shown in Figure 20. A band at 355 nm can be assigned to intraligand $\pi - \pi^*$ transitions while a broad band located in the visible region at 462 nm is attributed to the metal-to-ligand charge transfer (MLCT) transitions [22]. As the concentration of DNA increased, both absorption bands displayed clear hypochromism but no obvious red shift. This observation is in agreement with recently published reports [23,24]. These studies suggested an intercalation mode of complex-DNA interaction, which usually results in hypochromism and bathochromism as a direct consequence of interaction between the aromatic chromophore and the base pairs of DNA.

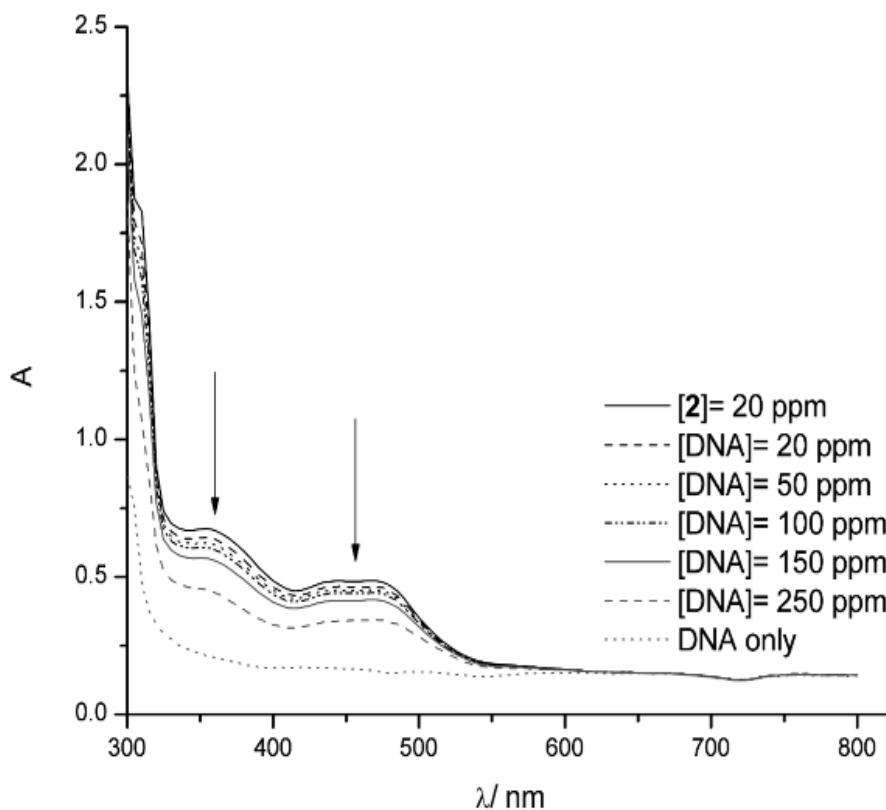


Figure 20. Absorption spectra of complex **2** in DMSO (0.1 mM PBS) at pH = 7 upon the addition of DNA, [Ru] = 20 ppm, [DNA] = 0-250 ppm. Arrow shows the absorbance changing upon increasing DNA.

4.6.2. Cyclic voltammetry

Electrochemical measurements were performed for complex **2** as a useful complement method for UV-vis spectroscopic investigation of complex-DNA interaction. Cyclic voltammograms were recorded in the presence of increasing amounts of complex **2** (Figure 21). After addition of DNA, two reversible one-electron redox processes are detected. Shifts of $E_{1/2}$ toward more positive values in a positive potential range ($0.20 < E_{1/2} < 0.90$ V) indicate ability of this Ru(II) complex to interact with DNA as a result of intercalation mode [25].

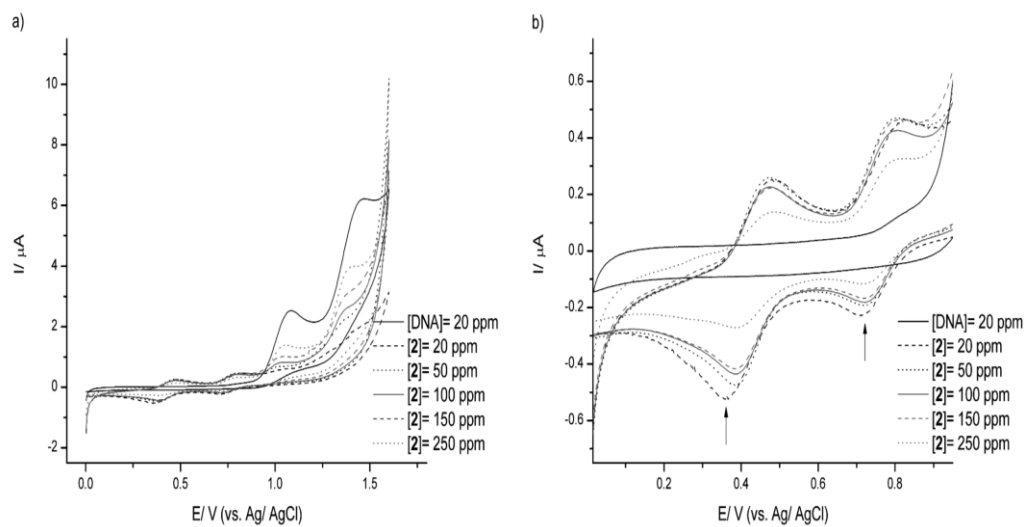


Figure 21. The cyclic voltammograms recorded in DMSO (0.1 mM PBS) at a boron-doped electrode upon the addition of the complex **2** ([DNA] = 20 ppm and [2] = 0-250 ppm) in a potential range a) $0.00 < E_{1/2} < 1.60$ V and b) $0.00 < E_{1/2} < 0.90$ V. Arrow shows $E_{1/2}$ shifts changing upon increasing complex's concentration.

References of Results and Discussion

1. F. H. Allen. *Acta Cryst.* **B58** (2002) 380.
2. D. Cabral, P. C. Howlett, J. M. Pringle, X. Zhang, D. MacFarlane. *Electrochim. Acta* **180** (2015) 419.
3. S. Bellinger-Buckley, T. Chang, S. Bag, D. Schweinfurth, W. Zhou, B. Torok, B. Sarkar, M. Tsai, J. Rochford. *Inorg. Chem.* **53** (2014) 5556.
4. P. Sengupta, S. Ghosh, T. C. W. Mak, *Polyhedron* **20** (2001) 975.
5. M. K. Nazeeruddin, S. M. Zakeeruddin, R. Humphry-Baker, M. Jirousek, P. Liska, N. Vlachopoulos, V. Shklover, C. H. Fischer, M. Grätzel, *Inorg. Chem.* **38** (1999) 6298.
6. D. Cabral, P. C. Howlett, J. M. Pringle, X. Zhang, D. MacFarlane, *Electrochim. Acta* **180** (2015) 419.
7. A. C. G. Hotze, S. E. Caspers, D. de Vos, H. Kooijman, A. Spek, Flamigni, M. Bacac, G. Sava, J. G. Haasnoot, J. Reedijk. *J. Biol. Inorg. Chem.* **9** (2004) 354.
8. L. Mishra, A. K. Yadaw, R. Sinha, A. K. Singh. *Indian J. Chem. Sect A-Inorg. Bio-Inorg. Phys. Theor. Anal. Chem.* **40** (2001) 913.
9. L. Marcélis, C. Moucheron, A. Kirsch-De Mesmaeker. *Philos. Trans. A. Math. Phys. Eng. Sci.*, **371** (2013) 20120131.
10. P. C. A. Bruijninch, P. J. Sadler. *Advances in Inorganic Chemistry*, R.van Eldik, C.D. Hubbard (Eds), Vol 61, pp.1, (2009).
11. C. A. Puckett, J. K. Barton. *J. Am. Chem. Soc.*, **129** (2007) 46.
12. C. A. Puckett, J. K. Barton. *Biochemistry*, **47** (2008) 11711.
13. S. Nikolić, D. M. Opsenica, V. Filipović, B. Dojčinović, S. Arandelović, S. Radulović, S. Grgurić-Šipka. *Organometallics*, **34** (2015) 3464.
14. Y. Zhang, L. Lai, P. Cai, G. Cheng, X. Xu, Y. Liu. *New J. Chem.*, **39** (2015) 5805.
15. M. Gielen, E. R. T. Tiekink. *Metallotherapeutic drugs and metal-based diagnostic agents*, John Wiley & Sons Ltd, Chichester (2005).
16. M. A. Jakupec, M. Galanski, V. B. Arion, C. G. Hartinger, B. K. Keppler. *Dalton Trans.* 183 (2008).
17. J. A. Fernandez-Pol, D. J. Klos, P. D. Hamilton. *Anticancer Res.*, **21** (2001) 3773.

18. S. G. Menon, M. C. Coleman, S.A. Walsh, D. R. Spitz, P. C. Goswami. *Antioxid. Redox Sign.* **7** (2005) 711.
19. H. H. W. Chen, M. T. Kuo. *Met. Based Drugs* **2010** (2010) 1.
20. Y. H. Han, S. Z. Kim, S. H. Kim, W. H. Park. *Int. J. Onco.* **33** (2008) 205.
21. Y. Fu, A. Habtemariam, A. M. B. H. Basri, D. Braddick, G. J. Clarkson, P. J. Sadler. *Dalton Trans.* **40** (2011) 10553.
22. X. W. Liu, Y. M. Shen, Z. X. Li, X. Zhong, Y. D. Chen, S. B. Zhang. *Spectrochim. Acta A* **149** (2015) 150.
23. A. M. Pyle, J. P. Rehmann, R. Meshoyrer, C. V. Kumar, N. J. Turro, J. K. Barton. *J. Am. Chem. Soc.* **111** (1989) 3051.
24. V. R. Putta, R.R. Mallepally, S. Avudoddi, P. K. Yata, N. Chintakuntla, D. Nancherla, K. Nagasuryaprasad, S. S. Surya, S. Sirasani. *Anal. Biochem.* **485** (2015) 49.
25. X. Totta, A. A. Papadopoulou, A. G. Hatzidimitriou, A. Papadopoulos, G. Psomas. *J. Inorg. Biochem.* **145** (2015) 79.

5. CONCLUSION

In this thesis synthesis and structural characterization of new ruthenium(II) bipyridyl complexes of general formula, $[\text{RuL}(\text{bpy})_2]\text{PF}_6$, (**HL** = 3-methylpyridine-2-carboxylic acid, 6-methylpyridine-2-carboxylic acid, 5-bromopyridine-2-carboxylic acid and 6-bromopyridine-2-carboxylic acid) were described. All compounds were characterized by various methods (NMR and IC spectroscopy, mass spectrometry and elemental analysis), including X-ray crystallography for complexes **3**, **4** and **5**. The octahedral Ru(II) complex cation consists of two bidentate bipyridyl ligands and one *ON* bidentate picolinate ligand, counterbalanced by one PF_6^- anion. Electrochemical properties of the synthesized complex were investigated and the obtained results indicate that its electrochemical behavior is in accordance with literature data for Ru(II) complexes.

Complexes showed moderate cytotoxicity, which may be due to the unfavorable ligand dissociation kinetics and off-target reactivity, when once in solution.

Still, minor variations in the structure of the co-ligand resulted in variations in the resulting IC_{50} values obtained in HeLa cells. Complex **2** exhibited the highest activity in cervical cancer HeLa cells, with IC_{50} value being 132.26 ± 4.99 (μM). Combinational drug studies revealed that L-BSO did not affect cytotoxicity of the complex **2**, though it modulated its effect on the cell cycle, by enhancing arrest in the S phase, and increasing Sub-G1 peak (fragmented DNA). Among ruthenium compounds bearing polypyridine moieties, several of them have proven to be mitochondria-targeting anticancer drug candidates, which often induce redox reactions inside cancer cells, resulting in an increase of reactive oxygen species (ROS). However, combinational drug studies using the ROS scavenger, NAC, did not affect the activity of the complex **2**. For investigation of the binding mode of the complex **2** to DNA, UV-vis and cyclic voltammetry were employed. Both techniques suggest an intercalative mode of binding signifying that the complex **2** probably acts as DNA intercalator.

6. SUPPLEMENTARY MATERIAL

SYNTHESIS, CHARACTERIZATION AND CYTOTOXICITY BIS(BIPYRIDINE) RUTHENIUM(II) COMPLEXES WITH PICOLINIC ACID DERIVATIVES

Afia Baroud

(Spectroscopic characterization of synthesized complexes)

Table of content:

Fig. S1. ^1H NMR spectrum of complex **1**.

Fig. S2. ^{13}C NMR spectrum of complex **1**.

Fig. S3. IR spectrum of complex **1**.

Fig. S4. MS spectrum of complex **1**.

Fig. S5. ^1H NMR spectrum of complex **2**.

Fig. S6. ^{13}C NMR spectrum of complex **2**.

Fig. S7. IR spectrum of complex **2**.

Fig. S8. MS spectrum of complex **2**.

Fig. S9. ^1H NMR spectrum of complex **3**.

Fig. S10. ^{13}C NMR spectrum of complex **3**.

Fig. S11. IR NMR spectrum of complex **3**.

Fig. S12. MS spectrum of complex **3**.

Fig. S13. ^1H NMR spectrum of complex **4**.

Fig. S14. ^{13}C NMR spectrum of complex **4**.

Fig. S15. IR spectrum of complex **4**.

Fig. S16. MS spectrum of complex **4**.

Fig. S17. ^1H NMR spectrum of complex **5**.

Fig. S18. IR spectrum of complex **5**.

Fig. S19. MS spectrum of complex **5**.

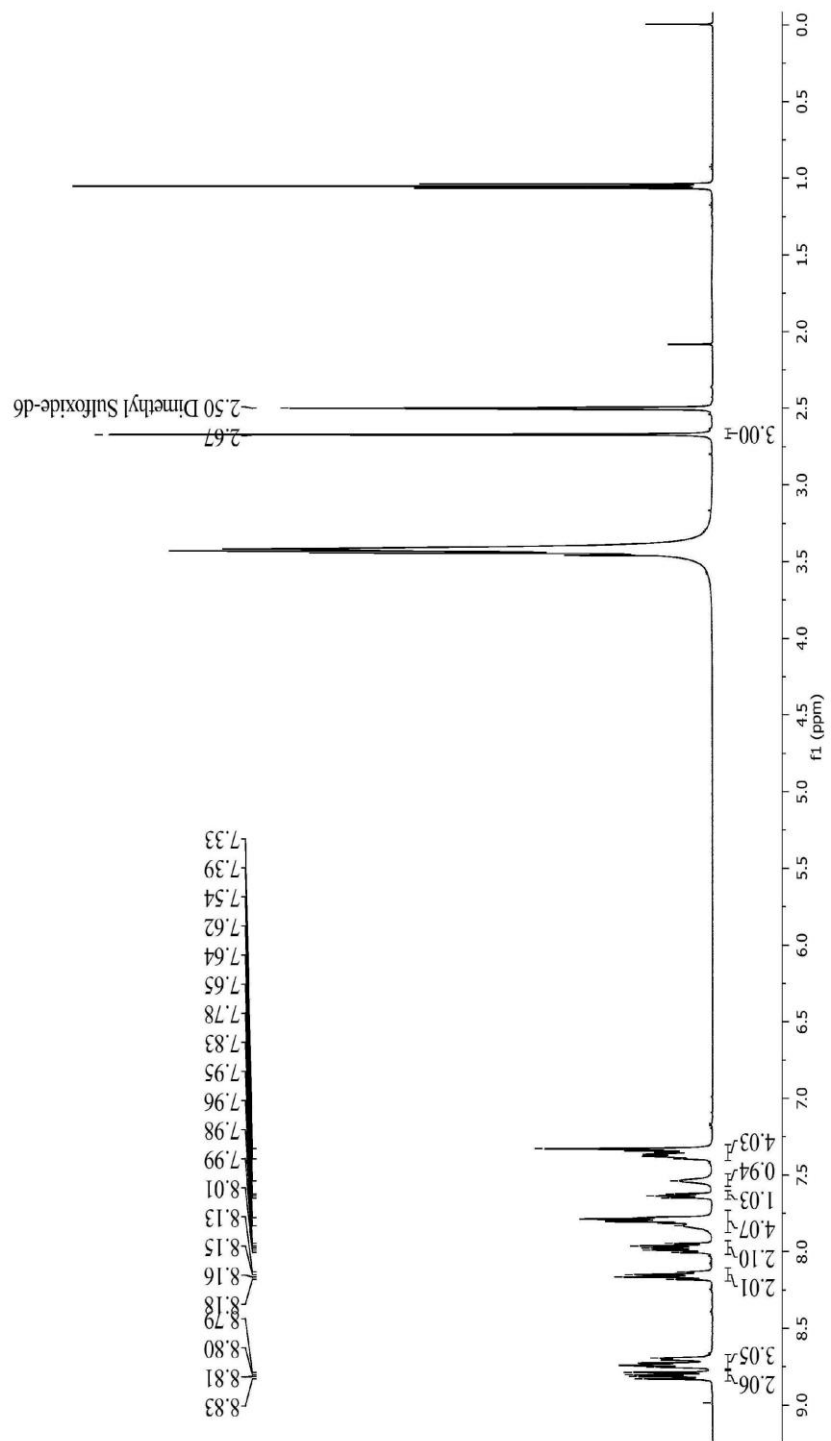


Fig. S1. ^1H NMR spectrum of **1**.

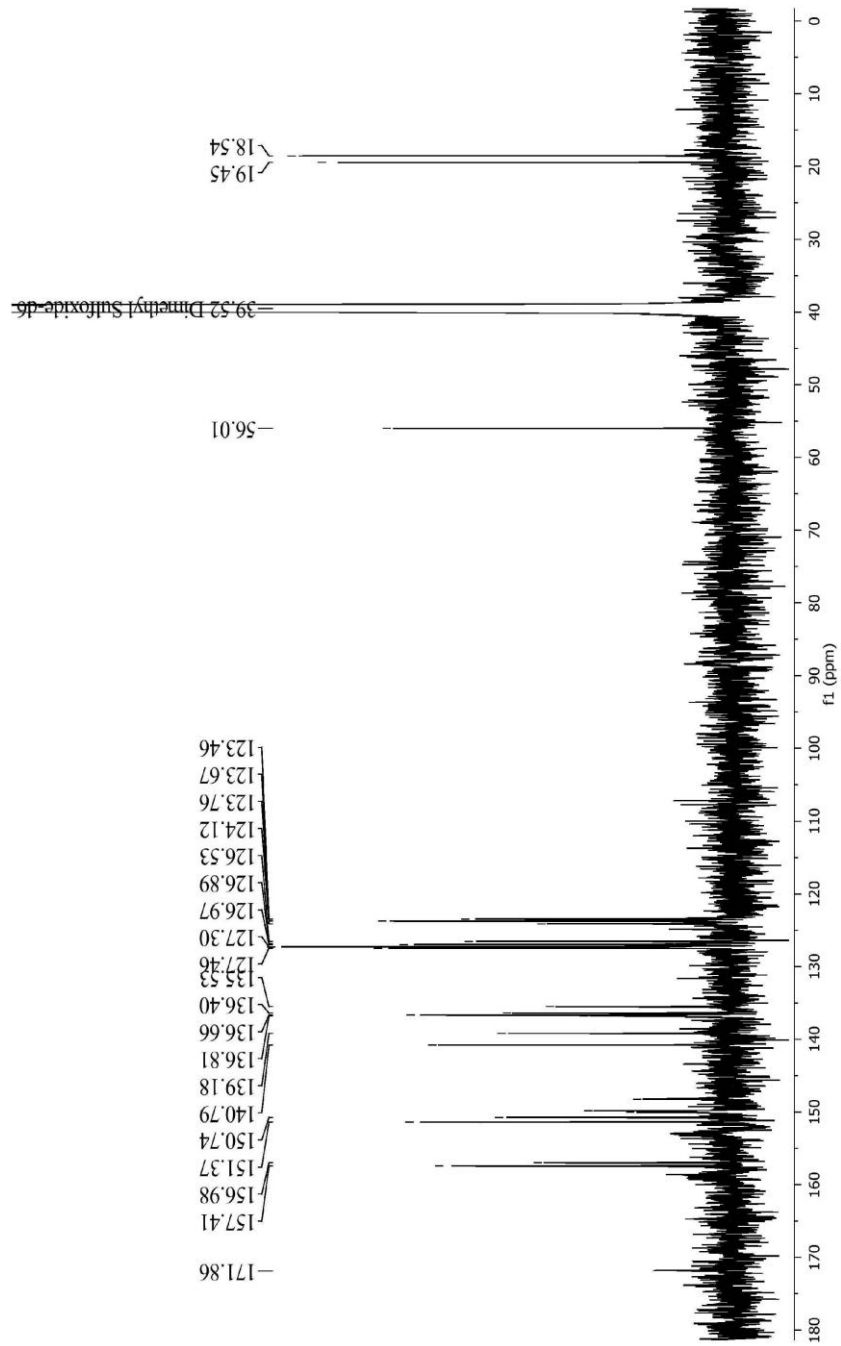


Fig. S2. ^{13}C NMR spectrum of **1**.

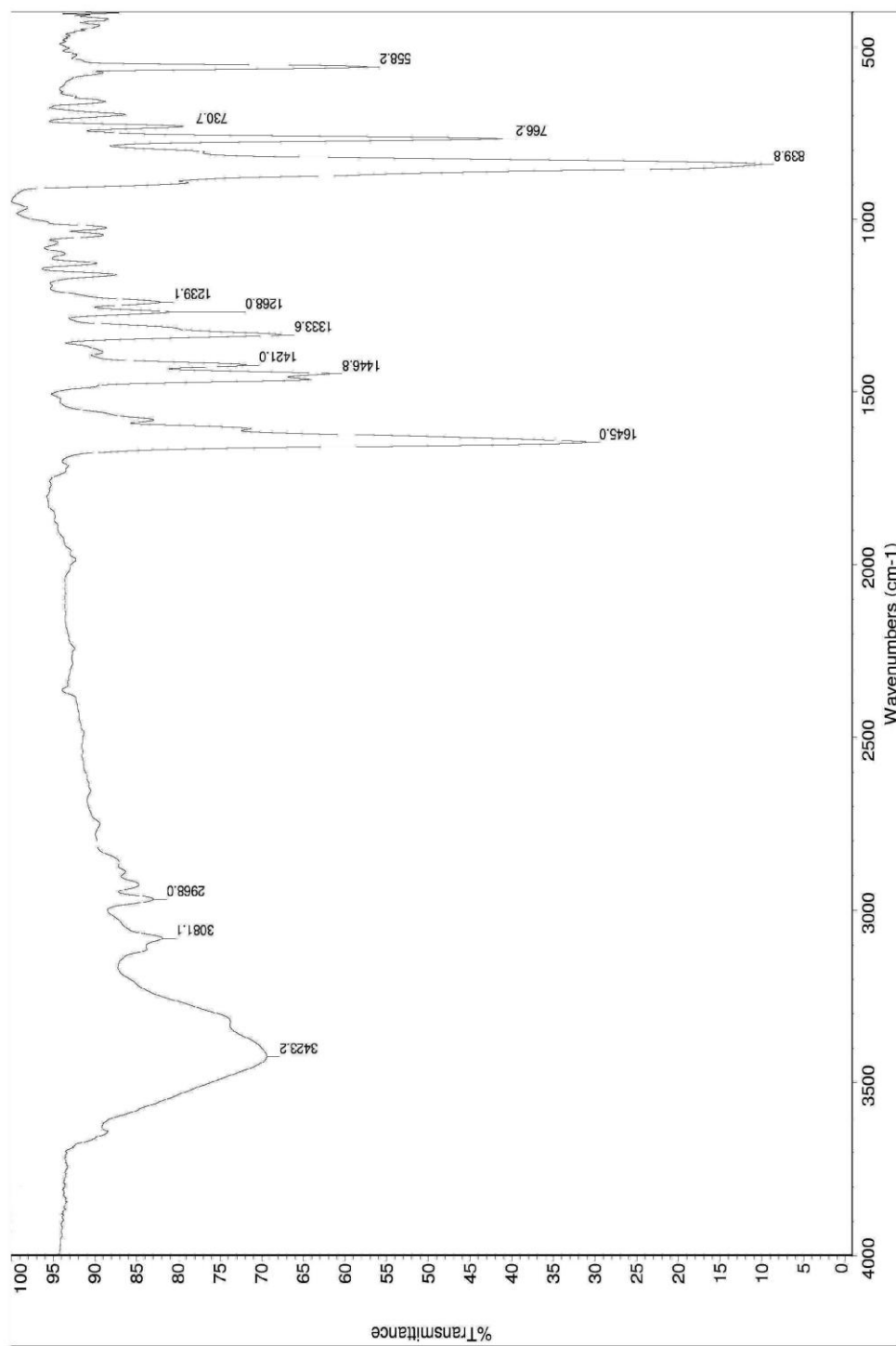
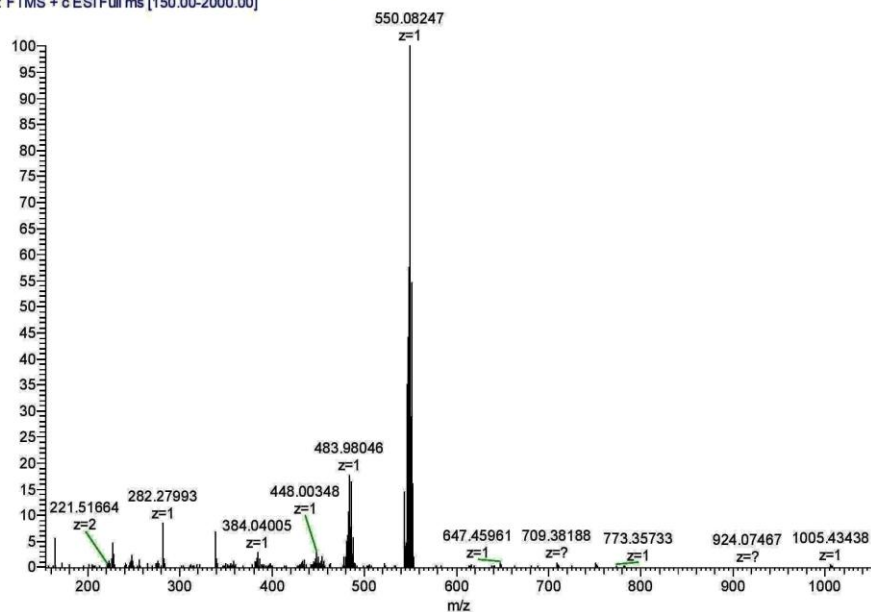


Fig. S3. IR spectrum of **1**.

OB3048 #1-55 RT: 0.01-0.50 AV: 55 NL: 1.83E7
T: FTMS + c ESI Full ms [150.00-2000.00]



Zoomed spectra

OB3048 #1-55 RT: 0.01-0.50 AV: 55 NL: 1.83E7
T: FTMS + c ESI Full ms [150.00-2000.00]

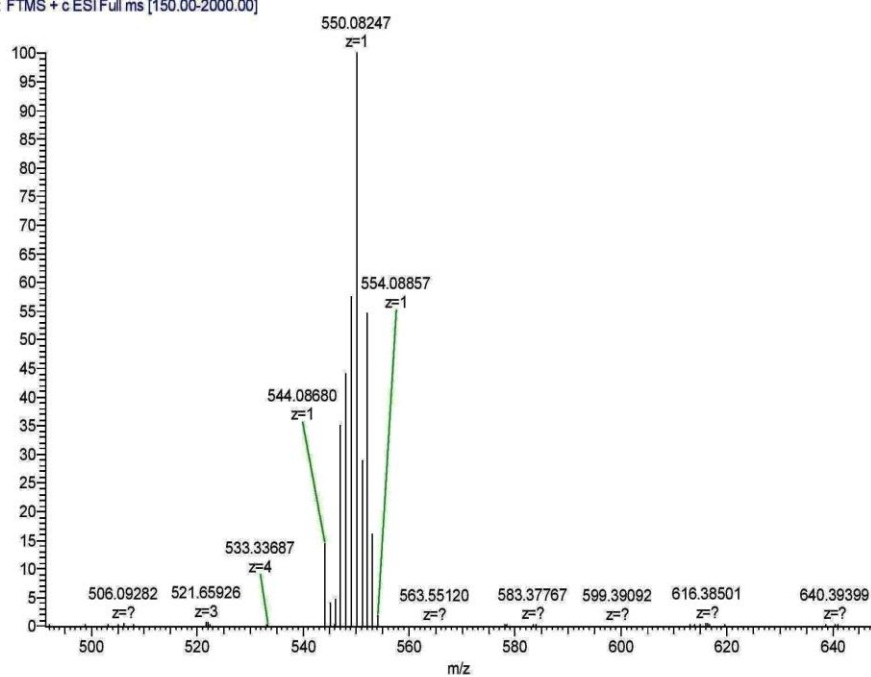


Fig. S4. MS spectrum of 1.

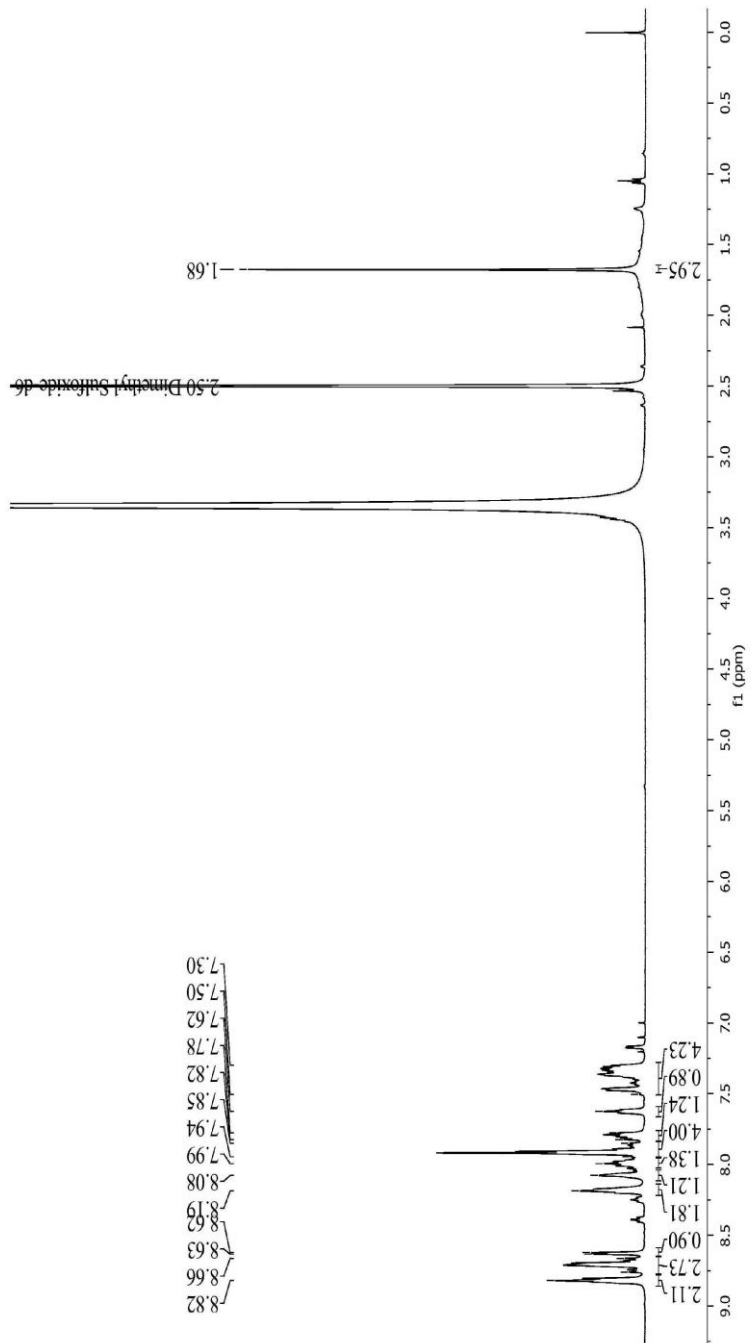


Fig. S5. ^1H NMR spectrum of **2**.

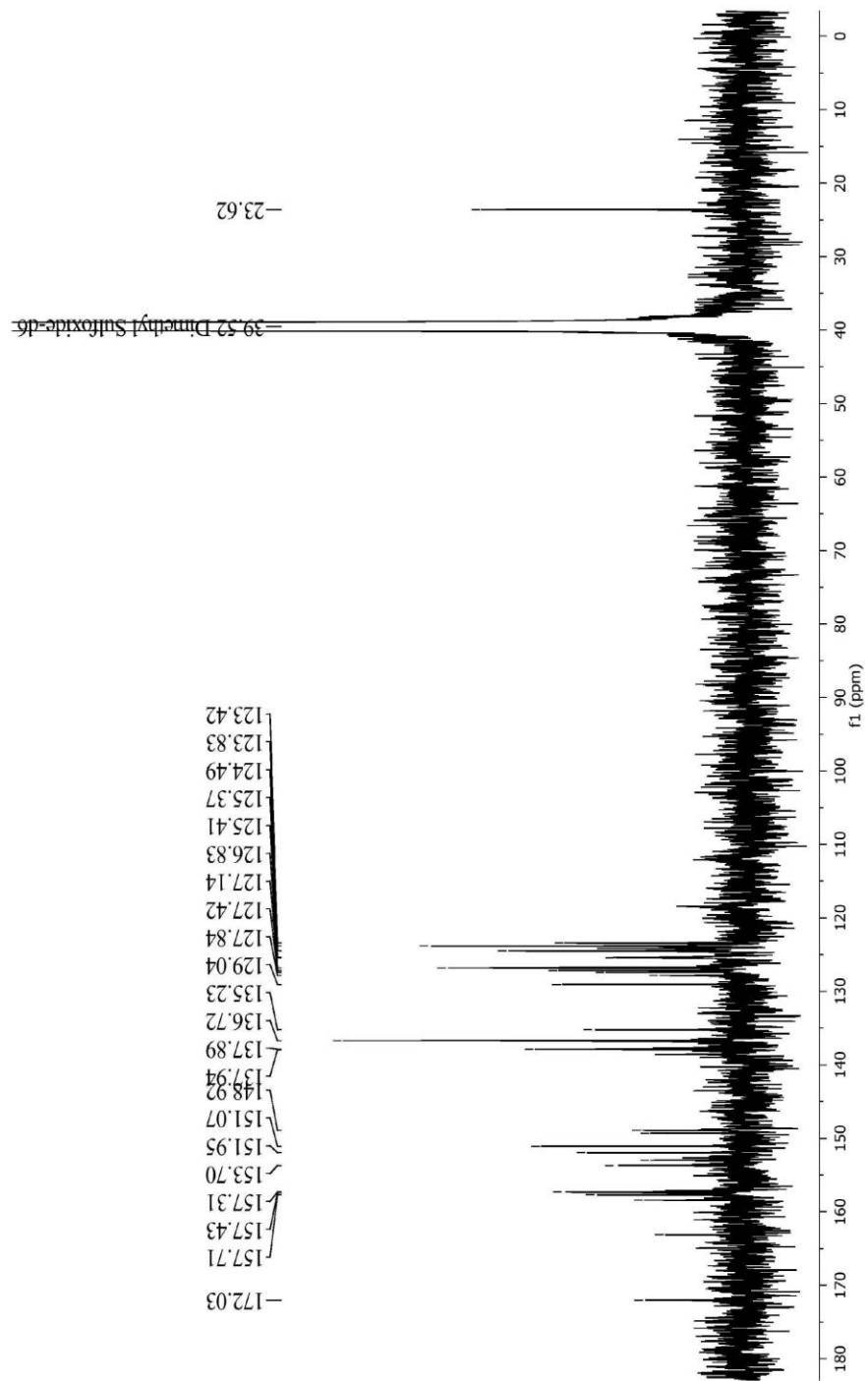


Fig. S6. ^{13}C NMR spectrum of **2**.

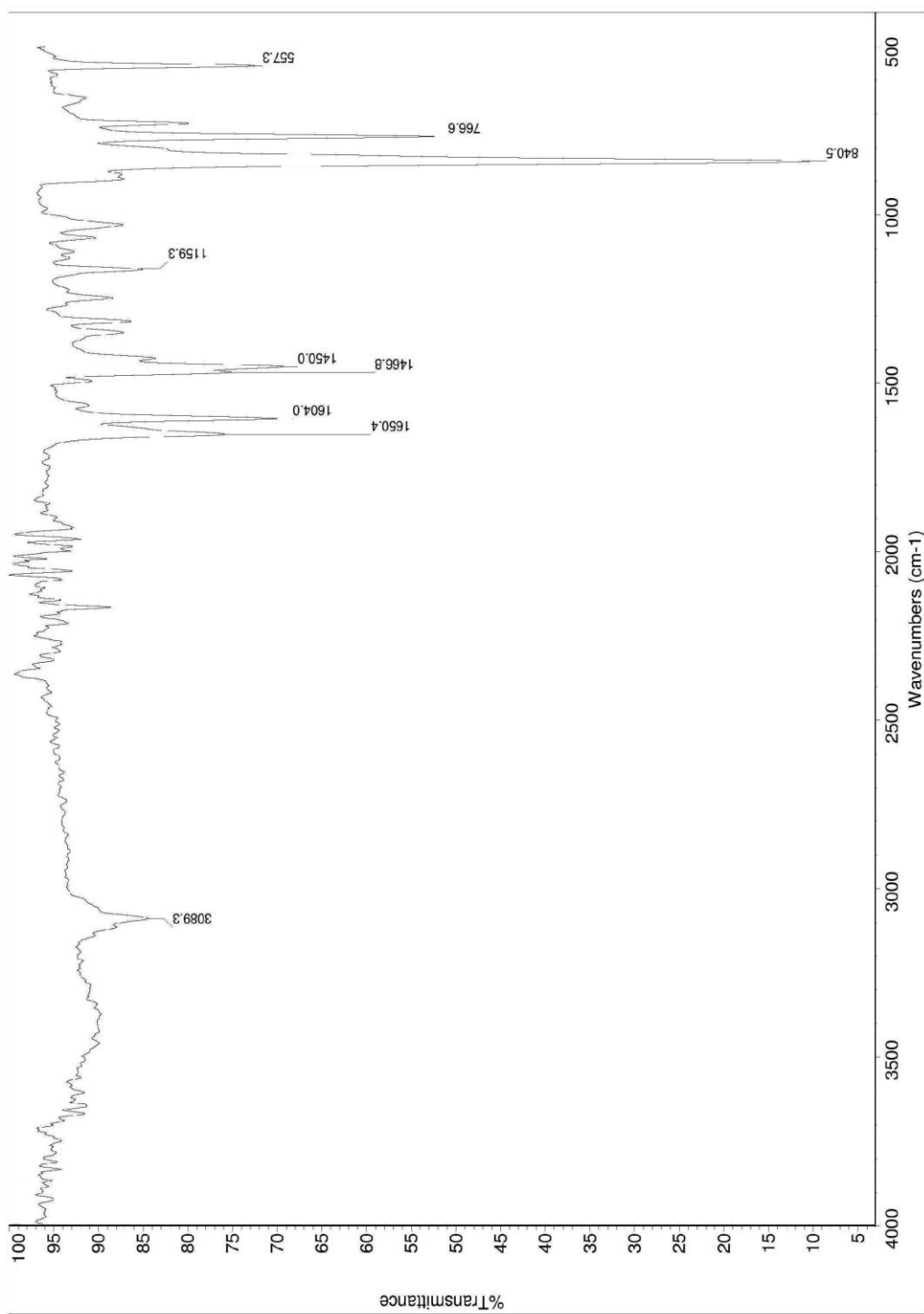
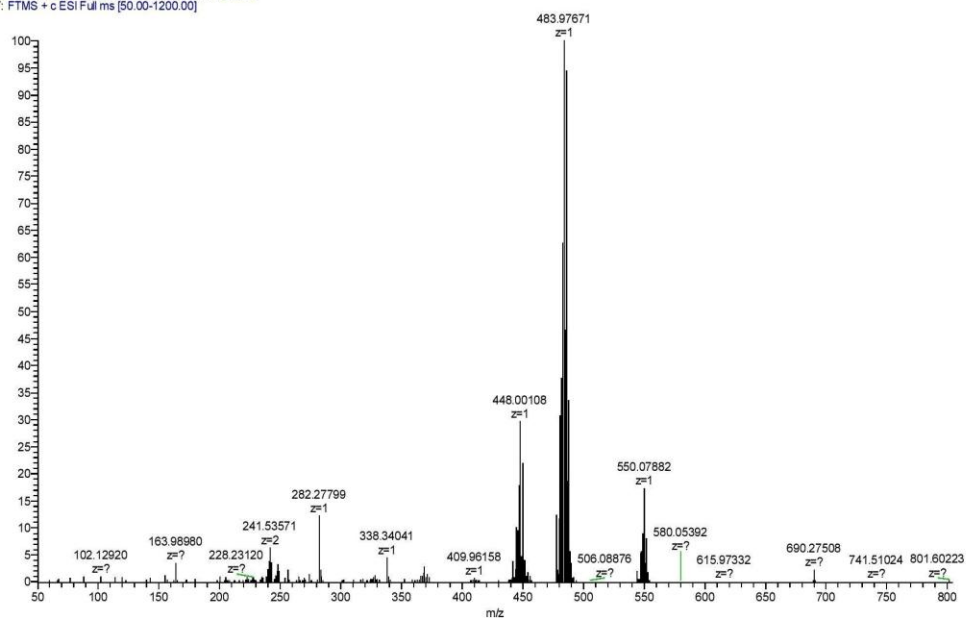


Fig. S7. IR spectrum of **2**.

OB2535 #1-54 RT: 0.01-0.50 AV: 54 NL: 5.99E6
T: FTMS + c ESI Full ms [50.00-1200.00]



OB2535 #49 RT: 0.45 AV: 1 NL: 9.74E5
T: FTMS + c ESI Full ms [50.00-1200.00]

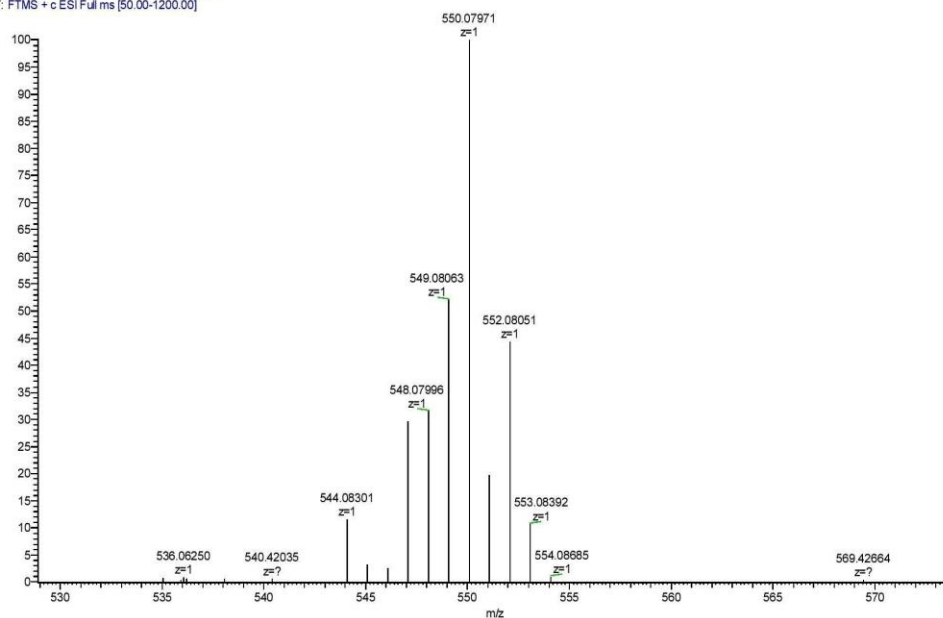


Fig. S8. MS spectrum of **2**.

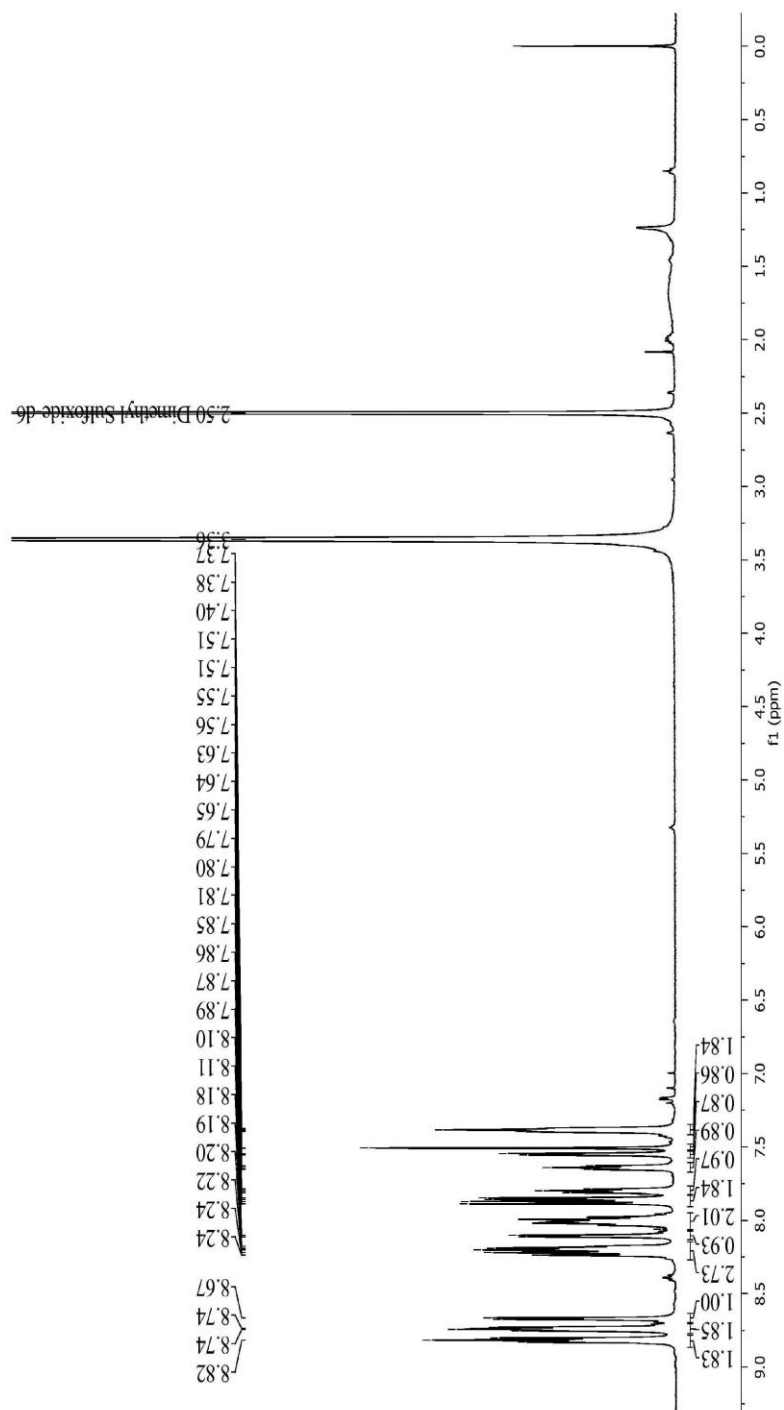


Fig. S9. ^1H NMR spectrum of **3**.

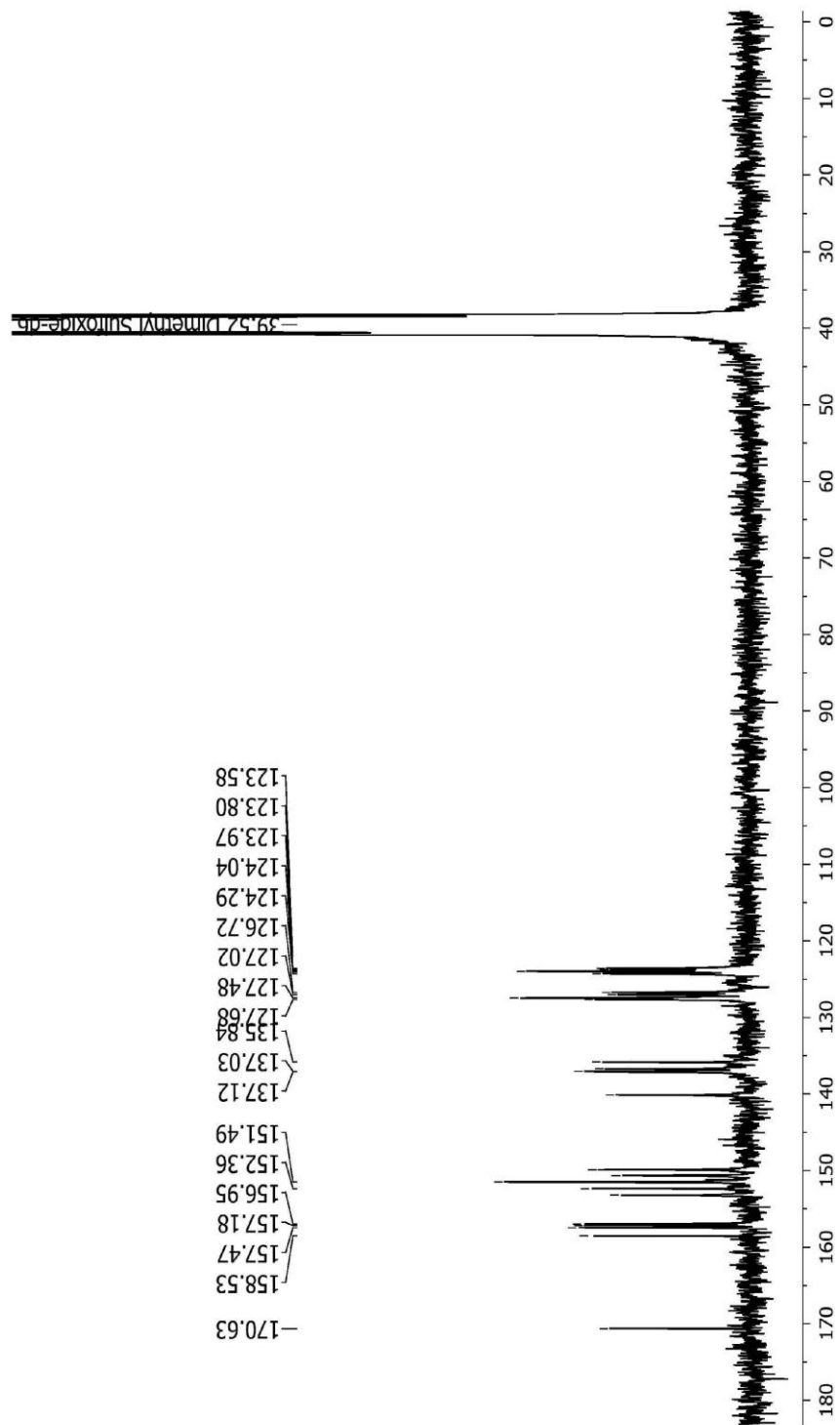


Fig. S10. ^{13}C NMR spectrum of **3**.

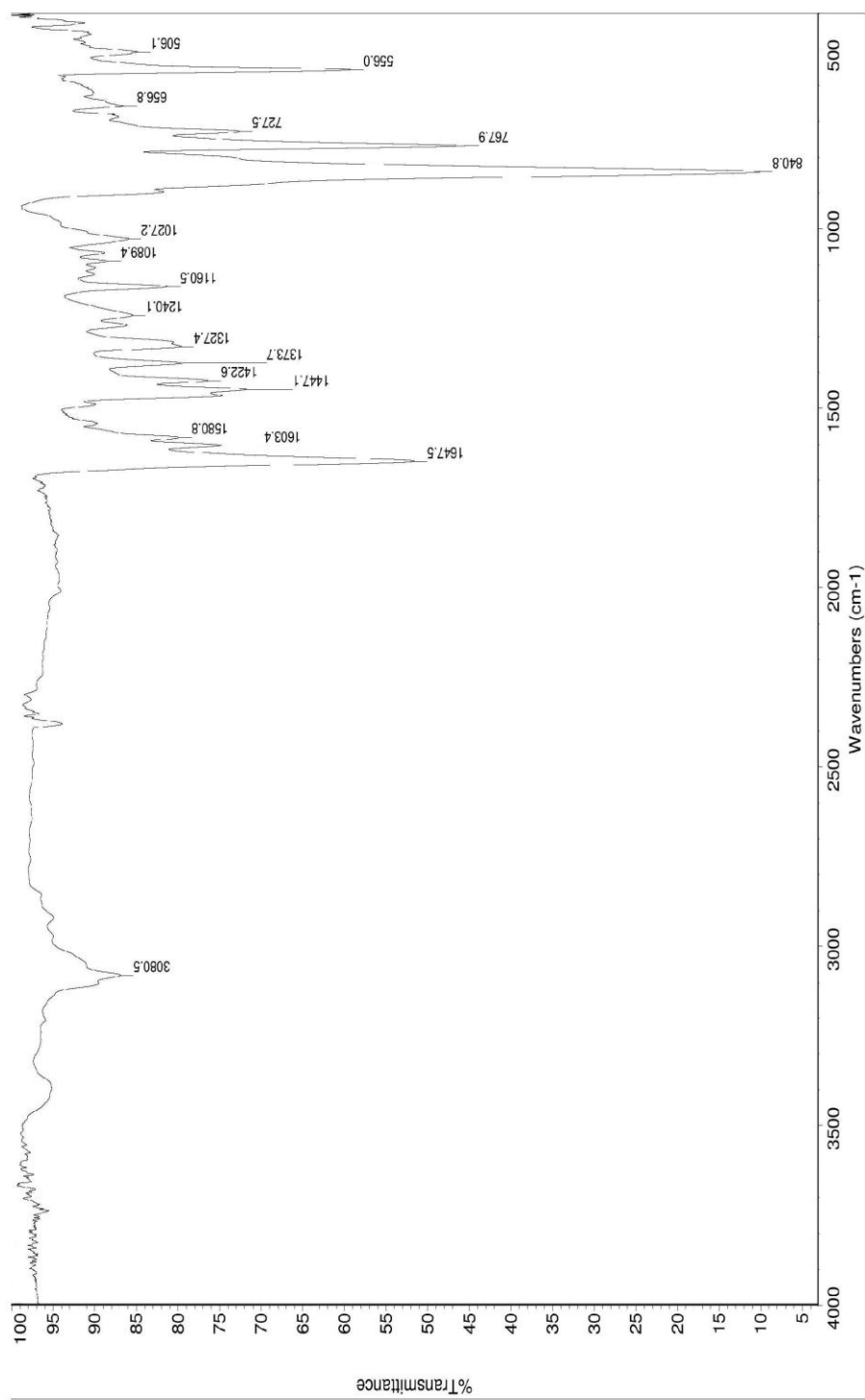
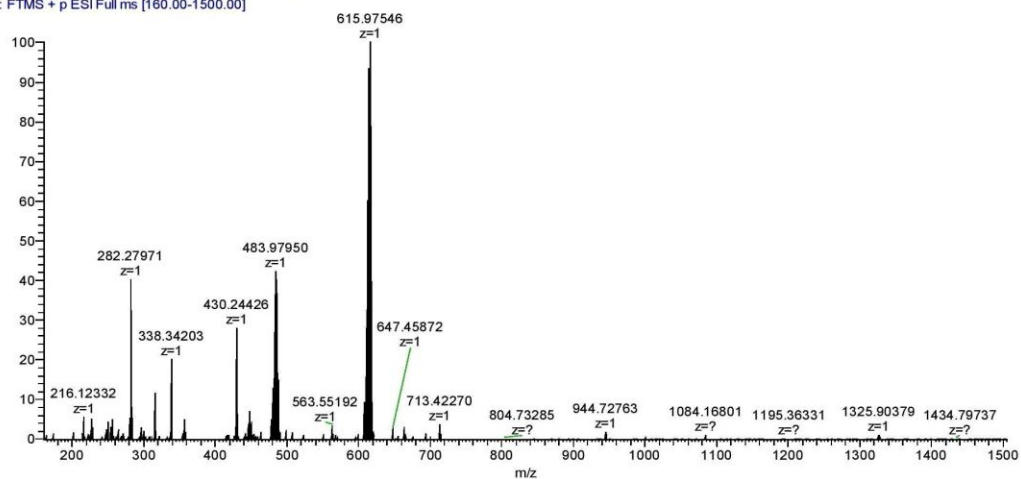


Fig. S11. IR spectrum of **3**.

OB3484 #1-34 RT: 0.01-0.50 AV: 34 NL: 2.50E7
T: FTMS + p ESI Full ms [160.00-1500.00]



Zoomed spectra

OB3484 #1-34 RT: 0.01-0.50 AV: 34 NL: 2.50E7
T: FTMS + p ESI Full ms [160.00-1500.00]

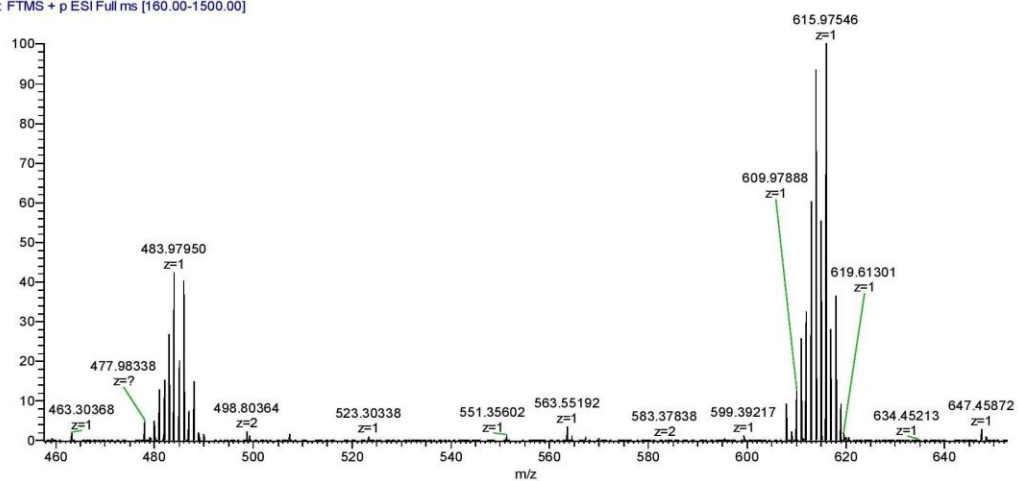


Fig. S12. MS spectrum of **3**.

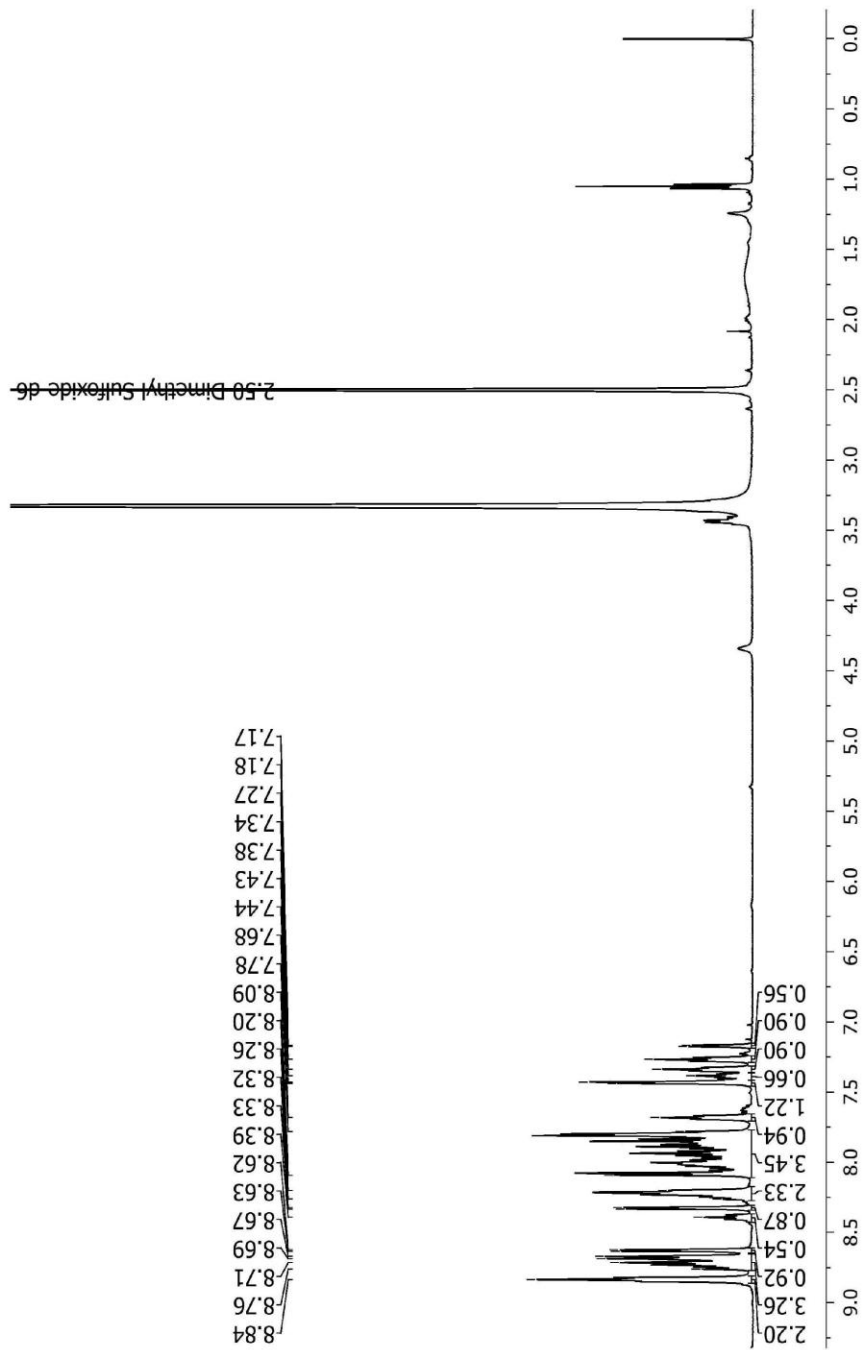


Fig. S13. ^1H NMR spectrum of **4**.

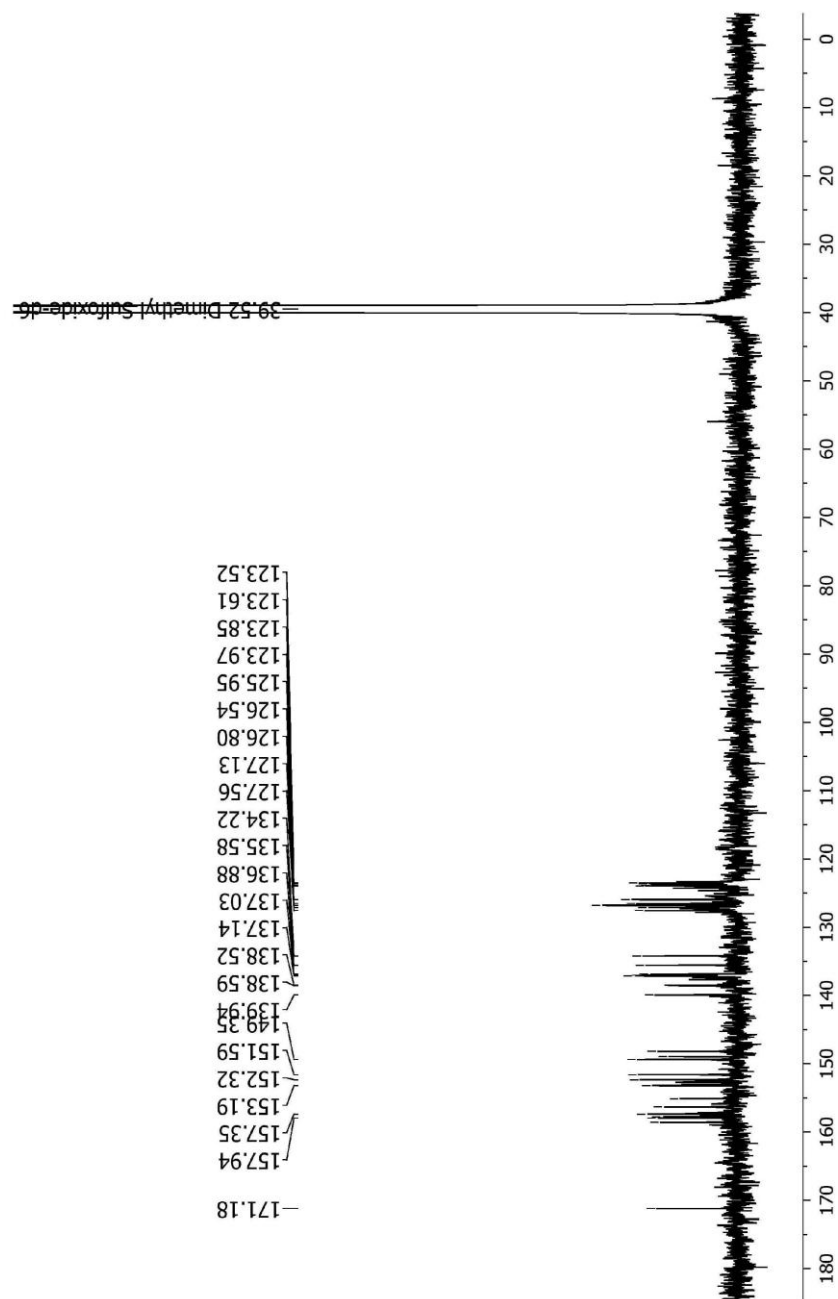


Fig. S14. ^{13}C NMR spectrum of **4**.

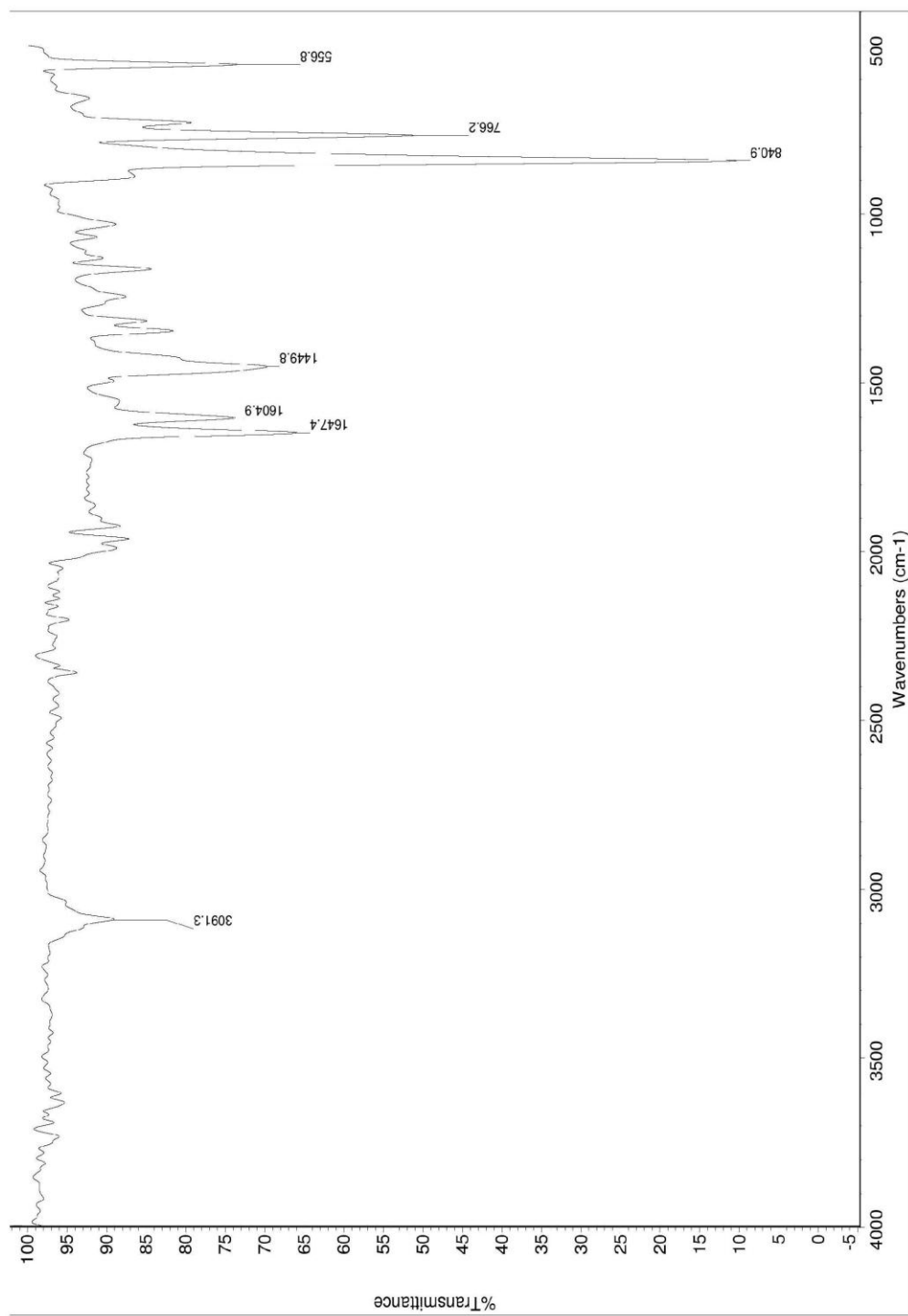
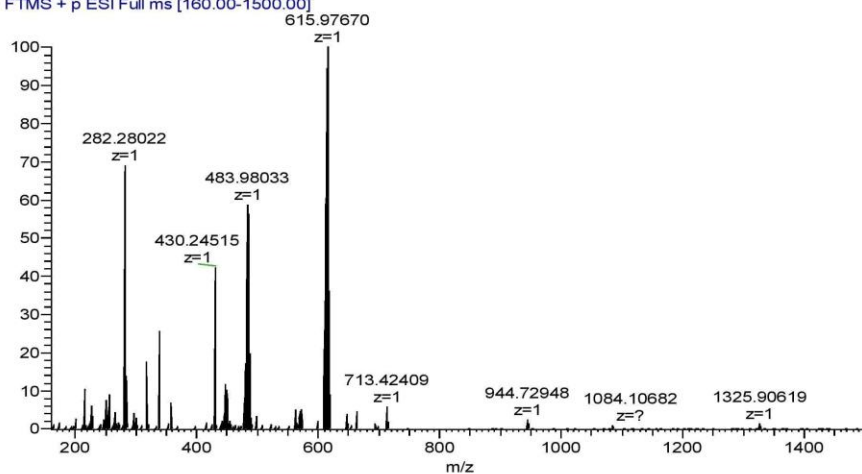


Fig. S15. IR spectrum of **4**.

OB3482 #1-34 RT: 0.00-0.50 AV: 34 NL: 1.42E7
T: FTMS + p ESI Full ms [160.00-1500.00]



Zoomed spectra

OB3482 #1-34 RT: 0.00-0.50 AV: 34 NL: 1.42E7
T: FTMS + p ESI Full ms [160.00-1500.00]

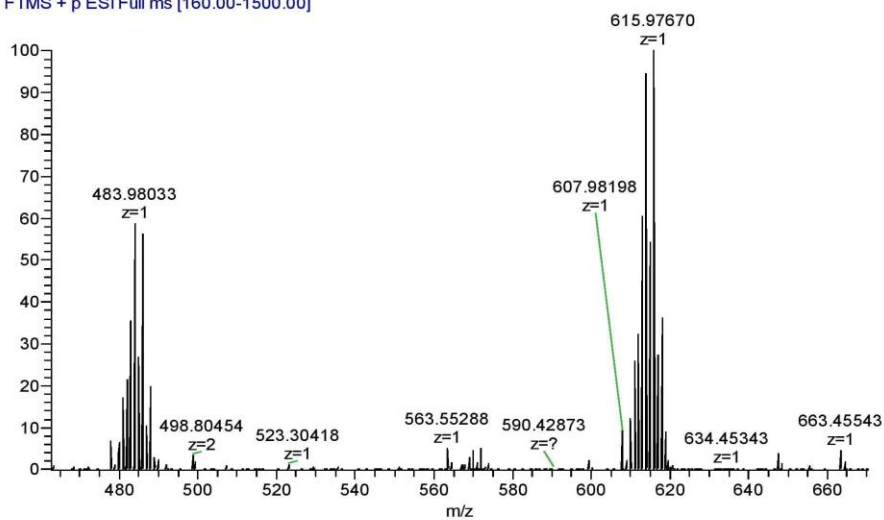


Fig. S16. MS spectrum of 4.

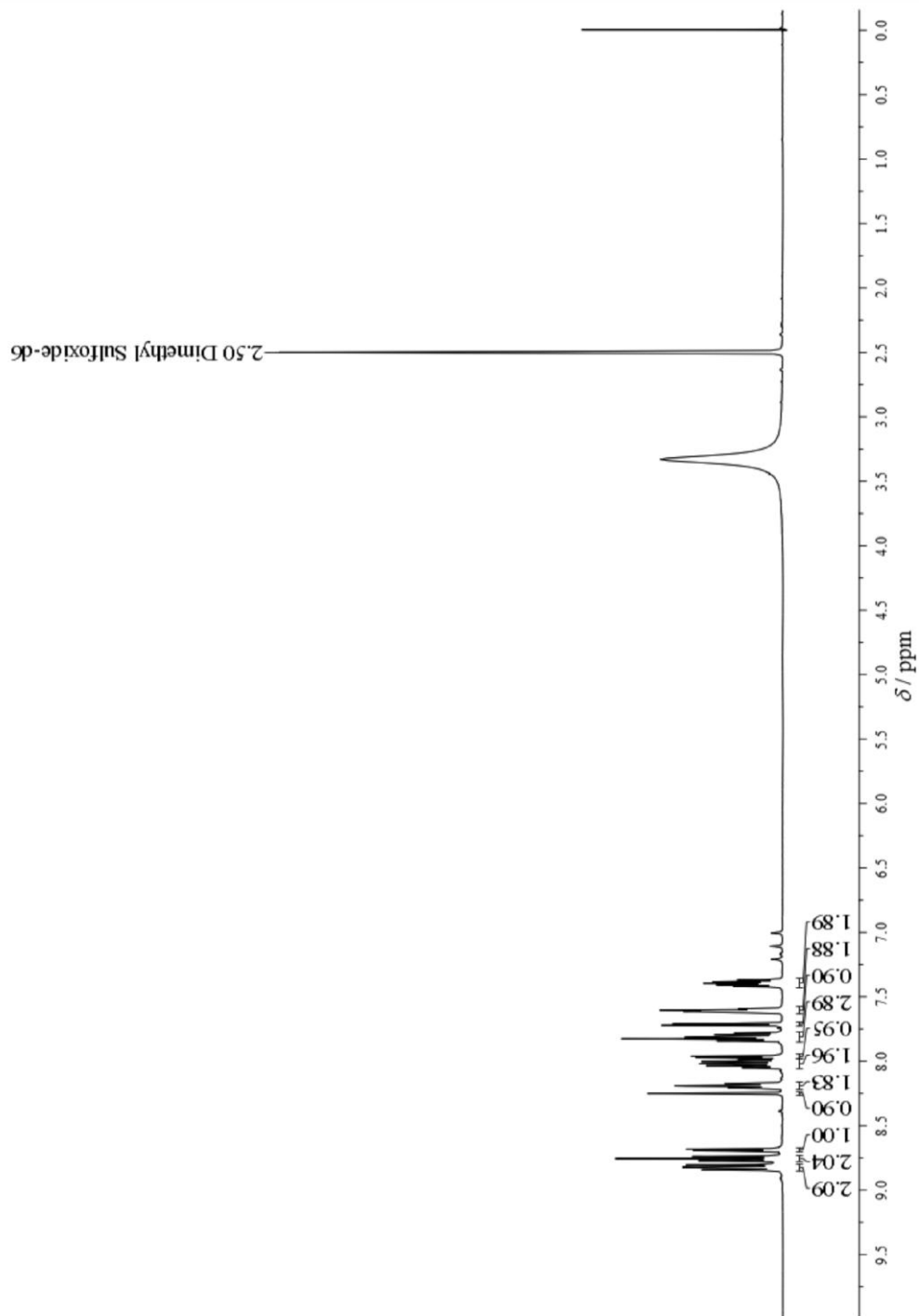


Fig. S17. ^1H NMR spectrum of **5**.

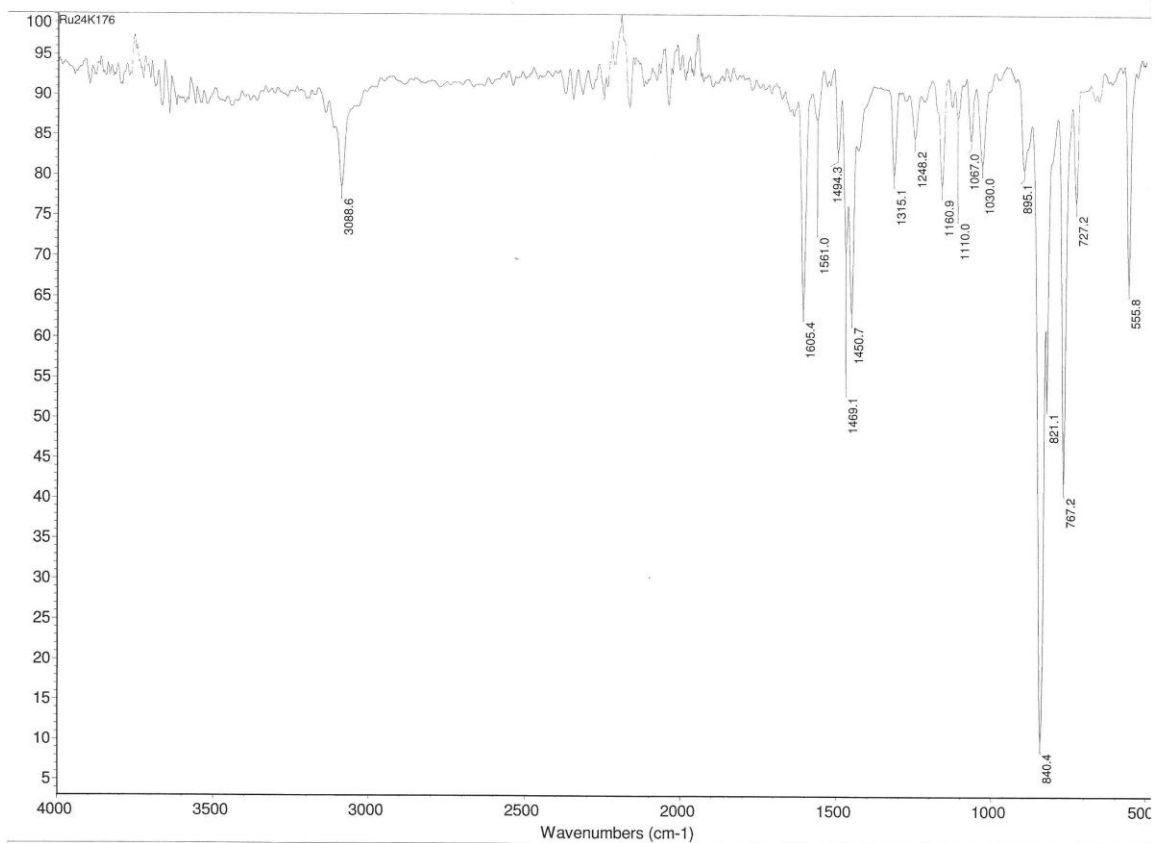


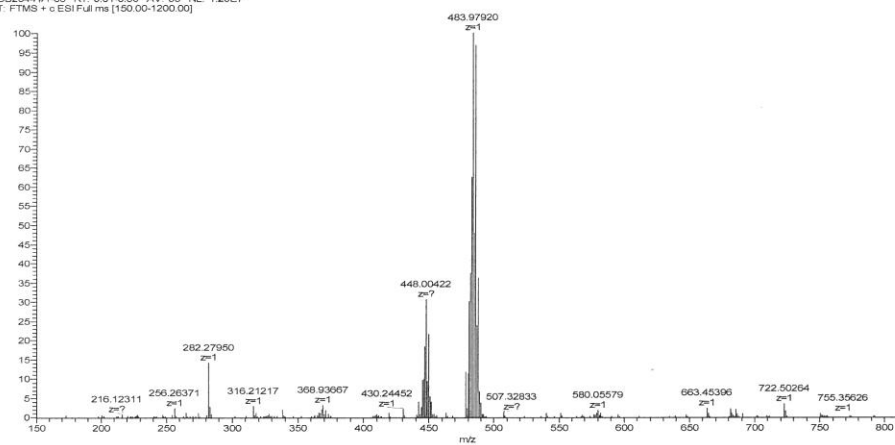
Fig. S18. IR spectrum of **5**.

Ru24K176

Raw file: OB2539

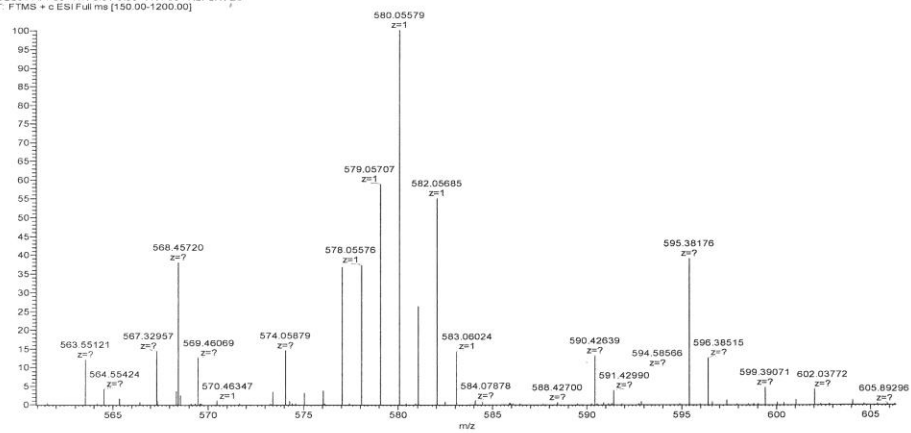
Uzorak: Ru24K176 2ug/mL in ACN

OB2544 #1-55 RT: 0.01-0.50 AV: 55 NL: 1.20E7
T: FTMS + c ESI Full ms [150.00-1200.00]



Zum gore prikazanog spektra u opsegu do 560 do 580 m/z.

OB2544 #1-55 RT: 0.01-0.50 AV: 55 NL: 2.17E5
T: FTMS + c ESI Full ms [150.00-1200.00]



Signal m/z 580.05579 odgovara Ru24K176 uz gresku odredjivanja od 0.2 ppm.

Fig. S19. Mass spectrum of **5**.

7. Curriculum Vitae

Afya A. Baroud, Msc in Chemistry

Date of birth: 08.03.1985

Place of birth: Bani Waleed, Libya

Education

2013-	PhD student at Faculty of Chemistry, University of Belgrade
Decembar 2012	Master of Science degree in Chemistry, Faculty of Chemistry, University of Belgrade
2010-2012.	MSc studies, Faculty of Chemistry, University of Belgrade
2003-2007.	Bachelor of Science degree in Chemistry, Faculty of Science, University 7 th of October, Bani Waleed, Libya
2000-2003.	General Certificate of Secondary Education in Science-Albark Akatif School, Bani Waleed, Libya
1992-2000.	Preparatory School Certificate, Alfajer Algadeid School, Bani Waleed, Libya

Publications

1. **A. A. Baroud**, Lj. E. Mihajlović-Lalić, D. Stanković, Marijana Kajzerberger, K. V. Hecke, S. Grgurić-Šipka, A. Savić: New ruthenium(II) bipyridyl complex: synthesis, crystal structure and cytotoxicity, *J. Serb. Chem. Soc.*, (2017) DOI: 10.2298/JSC170109025B.
2. **A. A. Baroud**, Lj. E. Mihajlović-Lalić, N. Gligorijević, S. Arandelović, D. Stanković, S. Radulović, K. V. Hecke, A. Savić, S. Grgurić-Šipka: Ruthenium(II) bipyridyl complexes:

from synthesis and crystal structures to electrochemical and cytotoxicity investigation, *J. Coord. Chem.*, 70 (2017) 831-847.

3. A. Savić, **A. A. Baroud**, Sanja Grgurić-Šipka: The new ruthenium(II)-bipyridyl complex with O,O'-diethyl-(S,S)-ethylenediamine-N,N'-di-2-(3-cyclohexyl)propanoate: synthesis and characterization. *Maced. J. Chem. Chem. Eng.*, 2014, 33, 59-64.

Conferences

1. **A. A. Baroud**, A. R. Savić, Ruthenium(II)-bipyridyl complex as PDT agent, *Prva konferencija Kluba mladih hemičara*, Beograd, **2012**. Izvodi radova HS P15, str. 62.

Прилог 1.

Изјава о ауторству

Потписана: Afya A. Baroud

број уписа ДХ54/2012

Изјављујем

да је докторска дисертација под насловом

Синтеза, карактеризација и цитотоксичност бис(бипиридин) рутенијум(II) комплекса са дериватима пиколинске киселине

- резултат сопственог истраживачког рада,
- да предложена дисертација у целини ни у деловима није била предложена за добијање било које дипломе према студијским програмима других високошколских установа,
- да су резултати коректно наведени и
- да нисам кршио/ла ауторска права и користио интелектуалну својину других лица.

Потпис докторанда

У Београду, 9.3.2017.

Прилог 2.

Изјава о истоветности штампане и електронске верзије докторског рада

Име и презиме аутора: Afya A. Baroud

Број уписа: ДХ54/2012

Студијски програм: доктор хемијских наука

Наслов рада: Синтеза, карактеризација и цитотоксичност бис(бипиридин) рутенијум(II) комплекса са дериватима пиколинске киселине

Ментор: др Сања Гргурић-Шипка, редовни професор Хемијског факултета, Универзитета у Београду

Потписани Afya A. Baroud

изјављујем да је штампана верзија мог докторског рада истоветна електронској верзији коју сам предао/ла за објављивање на порталу **Дигиталног репозиторијума Универзитета у Београду**.

Дозвољавам да се објаве моји лични подаци везани за добијање академског звања доктора наука, као што су име и презиме, година и место рођења и датум одбране рада.

Ови лични подаци могу се објавити на мрежним страницама дигиталне библиотеке, у електронском каталогу и у публикацијама Универзитета у Београду.

Потпис докторанда

У Београду, 9.3.2017.

Прилог 3.

Изјава о коришћењу

Овлашћујем Универзитетску библиотеку „Светозар Марковић“ да у Дигитални репозиторијум Универзитета у Београду унесе моју докторску дисертацију под насловом:

Синтеза, карактеризација и цитотоксичност бис(бипиридин) рутенијум(II) комплекса са дериватима пиколинске киселине

која је моје ауторско дело.

Дисертацију са свим прилозима предао/ла сам у електронском формату погодном за трајно архивирање.

Моју докторску дисертацију похрањену у Дигитални репозиторијум Универзитета у Београду могу да користе сви који поштују одредбе садржане у одабраном типу лиценце Креативне заједнице (Creative Commons) за коју сам се одлучио/ла.

1. Ауторство
2. Ауторство - некомерцијално
3. Ауторство – некомерцијално – без прераде
4. Ауторство – некомерцијално – делити под истим условима
5. Ауторство – без прераде
6. Ауторство – делити под истим условима

(Молимо да заокружите само једну од шест понуђених лиценци, кратак опис лиценци дат је на полеђини листа).

Потпис докторанда

У Београду, 9.3.2017.

1. Ауторство - Дозвољаваате умножавање, дистрибуцију и јавно саопштавање дела, и прераде, ако се наведе име аутора на начин одређен од стране аутора или даваоца лиценце, чак и у комерцијалне сврхе. Ово је најслободнија од свих лиценци.
2. Ауторство – некомерцијално. Дозвољаваате умножавање, дистрибуцију и јавно саопштавање дела, и прераде, ако се наведе име аутора на начин одређен од стране аутора или даваоца лиценце. Ова лиценца не дозвољава комерцијалну употребу дела.
3. Ауторство - некомерцијално – без прераде. Дозвољаваате умножавање, дистрибуцију и јавно саопштавање дела, без промена, преобликовања или употребе дела у свом делу, ако се наведе име аутора на начин одређен од стране аутора или даваоца лиценце. Ова лиценца не дозвољава комерцијалну употребу дела. У односу на све остале лиценце, овом лиценцом се ограничава највећи обим права коришћења дела.
4. Ауторство - некомерцијално – делити под истим условима. Дозвољаваате умножавање, дистрибуцију и јавно саопштавање дела, и прераде, ако се наведе име аутора на начин одређен од стране аутора или даваоца лиценце и ако се прерада дистрибуира под истом или сличном лиценцом. Ова лиценца не дозвољава комерцијалну употребу дела и прерада.
5. Ауторство – без прераде. Дозвољаваате умножавање, дистрибуцију и јавно саопштавање дела, без промена, преобликовања или употребе дела у свом делу, ако се наведе име аутора на начин одређен од стране аутора или даваоца лиценце. Ова лиценца дозвољава комерцијалну употребу дела.
6. Ауторство - делити под истим условима. Дозвољаваате умножавање, дистрибуцију и јавно саопштавање дела, и прераде, ако се наведе име аутора на начин одређен од стране аутора или даваоца лиценце и ако се прерада дистрибуира под истом или сличном лиценцом. Ова лиценца дозвољава комерцијалну употребу дела и прерада. Слична је софтверским лиценцама, односно лиценцама отвореног кода.